Supporting Information for:

Arabinoxyloglucan Oligosaccharides May Contribute to the Anti-Adhesive Properties of Porcine Urine After Cranberry Consumption

Christina M. Coleman,[#,*,†] Kimberly M. Auker,[†] K. Brian Killday,[‡] Parastoo Azadi,[§] Ian Black,[§] and Daneel Ferreira[#,*,†]

[†]Department of BioMolecular Sciences, Division of Pharmacognosy, and the Research Institute of Pharmaceutical Sciences, School of Pharmacy, University of Mississippi, University, Mississippi 38677, United States

[‡]Bruker BioSpin Corporation, Billerica, Massachusetts 01821, United States

[§]Complex Carbohydrate Research Center, University of Georgia, Athens, Georgia 30602, United States

[#]Correspondence
Christina M. Coleman: cmcoleman4321@gmail.com
Daneel Ferreira: dferreir@olemiss.edu

TABLE OF CONTENTS

LIST OF SUPPLEMENTARY TABLES

LIST OF SUPPLEMENTARY FIGURES

Supplementary Tables

These Tables are referred to and discussed within the main publication text (Main Text).

Table S1. Anti-Agglutination Assay Results for FF Sephadex LH-20 Column Fractions.

Sample Relative Activity				
FF1-1 ++	FF2-1 ++	FF3-1 ++	FF4-1 +	FF5-1 ++
FF1-2 ++	FF2-2 +	FF3-2 ++	FF4-2 +	FF5-2 ––
FF1-3 ––	FF2-3 +	FF3-3 ––	FF4-3 –	FF5-3 ––
FF1-4 ––	FF2-4 +	FF3-4 ––	FF4-4 ––	FF5-4 ––
FF1-5 –	FF2-5 ––	FF3-5 ––	FF4-5 ––	FF5-5 ––
FF1-6 +/–	FF2-6 +/–	FF3-6 +/–	FF4-6 ––	FF5-6 ––
FF1-7 ++	FF2-7 +/–		FF4-7 ––	FF5-7 ––
FF1-8 ––	FF2-8 ––		FF4-8 ––	FF5-8 –
FF1-9 ––				

Table S2. Details of Multiple Sephadex LH-20 Separations for the FF Aqueous Urine Sample.

The total amount of active material recovered from all five columns (combined to give FA, 1.747 g) accounted for 1.3% of the total loaded samples (133 g) and contained both active and inactive components.

column designation	FF1	FF2	FF3	FF4	FF5
amount of loaded material (g)	10.0	14.0	10.0	50.4	48.5
loaded volume & concentration[a]	45 mL 222 mg/mL	36 mL 388 mg/mL	31.5 mL 317 mg/mL	120 mL 417 mg/mL	100 mL 485 mg/mL
solvent composition	50% EtOH	70% EtOH	50% EtOH	70% EtOH	70% EtOH
column dimensions (cm; width x height)	5.5 x 32	7.5 x 5	5.5 x 34.5	10 x 24	10 x 24
solvent flow rate (mL/min)	1.8–2.0	1.0–1.2	1.2–1.4	2.0–4.0	3.0–5.0
active material total elution volume (mL)	150	50	114	456	572
active fractions (combined to give FA)	FF1-1 FF1-2 FF1-7[b]	FF2-1 FF2-2[b]	FF3-1 FF3-2	FF4-1 FF4-2	FF5-1 FF5-2[c]
total active material per column (g)	0.239	0.287	0.138	0.356	0.727
active % of loaded material	2.39%	2.05%	1.38%	0.71%	1.50%

[a] Samples were loaded in column solvent: *e.g.* FF1 loaded in 50% EtOH.
[b] Activity in this sample was the result of contamination with part of fraction FF1-2 during material transfers.
[c] These samples did not show activity but were included in recombined FA sample to ensure full recovery of potentially active metabolites.

Table S3. Details of the Sephadex LH-20 Separation for the Recombined, Enriched FA Sample.

The total amount of active material recovered from this column (0.917 g) accounted for 54.5% of the loaded FA sample, contains primarily active components, and is equivalent to 0.7% of the total amount of separated F samples (133 g).

column designation	FA
amount of loaded material [a]	1.683 g
loaded volume & concentration	5 mL; 337 mg/mL
column dimensions (width x height)	2.5 x 40.5 cm
solvent composition	75% EtOH
solvent flow rate	0.5–1.0 mL/min
active material total elution volume	200 mL
active fraction	FA1 (0.030 g); FA2 (0.887 g)
total active material per column	0.917 g
active % of loaded material	54.5%

[a] Approximately 0.06 g of FA was reserved as a bioassay testing control.

Table S4. Details of Sephadex LH-20 Separations for the H and I Urine Samples.

Combined oligosaccharide-containing fractions (1.334 g) comprised approximately 1–2% of the total amount of separated material (69 g) and contained oligosaccharides with putative activity as well as other, unrelated compounds.

column designation	HF1	HF2	IF1	IF2
amount of loaded material (g)	10	40	30	14
loaded volume & concentration	30 mL 333 mg/mL	125 mL 320 mg/mL	50 mL 300 mg/mL	50 mL 280 mg/mL
column dimensions (cm; width x height)	7 x 38	10 x 25	7 x 38	7 x 38
solvent composition	70% EtOH	70% EtOH	70% EtOH	70% EtOH
solvent flow rate (mL/min)	1.0–1.5	1.5–2.0	1.0–1.5	1.0–1.5
total elution volume for oligosaccharide-containing fractions[a] (mL)	350	450	380	200
oligosaccharide-containing fractions[a]	HF1-1 HF1-2	HF2-1 HF2-2	IF1-1 IF1-2 IF1-3	IF2-1[b] IF2-2[b]
oligosaccharide material per column (g)	0.148	0.607	0.425	0.154
active[c] % of loaded material	1.48%	1.52%	1.42%	1.10%

[a] HF1 fractions were tested in the bioassay. HF2, IF1, and IF2 fractions were compared by HPLC to HF1, FA1, and FA2 fractions to direct isolation efforts while conserving material.
[b] The IF2 fractions were combined with the respective IF1 fractions prior to later separations.
[c] Putative activity based on composition comparisons using HPLC and NMR.

Table S5. Glycosyl Composition Analysis Results for Compound **1**.

Residue	weight (μg)	mole %
arabinose (Ara)	26.5	22.0
ribose (Rib)	0.0	0.0
rhamnose (Rha)	0.0	0.0
fucose (Fuc)	0.0	0.0
xylose (Xyl)	30.4	25.1
glucuronic Acid (GlcUA)	0.0	0.0
galacturonic acid (GalUA)	0.0	0.0
mannose (Man)	0.0	0.0
galactose (Gal)	0.0	0.0
glucose (Glc)	76.7	52.9
N-acetyl galactosamine (GalNAc)	0.0	0.0
N-acetyl glucosamine (GlcNAc)	0.0	0.0
heptose (Hep)	0.0	0.0
3-deoxy-2-manno-2-octulsonic acid (KDO)	0.0	0.0
Sum		100

Supplementary Figures

These Figures are referred to and discussed within the main publication text (Main Text).

Figure S1. ^{1}H NMR spectra of synthesized A-type PAC pentameric and tetrameric oligomers, 400 MHz, Acetone-d_6.

These PAC samples were insoluble in D_2O and DMSO-d_6.

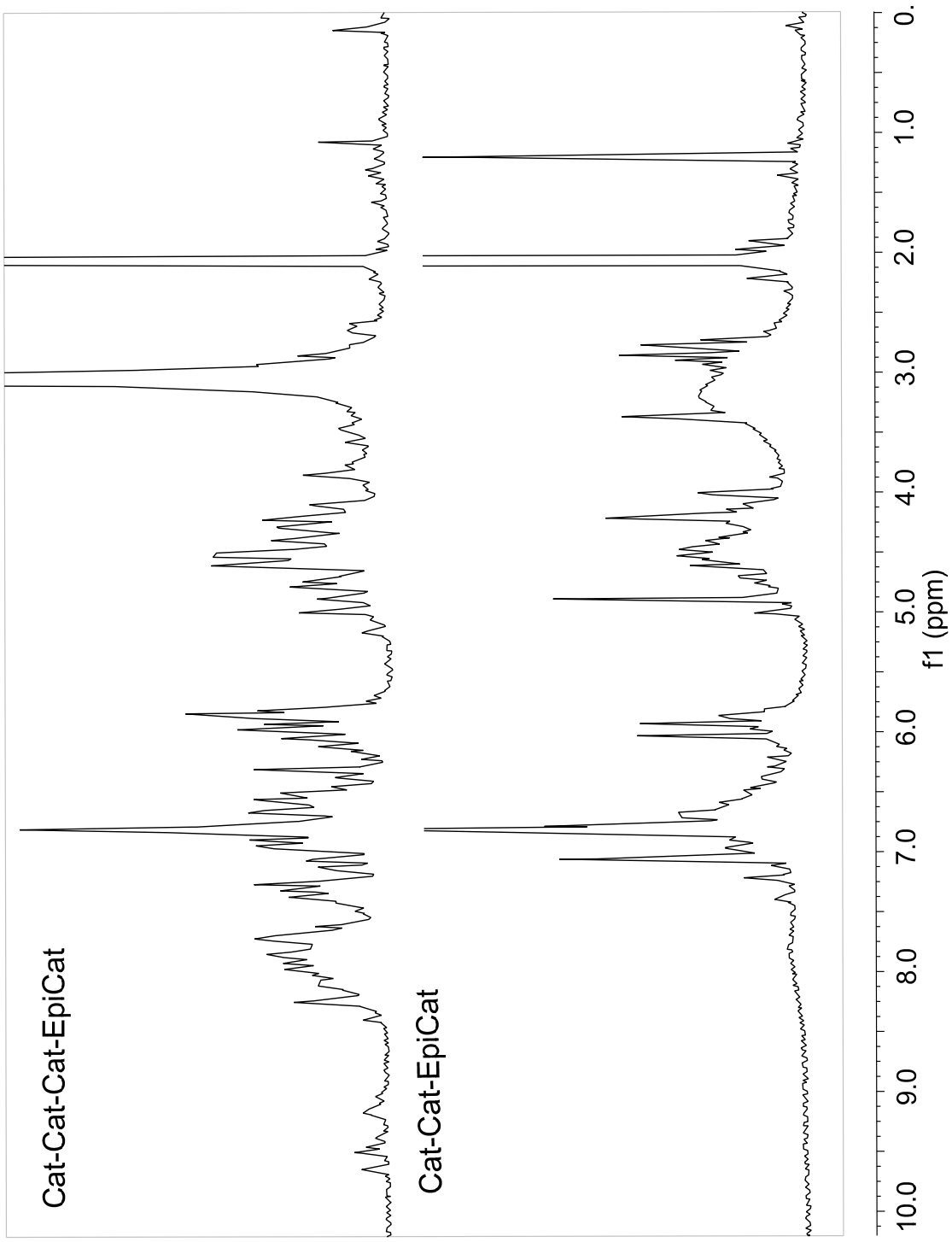

Figure S2. ^{1}H NMR spectra of FC1-1, HF, FA and HF1-1 samples, 400 MHz, D_2O.

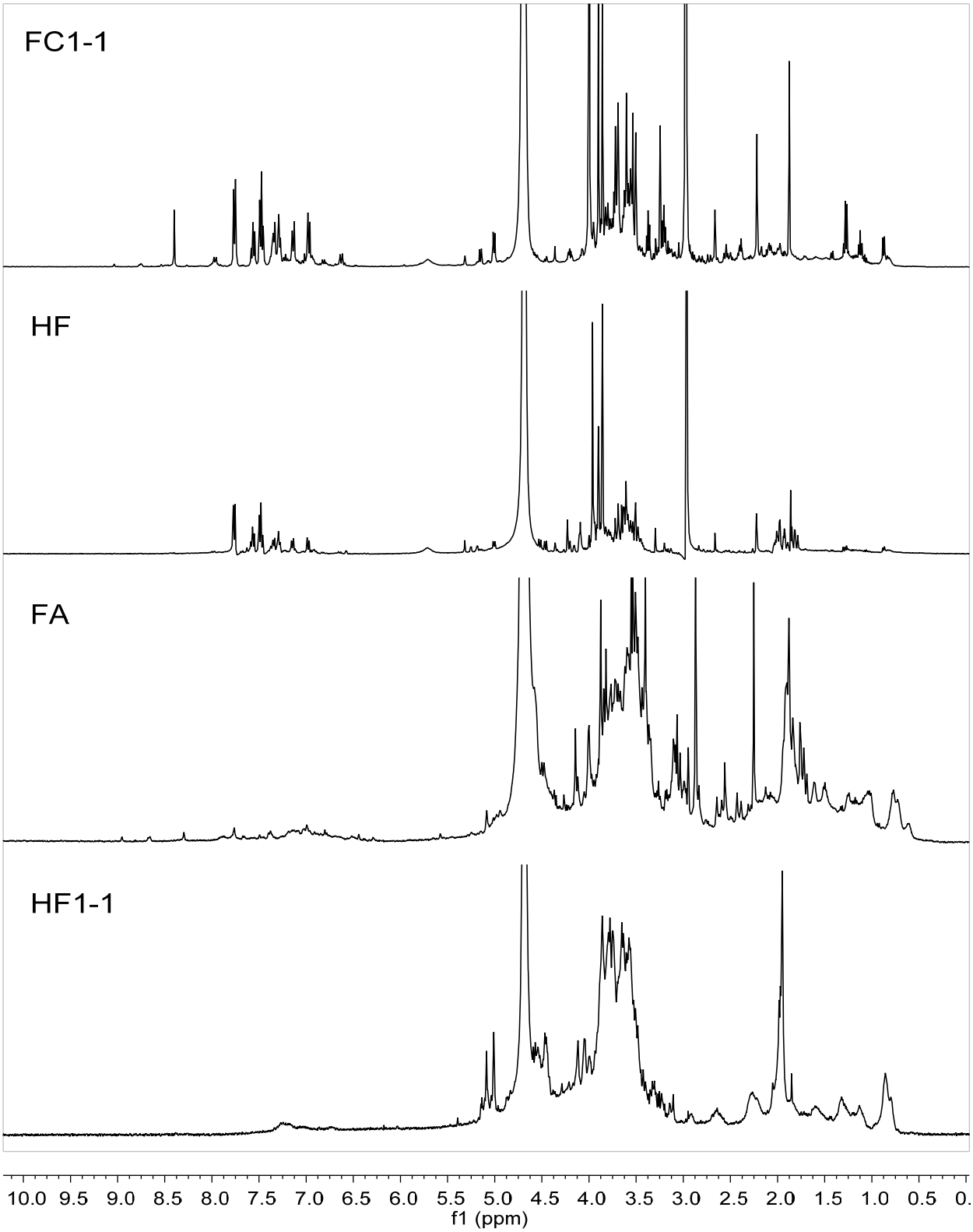

Figure S3. ^{1}H NMR spectra of FC1-1, HF, FA and HF1-1 samples; expansion of the aromatic region, 400 MHz, D_2O.

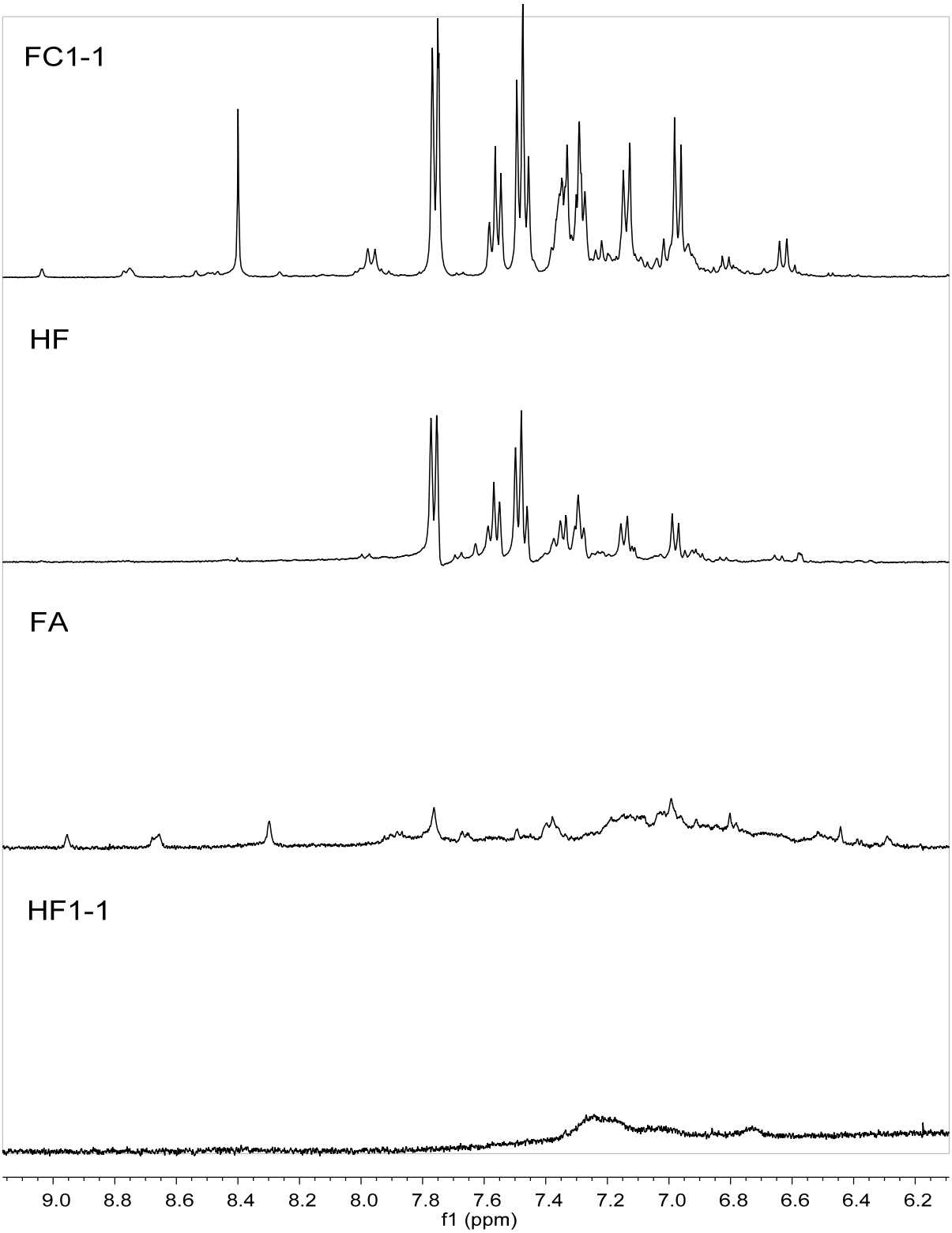

Figure S4. Analytical HPLC-UV (Max Plot) of Sephadex LH-20 fractions HF1-1, HF1-2, and HF1-3 (Atlantis dC_{18}).

The ELS-detectable components present at 16-25 min (box) in are not detectable by UV spectroscopy using wavelengths of 210-400 nm (Max Plot). Sample weight units are mg, Dilution units are µL.

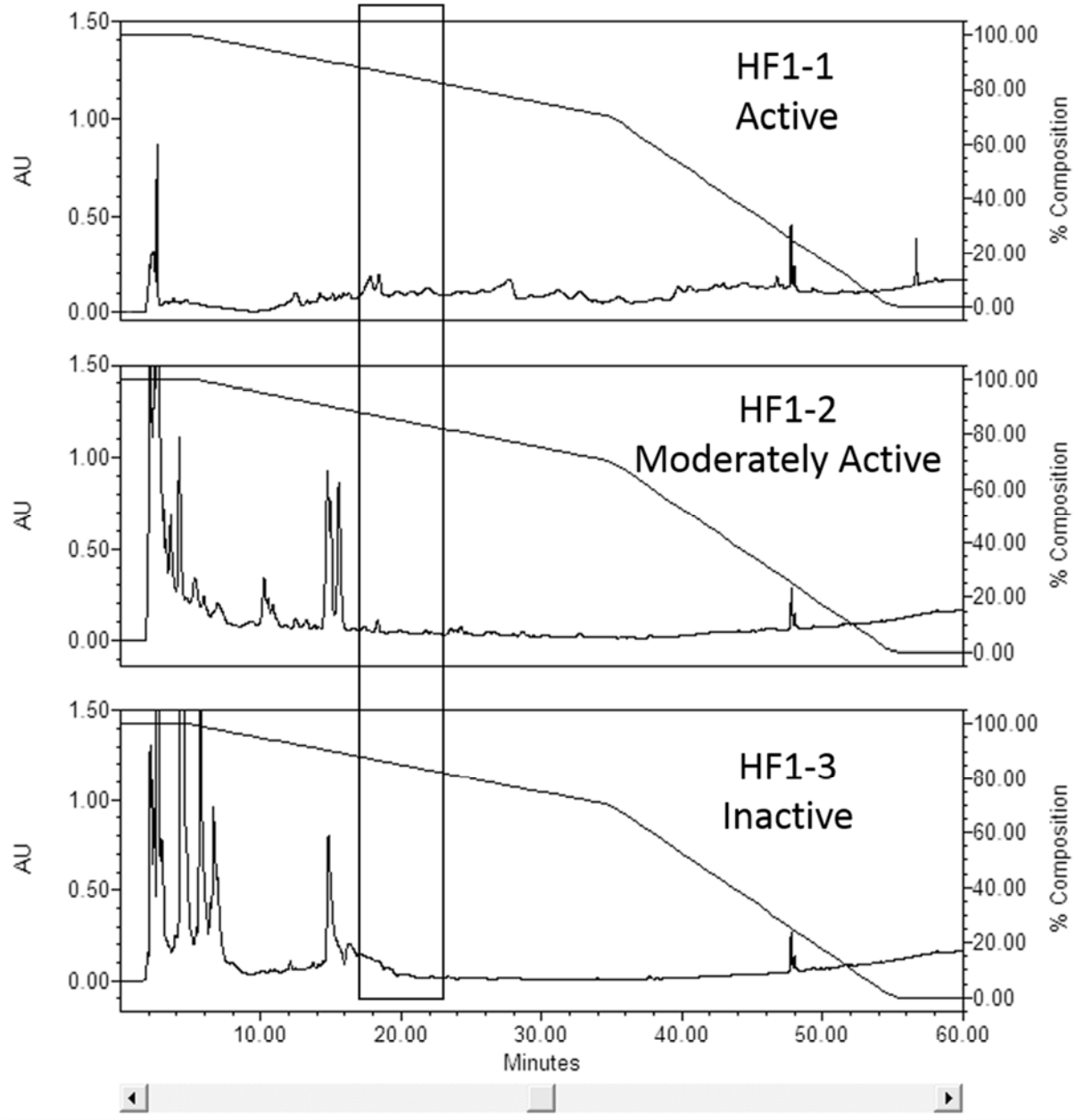

Visible	Vial	SampleName	Date Acquired	SampleWeight	Dilution	Injection Volume (uL)	Channel Name
☑	18	HF1-1 AtldC18-A R1	7/10/2009 1:08:44 AM CDT	2.00000	200.00000	50.00	MaxPlot 210.0 to 400
☑	19	HF1-2 AtldC18-A R1	7/10/2009 2:45:02 AM CDT	3.00000	300.00000	50.00	MaxPlot 210.0 to 400
☑	20	HF1-3 AtldC18-A R1	7/10/2009 4:21:20 AM CDT	2.60000	260.00000	50.00	MaxPlot 210.0 to 400

Figure S5. Expansions of the ^{1}H NMR spectrum of compound **1**, DMSO-d_6, 700 MHz.

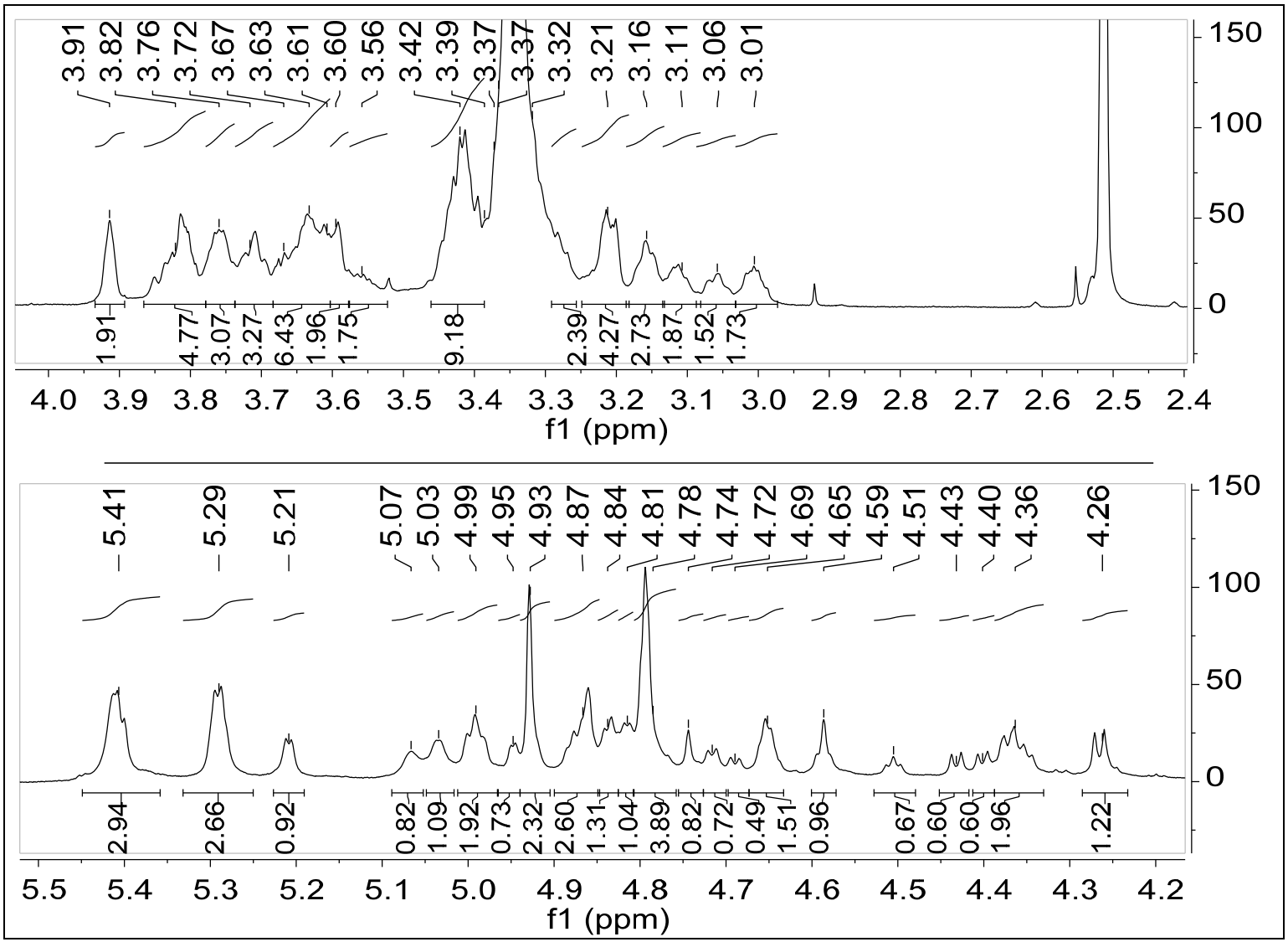

Figure S6. Expansions of the ^{13}C NMR spectrum of compound **1**, DMSO-d_6, 175 MHz.

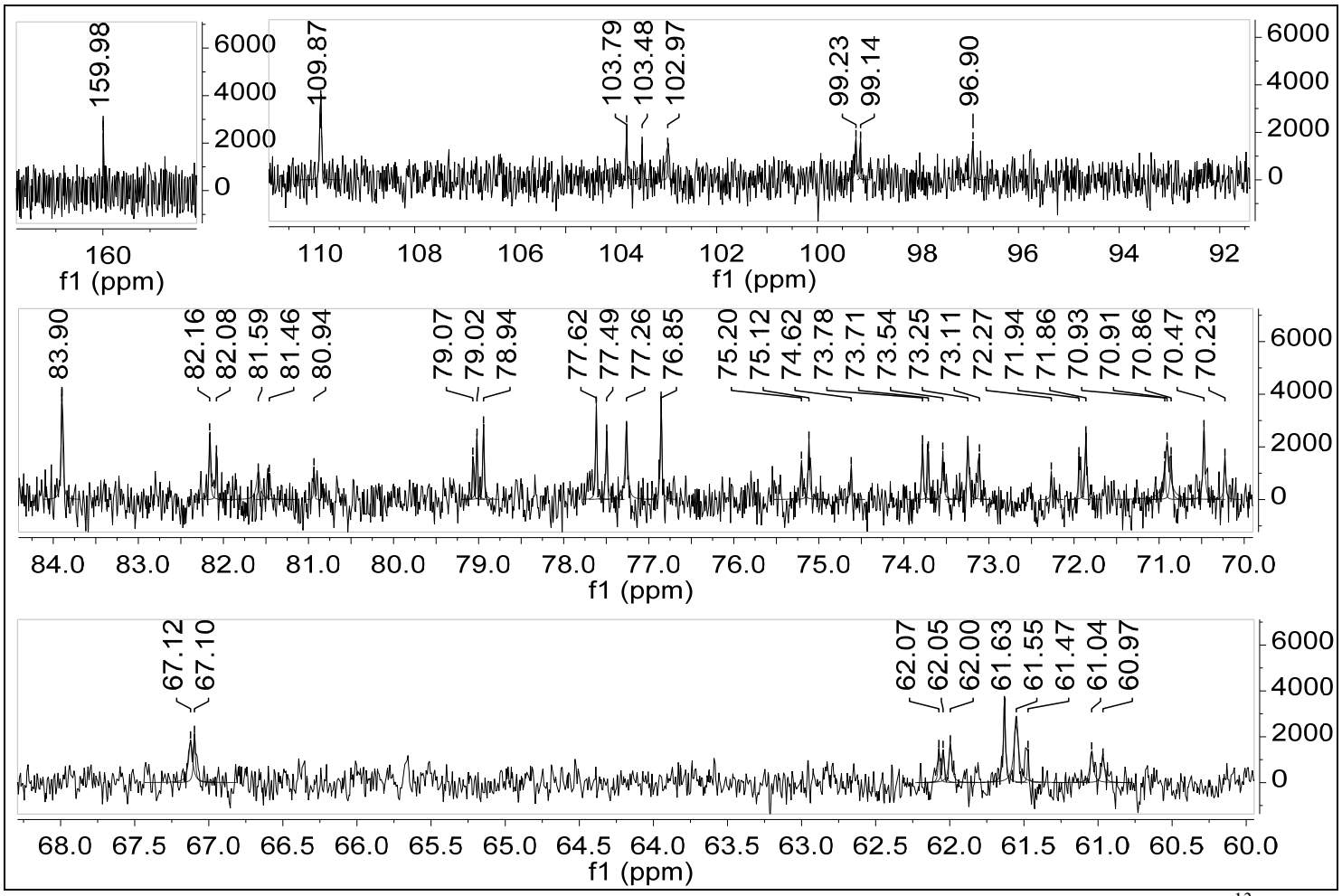

The values shown in Table 3 (Main Text) are based on consideration of this spectrum in conjunction with ^{13}C chemical shift values obtained from HSQC data (Figures S7 and S8). Although distinct signals could be detected, resonances that occurred close together were often assigned a single value (e.g., 61.7 for 61.63 and 61.55) due to signal overlap in correlation spectra. 2D NMR spectra also enabled the detection of signals that do not appear in this spectrum, including δ_C 92.2 (see Figure S8). The following resonances were not assigned to the structure of compound **1**: δ_C 159.98, 70.47, 70.23, 62.07.

Figure S7. Multiplicity-edited HSQC spectrum of compound **1** with an expansion, DMSO-d_6, 700/175 MHz.

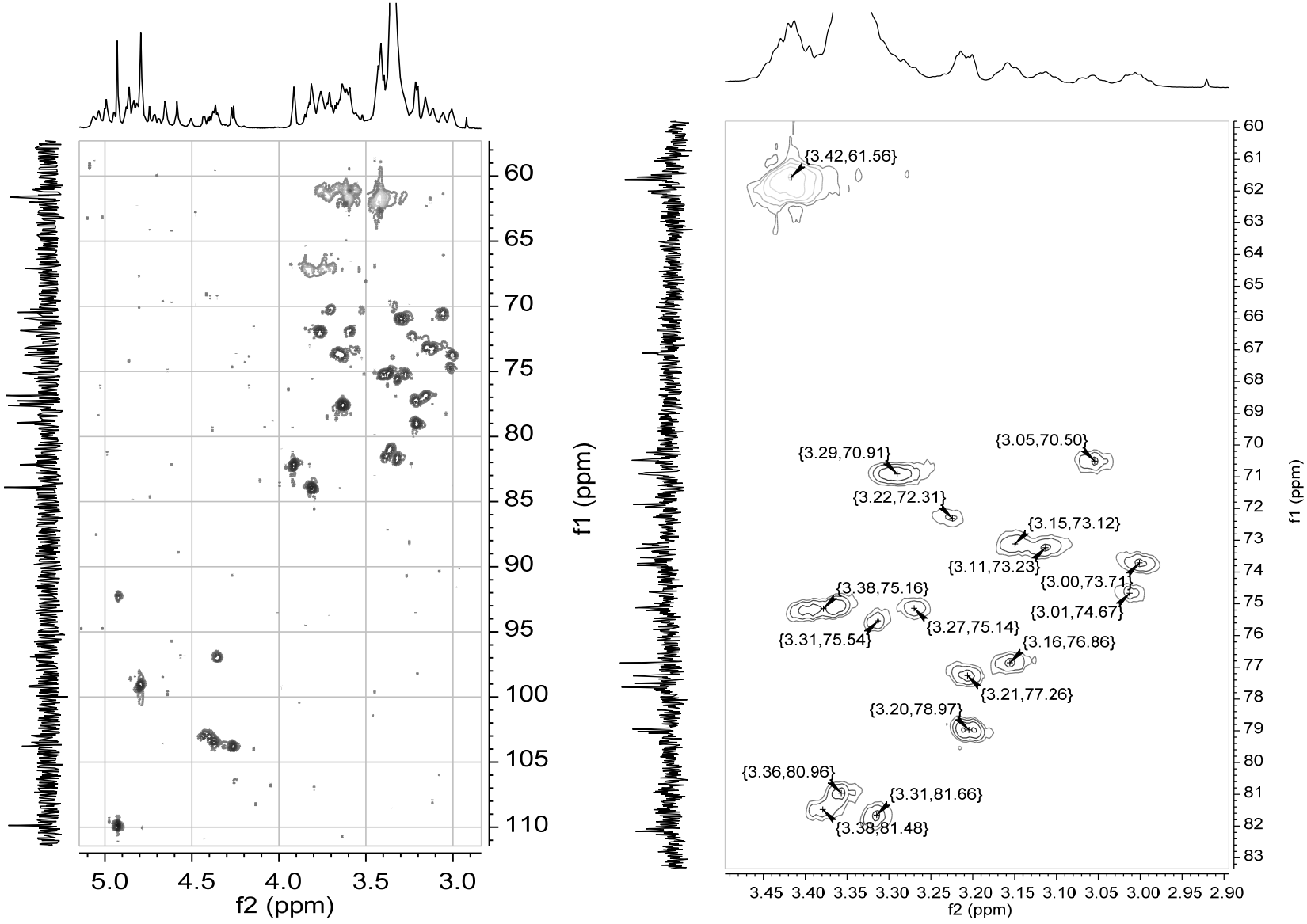

Figure S8. Additional expansions of the multiplicity-edited HSQC spectrum of compound **1**, DMSO-d_6, 700/175 MHz.

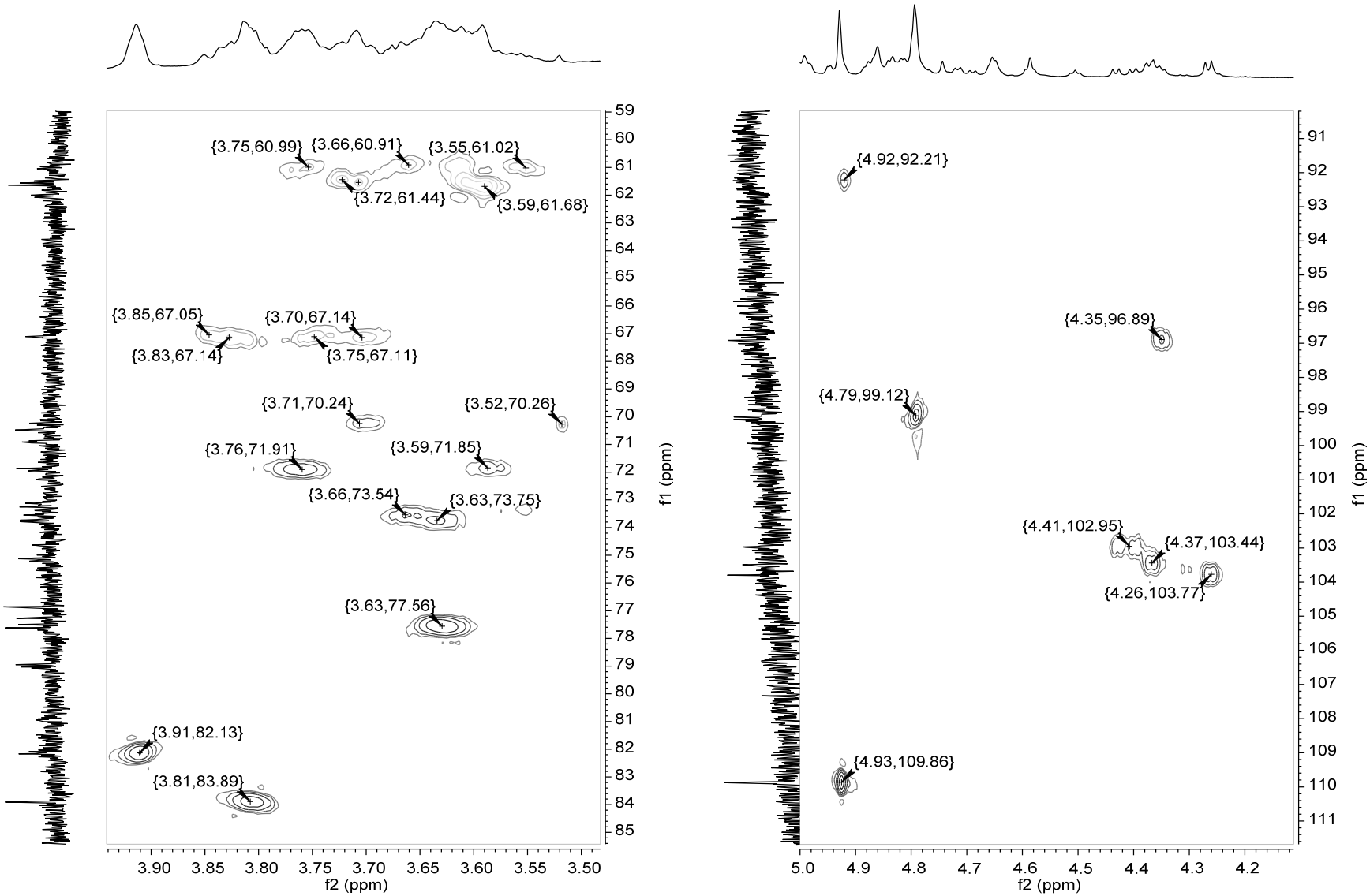

Figure S9. COSY spectrum for compound **1**, DMSO-d_6, 700 MHz.

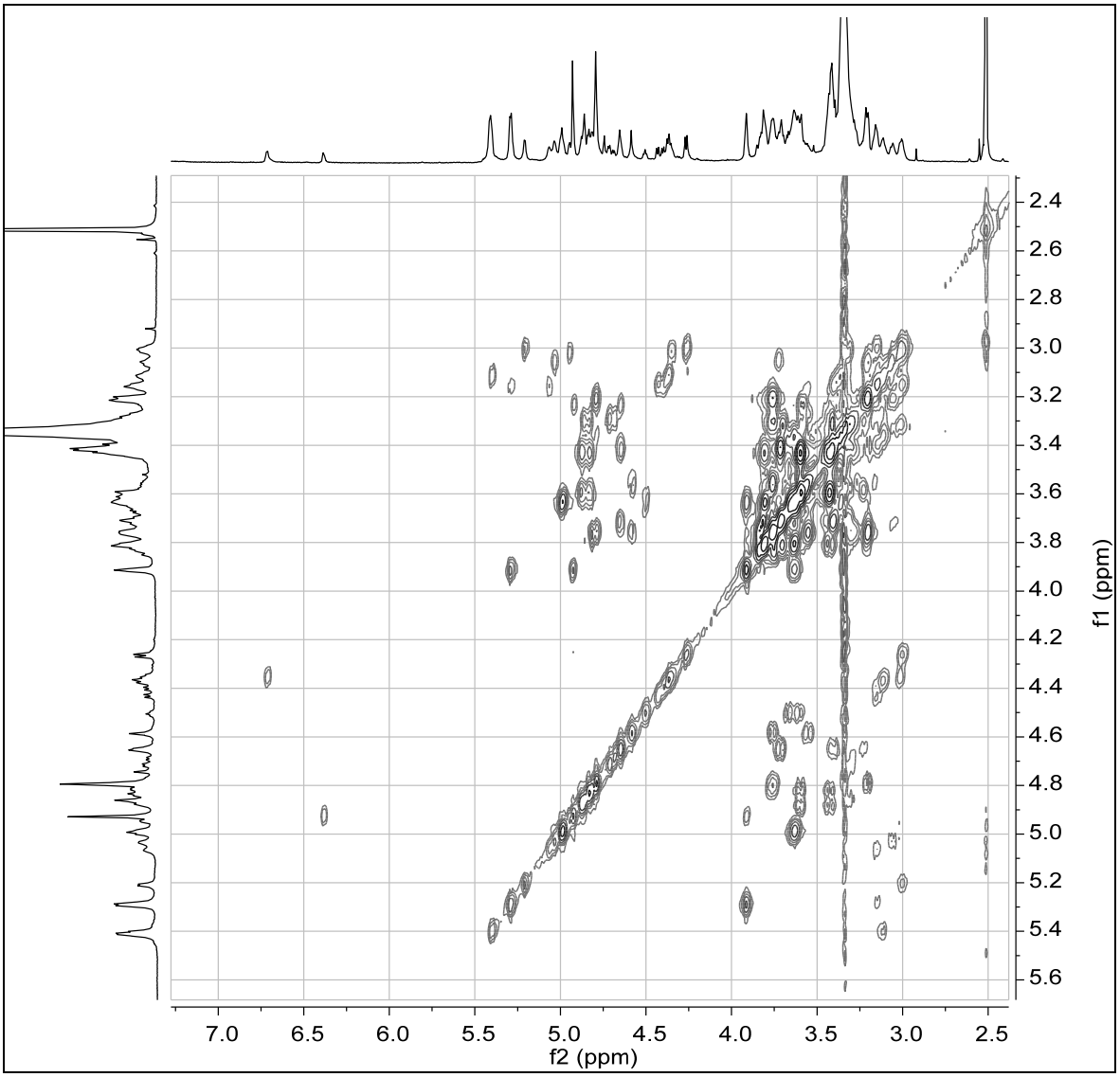

Figure S10. Expansions of the COSY spectrum for compound **1**, DMSO-d_6, 700 MHz.

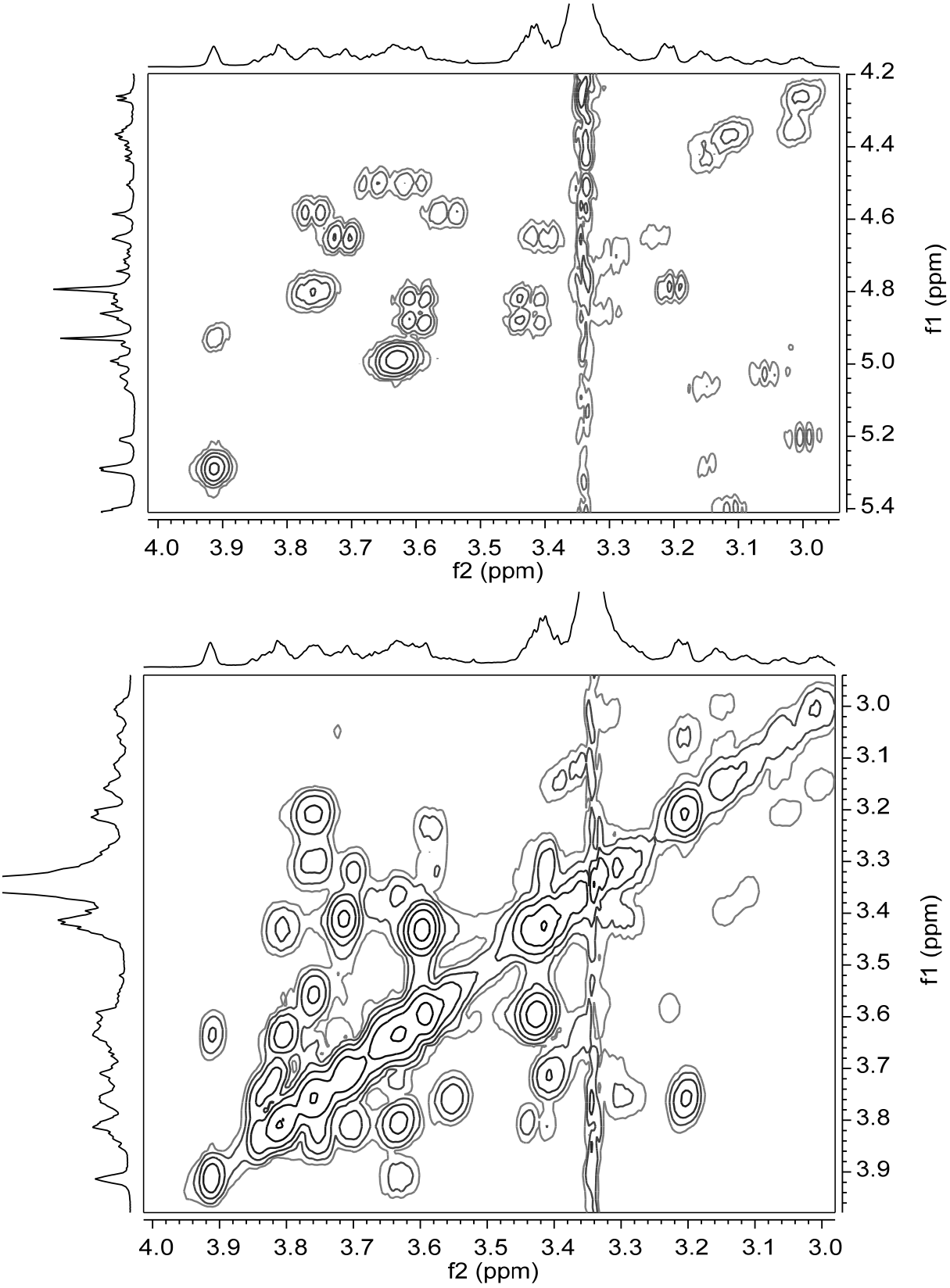

Figure S11. TOCSY spectrum of compound **1**, DMSO-d_6, 700 MHz.

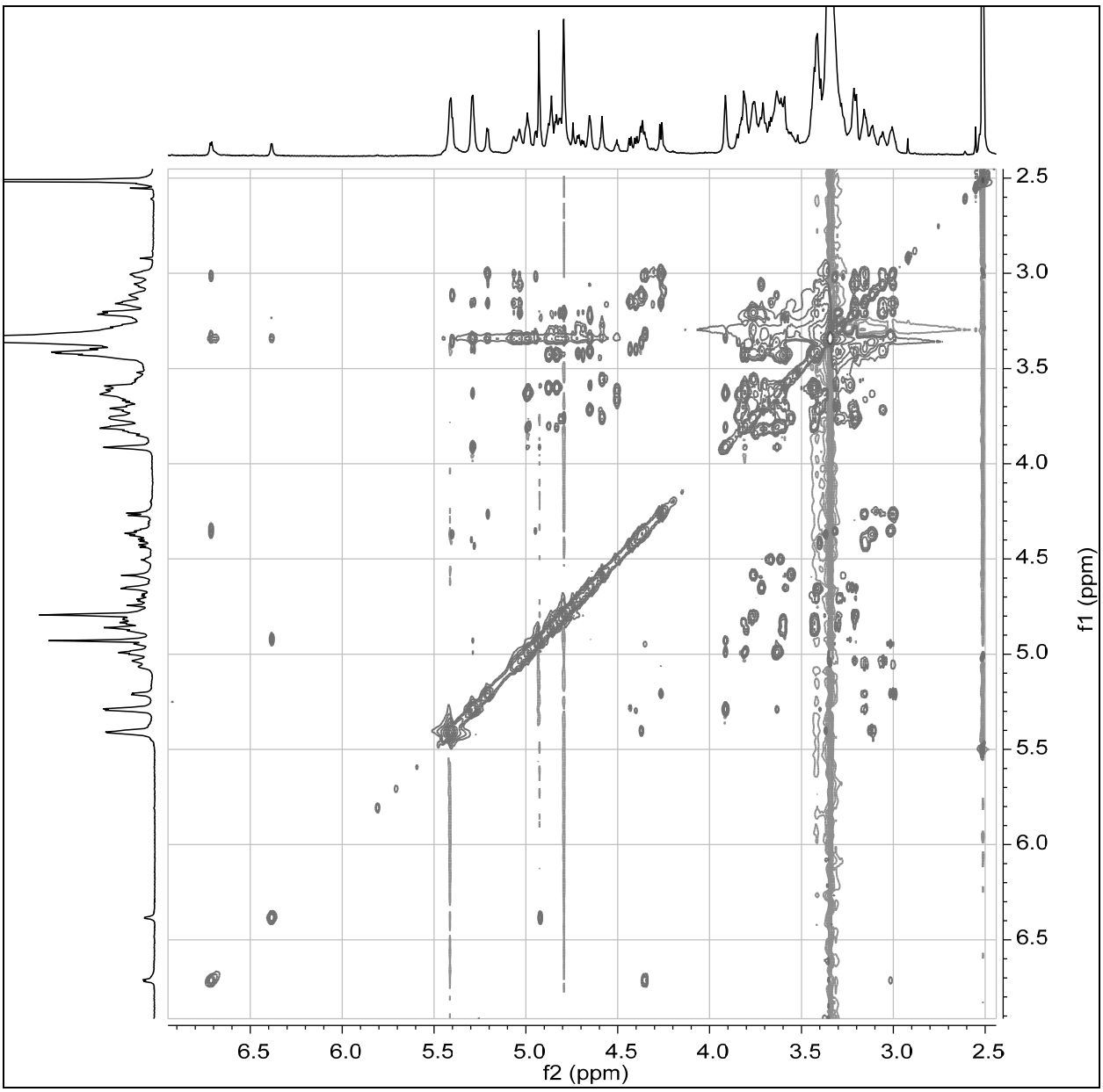

Figure S12. HMBC spectrum for compound **1** with an expansion, DMSO-d_6, 700 MHz.

Key HMBC correlations (arrows) supported the assignments of connectivity between monomer units and were consistent with the structure determined by the carbohydrate analyses (^{1}H/^{13}C ppm: 3.21/109.9; 4.27/81.0; 4.79/67.1; 4.93/78.9).

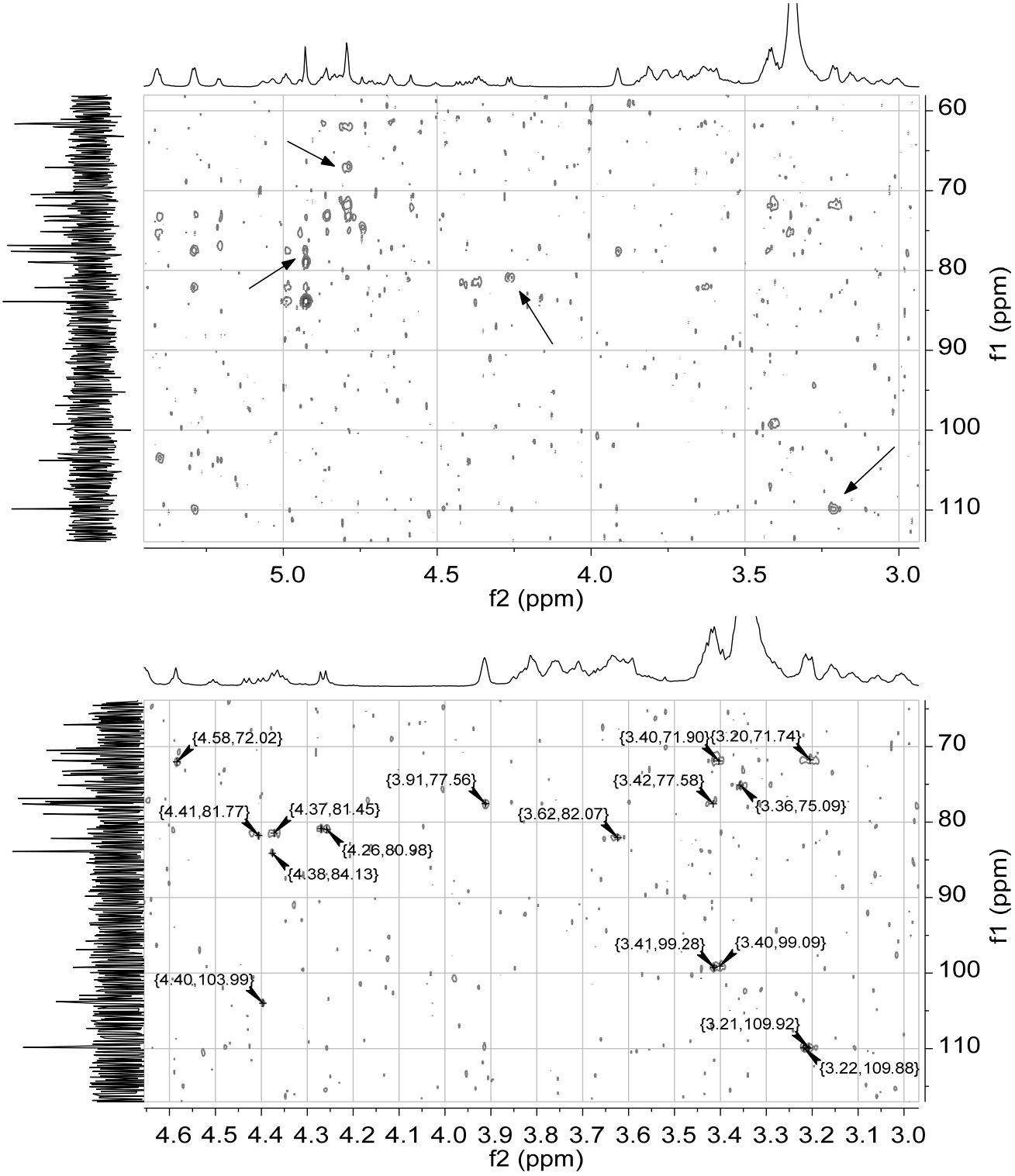

Figure S13. Expansions of the HMBC spectrum for compound **1**, DMSO-d_6, 700 MHz.

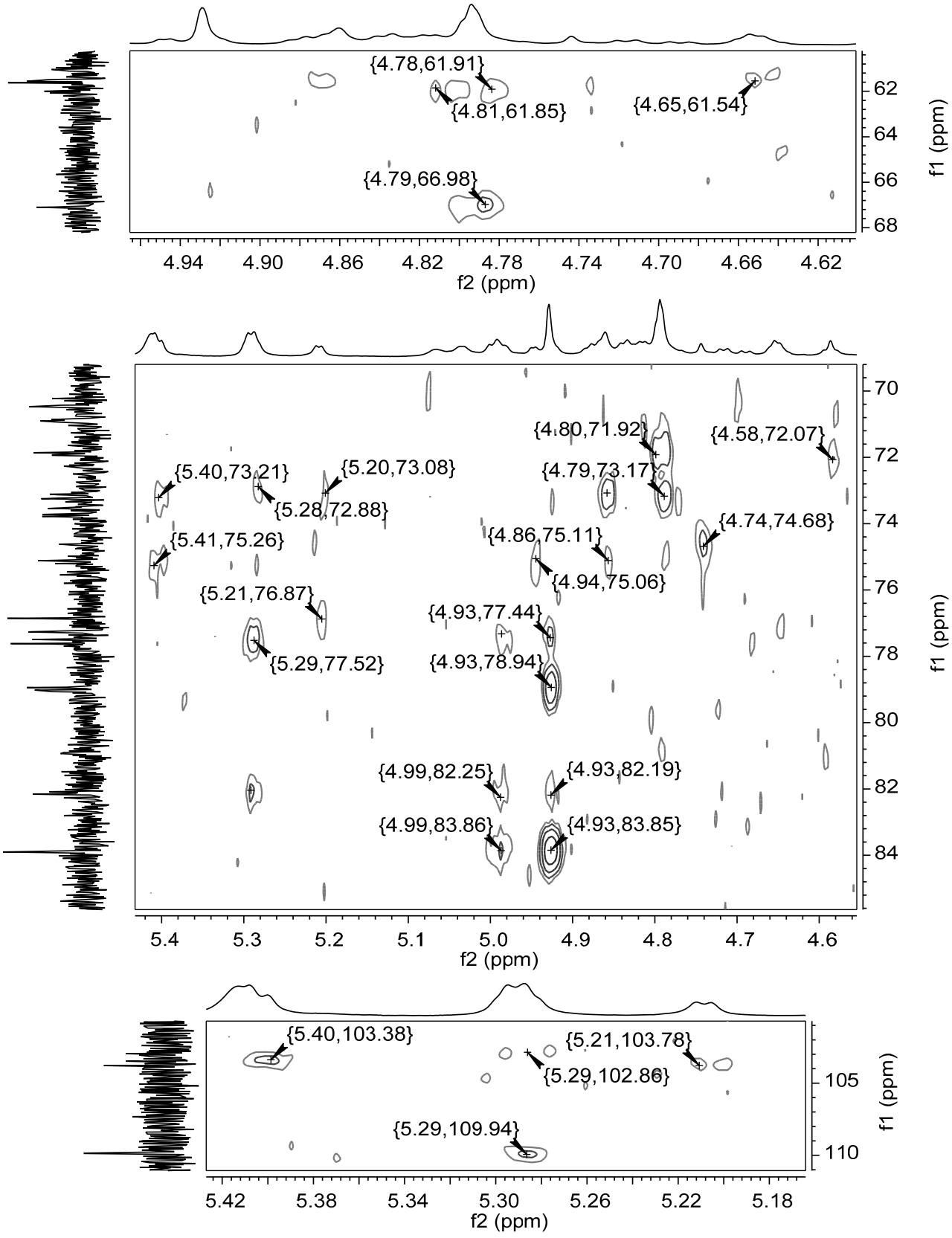

Figure S14. Results of the MALDI-MS analysis for compound **1** showing an *m/z* of 1218.117 corresponding to the sodium adduct of the compound in the (+) ionization mode.

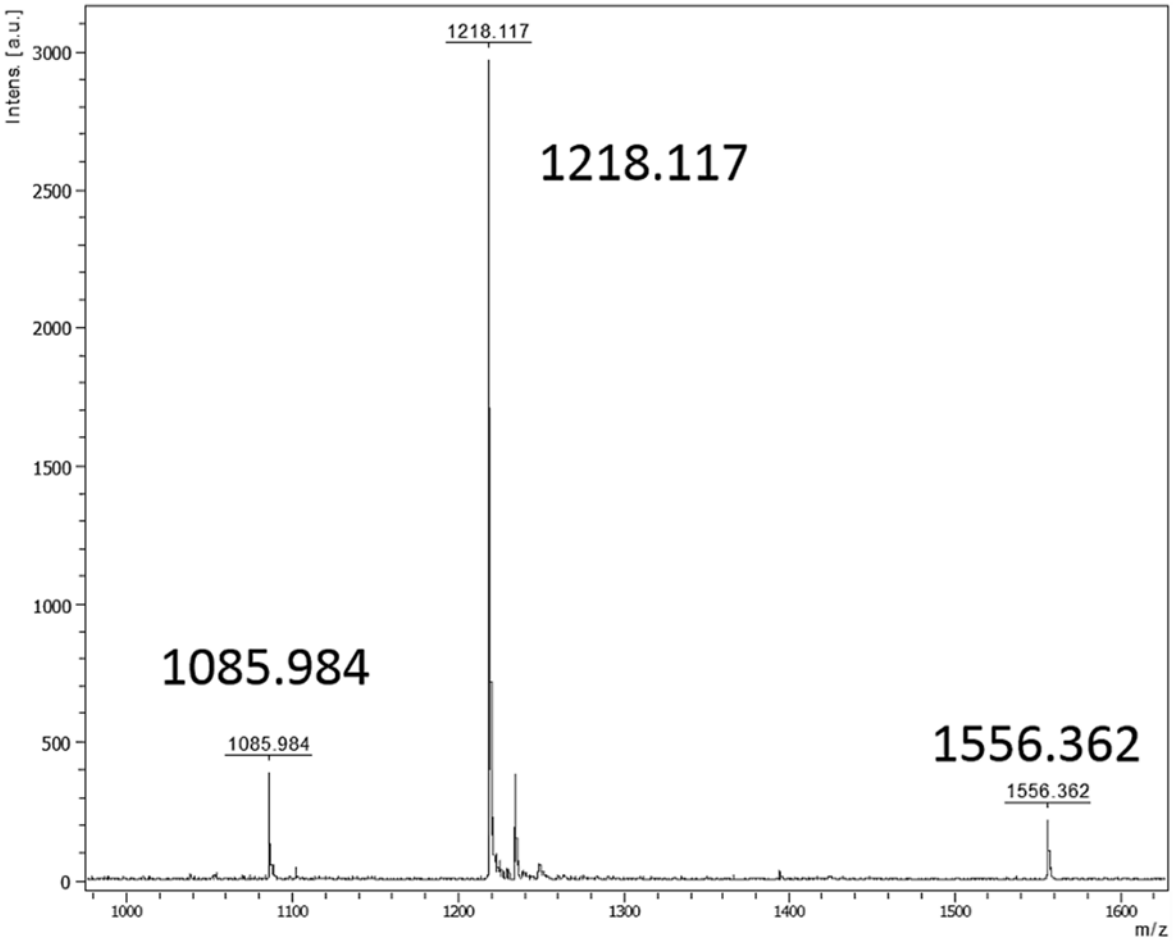

Figure S15. Results of the GC-MS analysis of the TMS derivatives of (*S*)-(+)-butyl glycosides of authentic standards D-Glc, L-Ara, D-Xyl and compound **1**.

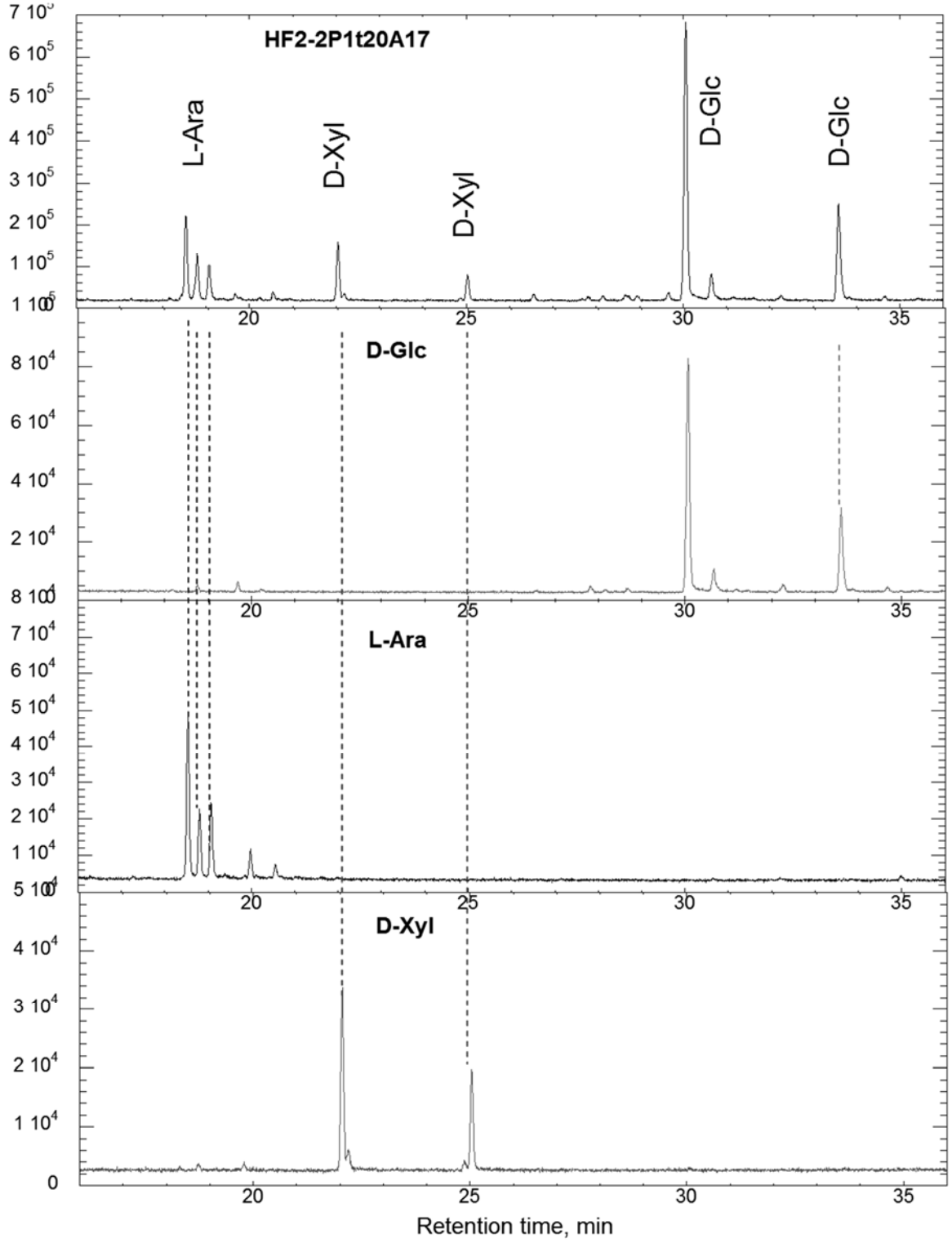

Figure S16. Analytical HPLC-ELSD comparison of cranberry material (CJ and CJA) and urine fractions (HF2-2 and HF1-1).

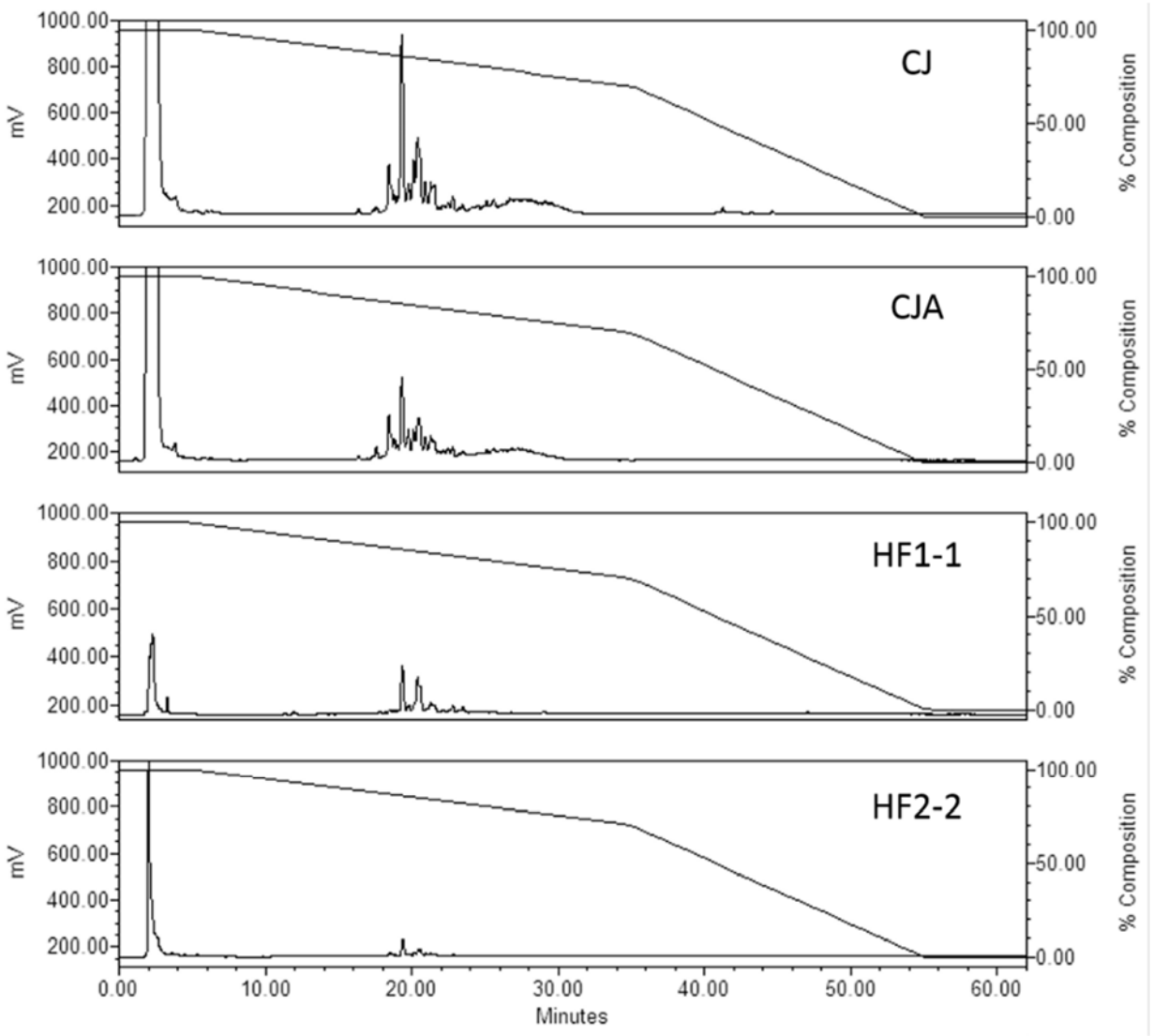

Figure S17. Comparison of the ^{1}H NMR spectra for major CJ-P1 oligosaccharide fractions, DMSO-d_6, 400 MHz.

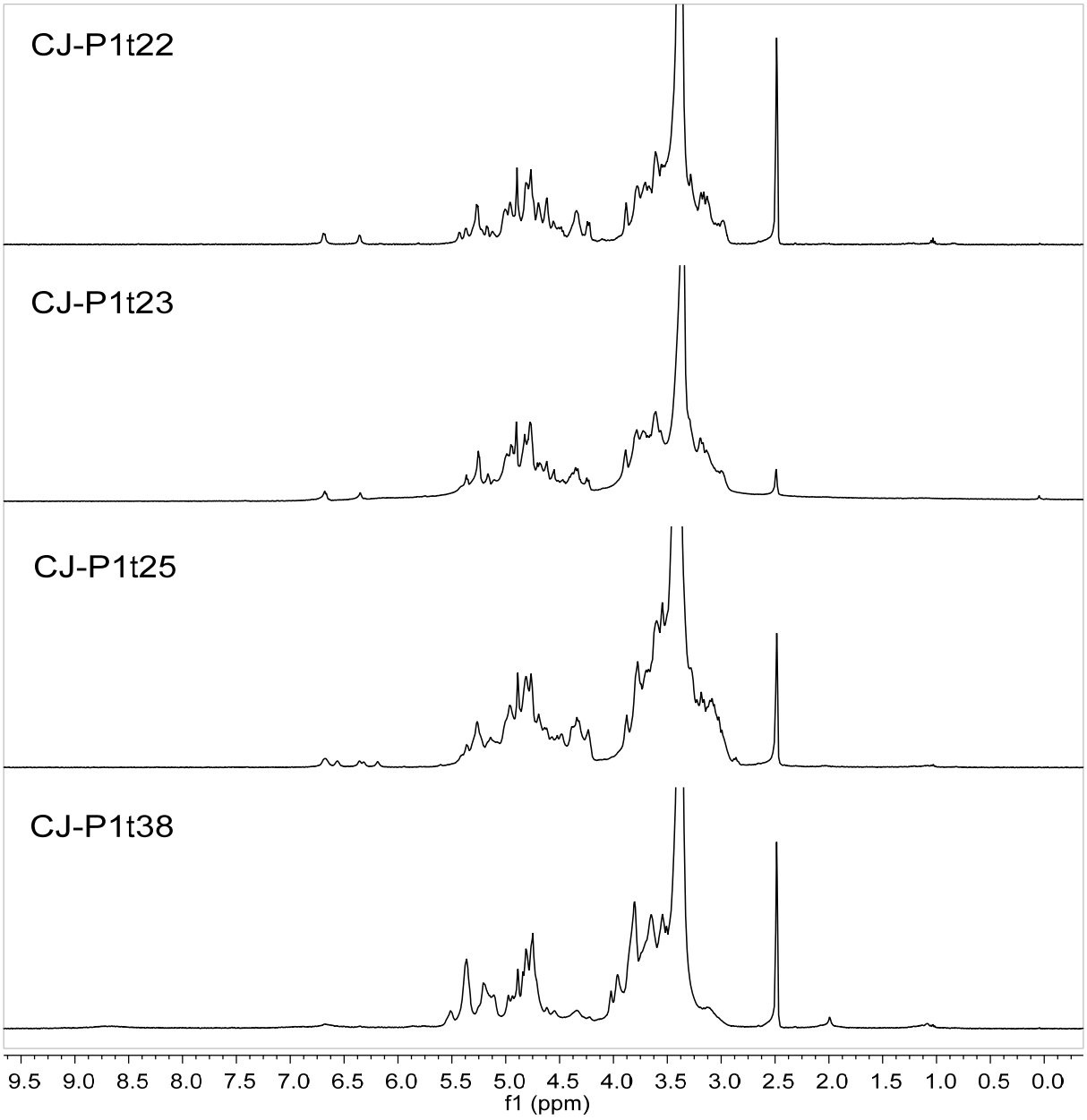

Supplementary Methods, Results and Discussion

This section of the Supporting Information provides additional details and discussion points not included in the main manuscript with the objective of aiding future investigations into the subject area of cranberry anti-adhesive urinary metabolites. Several Figures containing HPLC chromatograms also contain instrument data associated with those chromatograms. This data may include sample weight (g), dilution (µL), injection volume (µL), data input channel descriptions (SATIN = ELSD), acquisition dates and times, and acquisition method sets used. The same method set name does not always contain the same method but usually indicates the HPLC column used.

Section S1. Bioassay Scoring

a. Visual Agglutination Scoring

The microscopic evaluation for agglutination involved a visual assessment using a 0–4 scale (Table S6). For example, a visual agglutination score (VAS) of '0' represented 90–100% HRBC agglutination (Figure S18a) and therefore no inhibition of *E. coli* adhesion by the test sample, while a score of '4' represented 0–5% HRBC agglutination (Figure S18b) and total inhibition of *E. coli* adhesion by the test sample. Dilution endpoints were reported as the lowest dilution concentration at which the sample received a VAS of '1' or '2' with the next dilution receiving a VAS of '0' and having no anti-agglutination activity. Lower concentration dilution endpoints therefore indicated higher relative anti-agglutination activity.

b. Sample Relative Activity Scale

Assay results were interpreted using a qualitative scale similar to one previously published in association with this assay.[1] This scale assigned one of five assessments to each sample tested, based on four different criteria (Table S7). Scoring criteria were applied in the order shown to determine the probable activity of individual samples and assign a qualitative value. The majority of assignments were made based primarily on dilution endpoints, with secondary consideration given to the number of two-fold dilutions applied to each sample. The third and fourth criteria, involving the comparisons of fractions to parent materials or replicates, respectively, were considered but were given lower priority as they did not apply for all samples. Samples were assessed within an individual sample set test date and then across test dates. The dilution endpoints and number of two-fold dilutions for individual samples are discussed elsewhere.[2] Replicates were not available for most samples.

Table S6. Assignment Criteria for VAS Values Associated with UPEC-HRBC Agglutination.

VAS	HRBC Agglutination (%)	Inhibition of *E. coli* Adhesion by Test Sample (%)
0	90–100	0
1	60–90	10–40
2	30–60	40–70
3	5–30	70–95
4	0–5	95–100

Figure S18. Light microscope image of HRBC agglutination by *E. coli* in the presence of inactive (a) and active (b) samples.

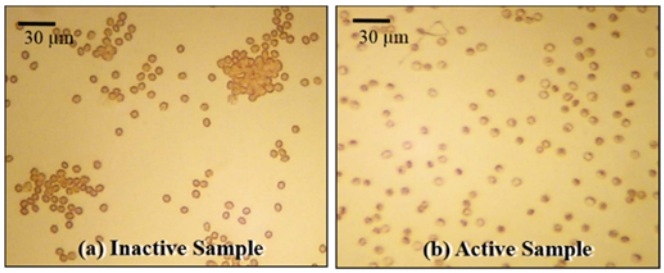

Table S7. Description of the Qualitative Scale Used to Interpret the Results Provided by the UPEC-HRBC Anti-Agglutination Assay.

Criteria:		First	Second	Third	Fourth
scale	assessment of sample activity	dilution endpoint range	no. of two-fold dilutions	sample compared to parent fraction:	replicates (if available):
+ +	active	< 10 mg/mL	5+	more active	show activity
+	probably active	10–30 mg/mL	4	more active	show activity
+/–	may or may not be active	30–60 mg/mL	3	about the same	may or may not show activity
–	probably not active	60–100 mg/mL	2	less active	show no activity
– –	not active	> 100 mg/mL	0, 1	less active	show no activity

Section S2. Characterization of Putative Active Components

a. Control Urine Extraction and Fractionation

Approximately 1.5 L raw control urine was centrifuged and filtered and the clarified urine (1.5 L) was extracted with EtOAc (2 x 375 mL). Both fractions were concentrated, diluted, and lyophilized as before. The aqueous fraction could not be successfully dried by lyophilization and instead produced a concentrated, viscous material with about 90–95% of the original water removed. A portion of this material (FC1, 15–20 mL, resulting from 250 mL of the concentrated aqueous fraction) was separated on a Sephadex LH-20 column (4 x 33 cm) using an isocratic 75% EtOH solvent system, a flow rate of 0.8–1.2 mL/min, and a collection time of 5 min/tube. Fraction composition was compared by TLC on silica (Sigma Aldrich silica gel 60, MeOH: EtOAc: water, 8:1:1, sprayed with ninhydrin) and tubes were combined to give three fractions, FC1-1 (3.539 g), FC1-2 (3.065 g), and FC1-3 (0.233 g). These three fractions were analyzed by analytical-scale reverse-phase HPLC (Atlantis dC_{18} sorbent) and NMR spectroscopy.

b. Analysis of FF and FA Fractions

The anti-agglutination assay data for the FF sample Sephadex LH-20 fractions (Table S1) led to methods that allowed for satisfactory enrichment of the active 1–2% of total urine material. Active fractions consistently eluted within the first 1–3 fractions of each Sephadex LH-20 column regardless of variations in column dimensions or EtOH percentages (Table S2). The total amount of active material enriched from the F urine samples accounted for ~0.7% of the starting material by weight, giving an estimated starting urine concentration for active metabolites of less than 0.14 mg/mL raw urine. Some of this material was used for method development and fraction characterization without success. Remaining anti-adhesive urine fractions from the five separate Sephadex LH-20 columns of the FF material were combined to give F Actives (FA; 1.75 g). This material was separated on Sephadex LH-20 (Table S3), to give five fractions: FA1 (0.030 g), FA2 (0.887 g), FA3 (0.270 g), FA4 (0.124 g), and FA5 (0.116 g). All FA fractions were submitted to bioassay and half of the recovered amount for fraction FA1 was required to improve the reliability of test results. LC-MicroTOF-MS of both FA1 and FA2 gave inconclusive results (not shown) regarding possible fraction composition. LC-MicroTOF-MS spectra were acquired with a Bruker MicroTOF-Agilent LC 1100 series instrument using a Phenomenex Luna C_8 column (4.6 x 150 mm) at 27 ^{o}C, with a flow rate of 0.4 mL/min and a 20 min gradient from 20–100% MeCN or MeOH with 0.1% formic acid.

The remaining amount of fraction FA1 was used primarily for analytical HPLC separations and comparative analyses due to its limited quantity. Method development with FA1 and FA2 used HPLC-UV with HILIC and XTerra MS C_{18} sorbents and various solvent systems with no success. In an example separation (Figure S19) the material eluting at ~270 min appears to be a major component of the FA1 sample with the scale used, but actually has a relatively low absorbance (0.07 AU), and would normally be considered part of a baseline. A preparative HILIC method similar to the one shows for these analytical separations was used to isolate the detectable components from the FA2 sample, especially those corresponding to the FA1 sample. All fractions isolated from FA1 and FA2 using UV detection, however, gave inconclusive or negative anti-adhesion assay results when submitted (data not shown).

Method development using remaining FA1 material led to attempts to use evaporative light scattering detection (ELSD) for monitoring HPLC elution of active fraction components. ELSD provided clear evidence that compounds were present in FA1 that lacked chromophores and therefore could not be detected by UV. Purification and structure elucidation for the UV-transparent compounds present in FA1 was impractical due to material limitations, but the same profile of compounds was present in HF1-1 and other active sub-fractions (Table S8).

c. Comparisons of Active Fractions to Control Urine Fractions and Standards

Analytical HPLC-ELSD spectra for FC1 Sephadex LH-20 fractions (Figure S20) were collected using the same HPLC-ELSD method as applied to HF1-1. Baseline expansions of the region of interest (18-24 min) for Fraction FC1-1 show no evidence of possible oligosaccharide components. The components visible in this region for FC1-1 and FC1-3 contain chromophores detectable by UV.

Active urine fractions FA1 and FA2 were compared to standards of various compounds via TLC. Standards used included galacturonic acid, apple pectin, D-glucose, sucrose, fructose, corn starch, sodium citrate, epicatechin, and various PAC oligomers. Samples were spotted on silica gel 60 TLC plates and dried. Plates were developed using various TLC spray reagents, including ninhydrin, *p*-anisidine HCl, *p*-anisidine phthalate, diphenylamine in 10% EtOH, bromocresol green, vanillin, *p*-anisaldehyde with sulfuric acid, and others. Results (not shown) indicated the possible presence of carbohydrates or amino sugars and the absence of flavonoids, amino acids, lipids, or other compounds that could be indicated by TLC color reactions.

Analytical HPLC-ELSD chromatograms of carbohydrate standards (the monosaccharides glucose and fructose, and the disaccharide sucrose), using the optimized method applied to HF1-1, indicated that all three compounds eluted with 100% water before 5 min. These compounds were therefore not significantly retained by the C_{18} sorbent of the Atlantis dC_{18} column. Compounds such as these low-MW carbohydrates also elute at later retention times from gel-filtration chromatography sorbents such as Sephadex LH-20. In contrast, the oligosaccharide mixtures of interest from both cranberry and urine samples eluted near the void volume from the Sephadex LH-20 sorbent, indicating larger MW, and at ca. 20 min on the Atlantis dC_{18} analytical column with the method shown here, indicating retention on the specialized C_{18} sorbent of the column. The Waters Atlantis dC_{18} sorbent is designed for isolation methods using 100% water and is intended for separations of polar, neutral compounds.[3]

^{1}H NMR data comparisons between active fractions and various monosaccharides (glucose, fructose, sucrose), glucuronic acid, and pectin (Figure S21), indicated that active fractions contained resonances most similar to those of pectin, with less apparent complexity.

d. Isolation Method Development

Samples of H and I Sephadex LH-20 fractions were assessed by analytical HPLC-ELSD to determine their composition prior to preparative and semi-preparative HPLC separations.

Comparisons of the HPLC-UV/ELSD spectra of active and inactive H and I urine sample fractions were used to guide isolation efforts (Figures S22-S26). The HF2 fraction series (Figures S24-S26) is representative of the HPLC-ELSD chromatographic profiles observed for the HF and IF Sephadex LH-20 column fractions.

Method development for HPLC separations was pursued under the new paradigm that the target compounds were carbohydrates with consideration given to the information obtained from previous separations.[2] The methods used for purification could not be changed completely without sacrificing the information obtained from previous separations and analyses of bioactive fractions. Purification for all components of the UV-transparent mixture was attempted, but these efforts were complicated by many factors related to the structural nature of the compounds, the complexity of the mixture, the physical limitations of the chromatographic systems used, and the overall resources available for the project. Fractions collected based on UV-detection were submitted to the bioassay but yielded negative or inconclusive results (data not shown).

Figure S19. Analytical HPLC-UV (210 and 256 nm) chromatograms of fractions FA1 and FA2 (HILIC).

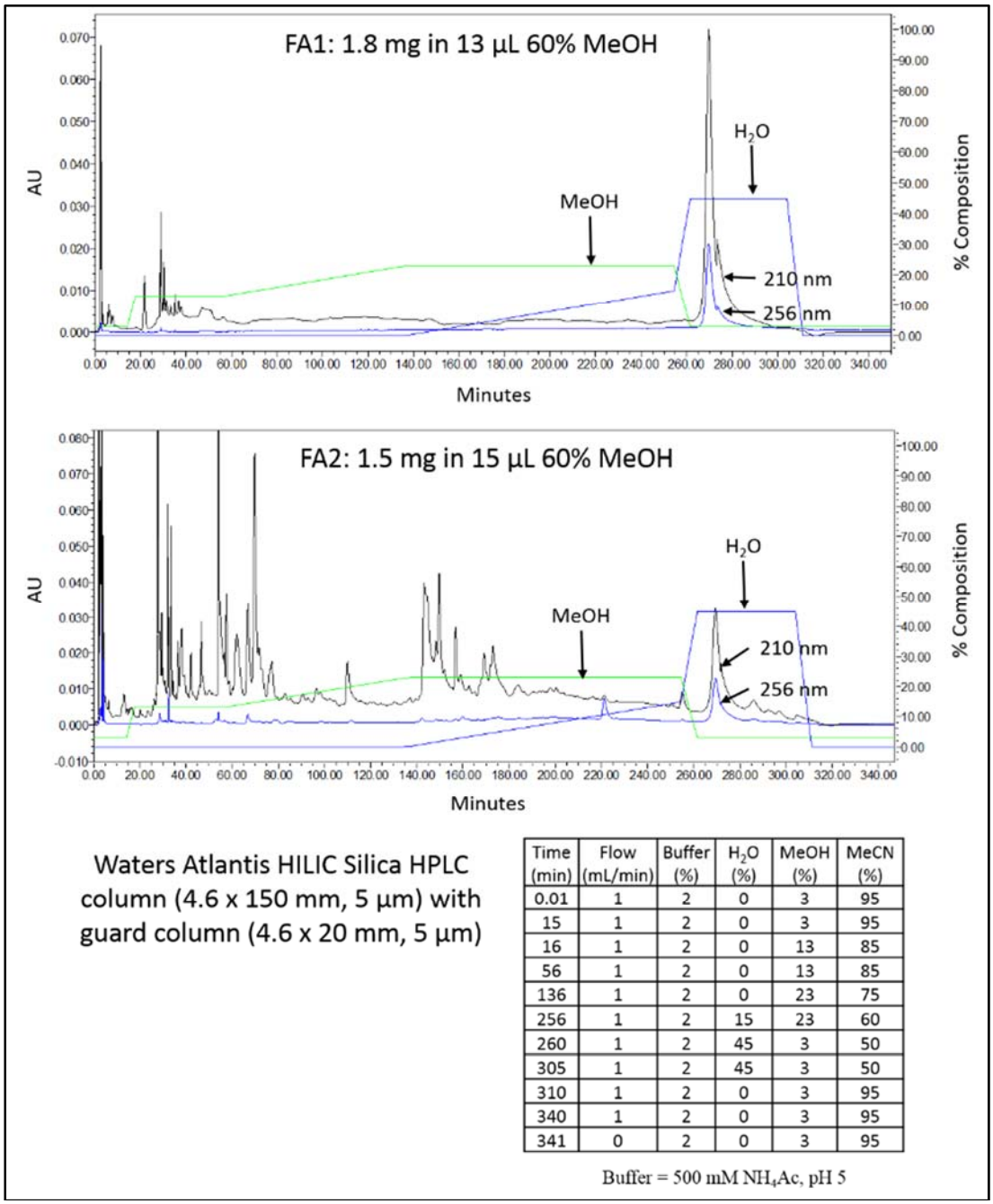

Time (min)	Flow (mL/min)	Buffer (%)	H_2O (%)	MeOH (%)	MeCN (%)
0.01	1	2	0	3	95
15	1	2	0	3	95
16	1	2	0	13	85
56	1	2	0	13	85
136	1	2	0	23	75
256	1	2	15	23	60
260	1	2	45	3	50
305	1	2	45	3	50
310	1	2	0	3	95
340	1	2	0	3	95
341	0	2	0	3	95

Buffer = 500 mM NH_4Ac, pH 5

Figure S20. Comparisons of the analytical HPLC-ELSD spectra for active urine fraction HF1-1 and control urine fractions (FC1-1, FC1-2, and FC1-3) (Atlantis dC_{18}).

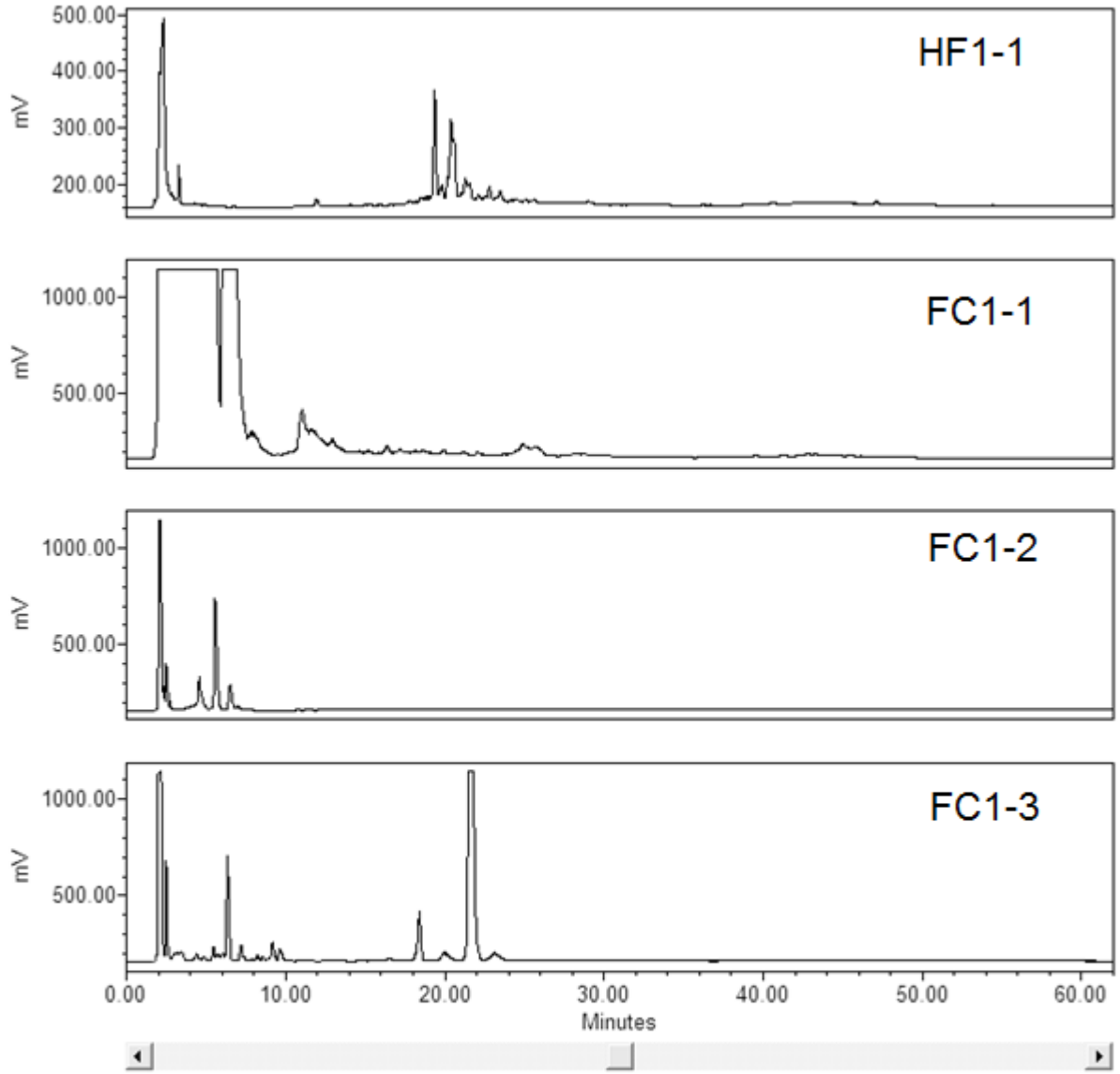

Visible	SampleName	SampleWeight	Dilution	Injection Volume (uL)	Channel Name	Date Acquired	Acq Method Set
☑	HF1-1 AtldC18A R1	2.60000	100.00000	20.00	SATIN	9/15/2010 12:49:50 PM CDT	AtldC18 A
☑	FC1-1-Liq AtldC18A R1	1.00000	300.00000	50.00	SATIN	9/15/2010 12:41:55 AM CDT	AtldC18 A
☑	FC1-2 AtldC18A R1	14.70000	300.00000	20.00	SATIN	9/15/2010 8:16:53 AM CDT	AtldC18 A
☑	FC1-3 AtldC18A R1	12.10000	300.00000	25.00	SATIN	9/15/2010 9:47:49 AM CDT	AtldC18 A

Figure S21. ^{1}H NMR spectrum for apple pectin reference material (Sigma Aldrich), D_2O, 400 MHz.

The overlapping resonances between 3–5.5 ppm are indicative of numerous monomeric carbohydrate substituents with similar chemical shift values.

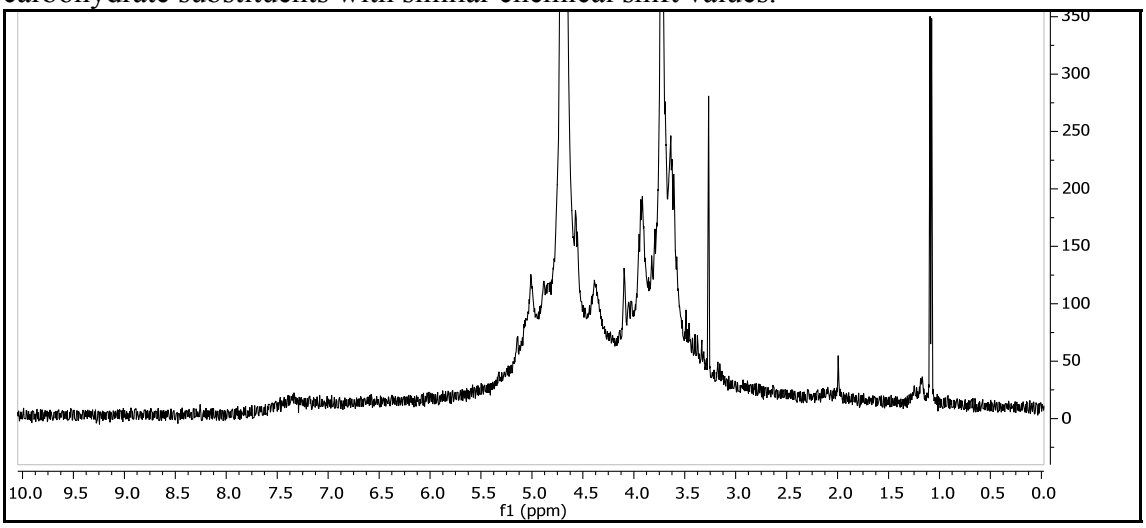

Figure S22. Analytical HPLC-ELSD chromatograms for IF1-1, IF1-2, and IF1-3 (Atlantis dC_{18}).

This set of chromatograms shows that the components of interest (box, 18–28 min) were readily detectable in Sephadex LH-20 fractions IF1-2 and IF1-3 but could only be detected at trace levels in fraction IF1-1.

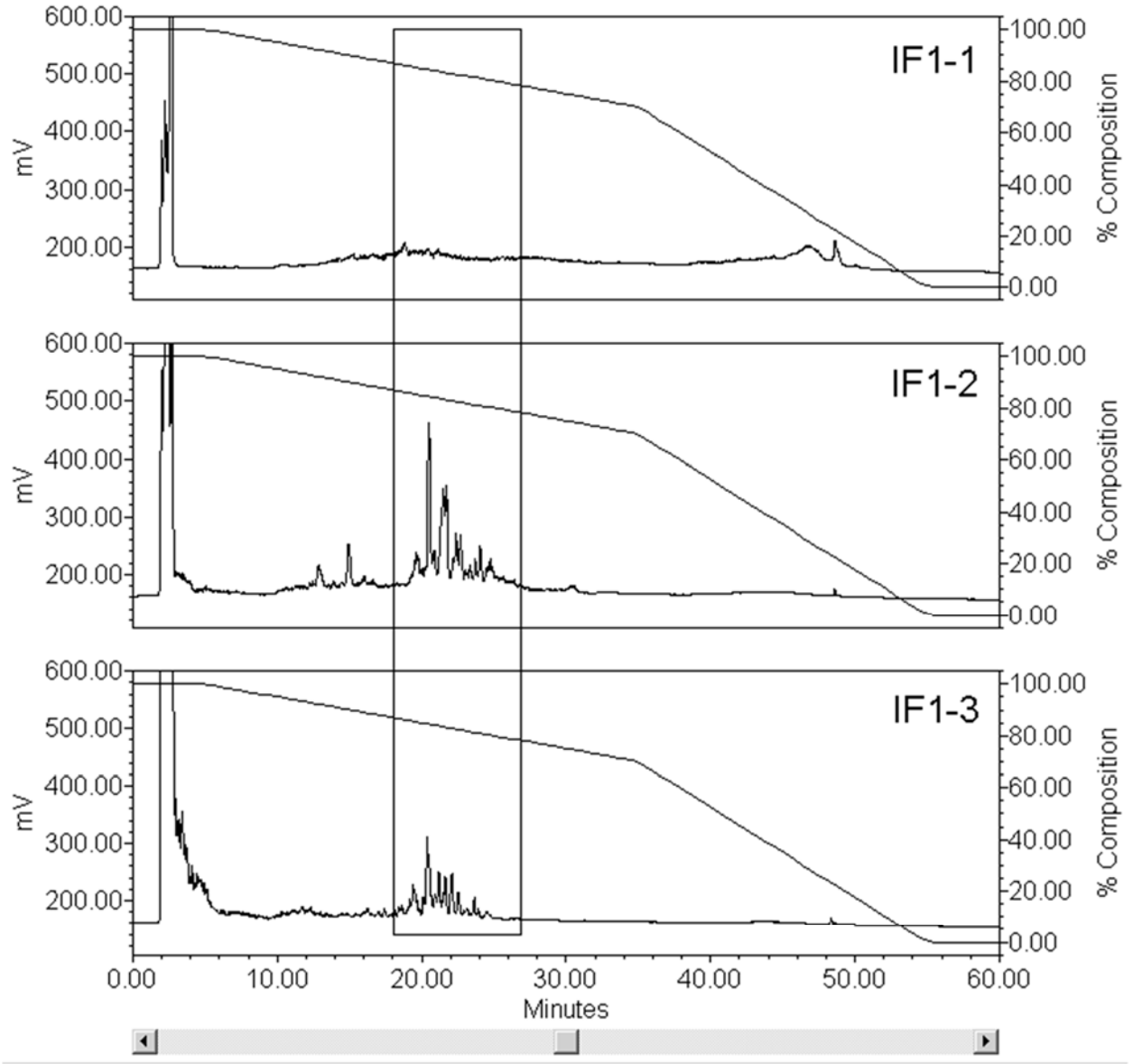

Visible	SampleName	SampleWeight	Dilution	Injection Volume (uL)	Date Acquired	Acq Method Set	Processed By	Channel
☑	IF1-1 AtldC18-A R3	2.80000	280.00000	50.00	7/9/2009 5:11:09 AM CDT	AtldC18 A	Christina	SATIN
☑	IF1-2 AtldC18-A R3	2.70000	270.00000	50.00	7/9/2009 6:47:22 AM CDT	AtldC18 A	Christina	SATIN
☑	IF1-3 AtldC18-A R1	2.50000	250.00000	50.00	7/9/2009 8:23:36 AM CDT	AtldC18 A	Christina	SATIN

Figure S23. Analytical HPLC-UV (Max-Plot) chromatograms for IF1-1, IF1-2, and IF1-3 (Atlantis dC_{18}).

This set of chromatograms shows that the components of interest in the IF fractions (box, 18–28 min) lacked chromophores.

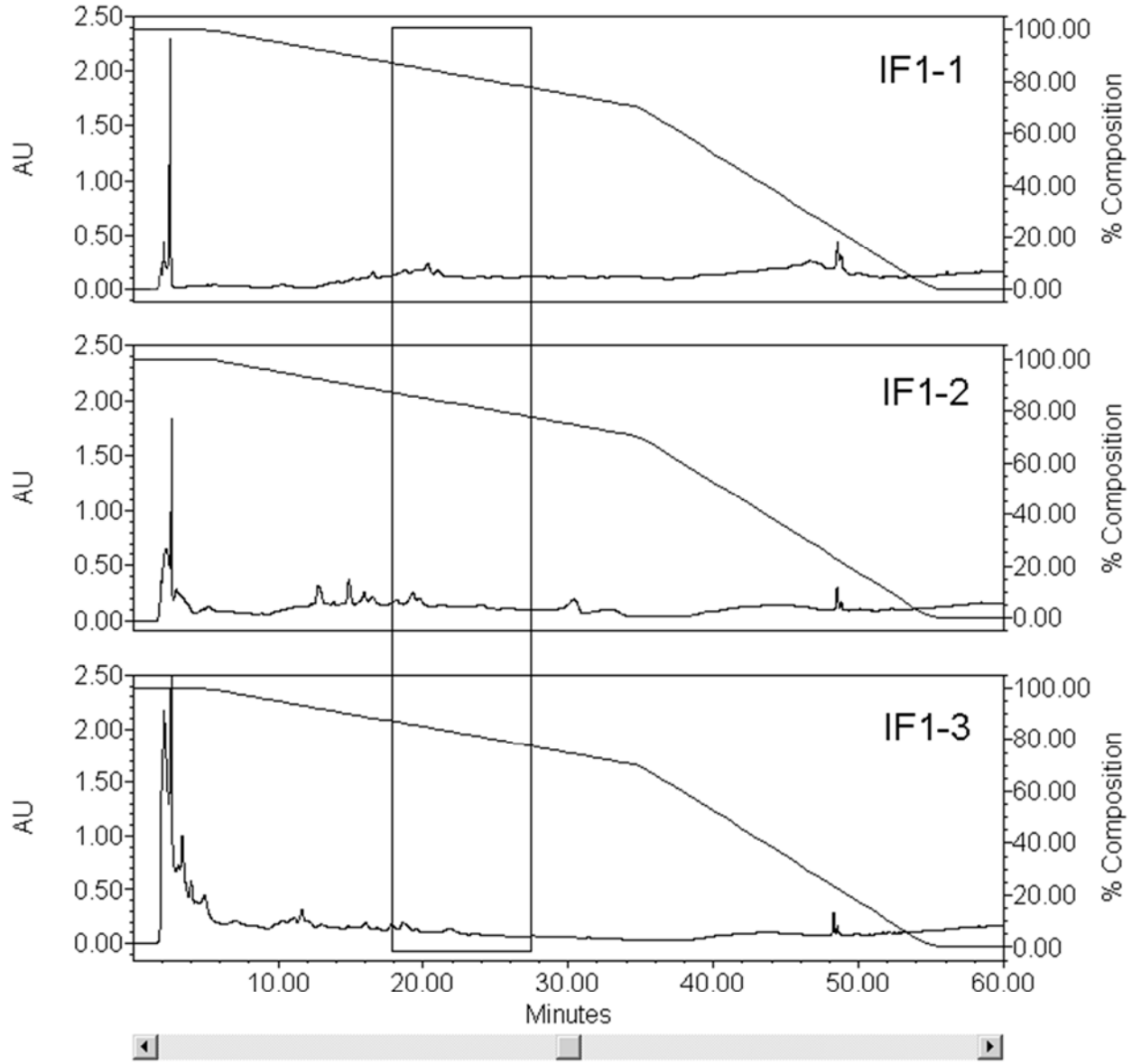

Visible	SampleName	SampleWeight	Dilution	Injection Volume (uL)	Date Acquired	Acq Method Set	Channel Name
☑	IF1-1 AtldC18-A R3	2.80000	280.00000	50.00	7/9/2009 5:11:09 AM CDT	AtldC18 A	MaxPlot 210.0 to 400.0
☑	IF1-2 AtldC18-A R3	2.70000	270.00000	50.00	7/9/2009 6:47:22 AM CDT	AtldC18 A	MaxPlot 210.0 to 400.0
☑	IF1-3 AtldC18-A R1	2.50000	250.00000	50.00	7/9/2009 8:23:36 AM CDT	AtldC18 A	MaxPlot 210.0 to 400.0

Figure S24. Analytical HPLC-ELSD chromatograms for HF2-1, HF2-2, and HF2-3 (Atlantis dC_{18}).

This chromatogram set shows that the components of interest (18–24 min, box) were predominantly present in Sephadex LH-20 fraction HF2-2 with trace amounts present in fractions HF2-1 and HF2-3.

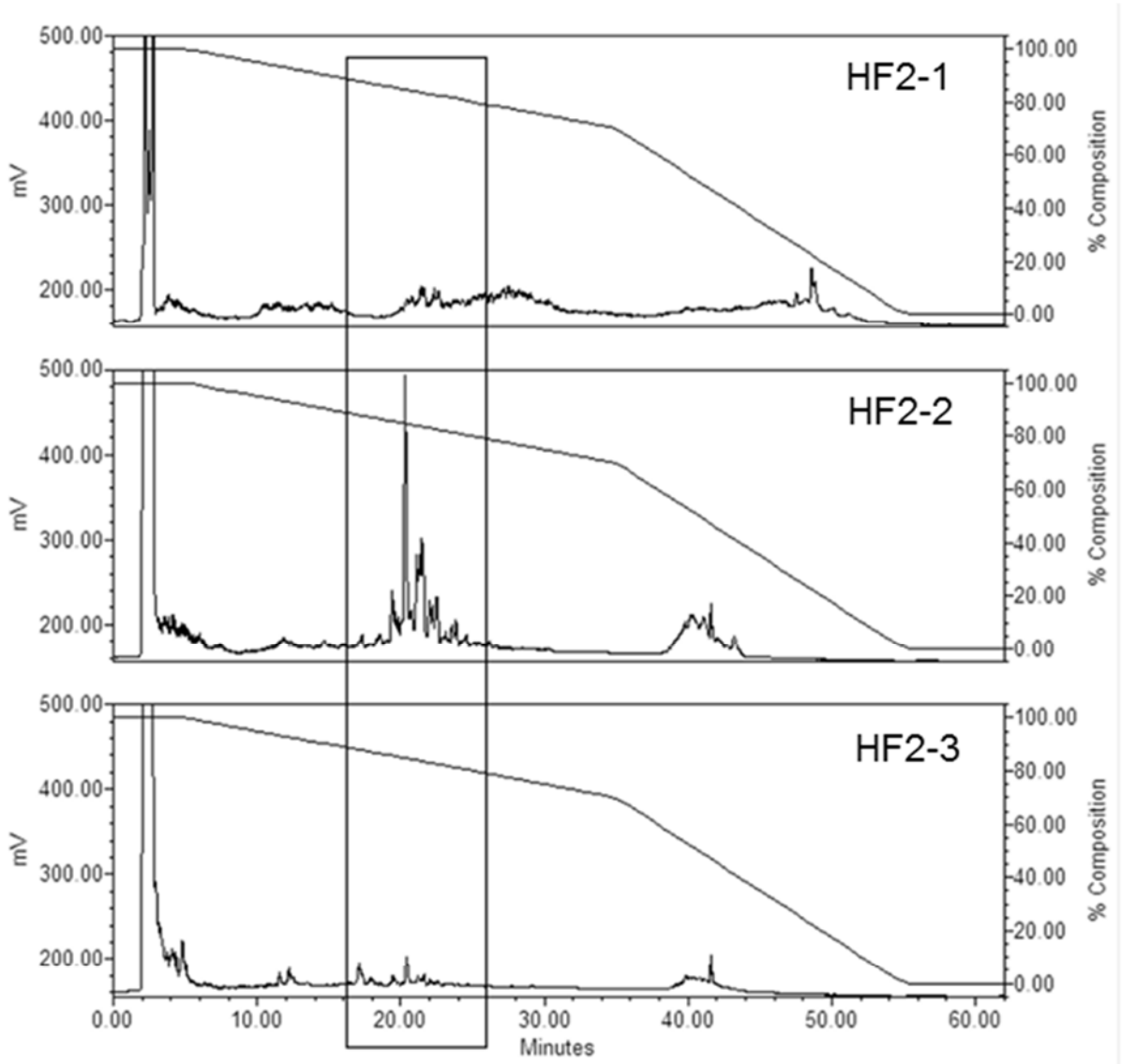

Visible	SampleName	SampleWeight	Dilution	Injection Volume (uL)	Channel Name	Date Acquired	Acq Method Set
☑	HF2-1 AtldC18-A R2	2.40000	240.00000	50.00	SATIN	7/9/2009 12:22:28 AM CDT	AtldC18 A
☑	HF2-2 AtldC18-A R3	2.40000	240.00000	50.00	SATIN	7/8/2009 9:45:57 PM CDT	AtldC18 A
☑	HF2-3 AtldC18-A R3	2.40000	240.00000	50.00	SATIN	7/8/2009 11:02:11 PM CDT	AtldC18 A

Figure S25. Analytical HPLC-ELSD chromatograms for HF2-2, HF2-3, HF2-4 and HF2-5 (Atlantis dC_{18}).

This chromatogram set shows that the components of interest (22–28 min) present in Sephadex LH-20 fraction HF2-2 were detected at trace levels in fraction HF2-3, and were not detected in fractions HF2-4, and HF2-5.

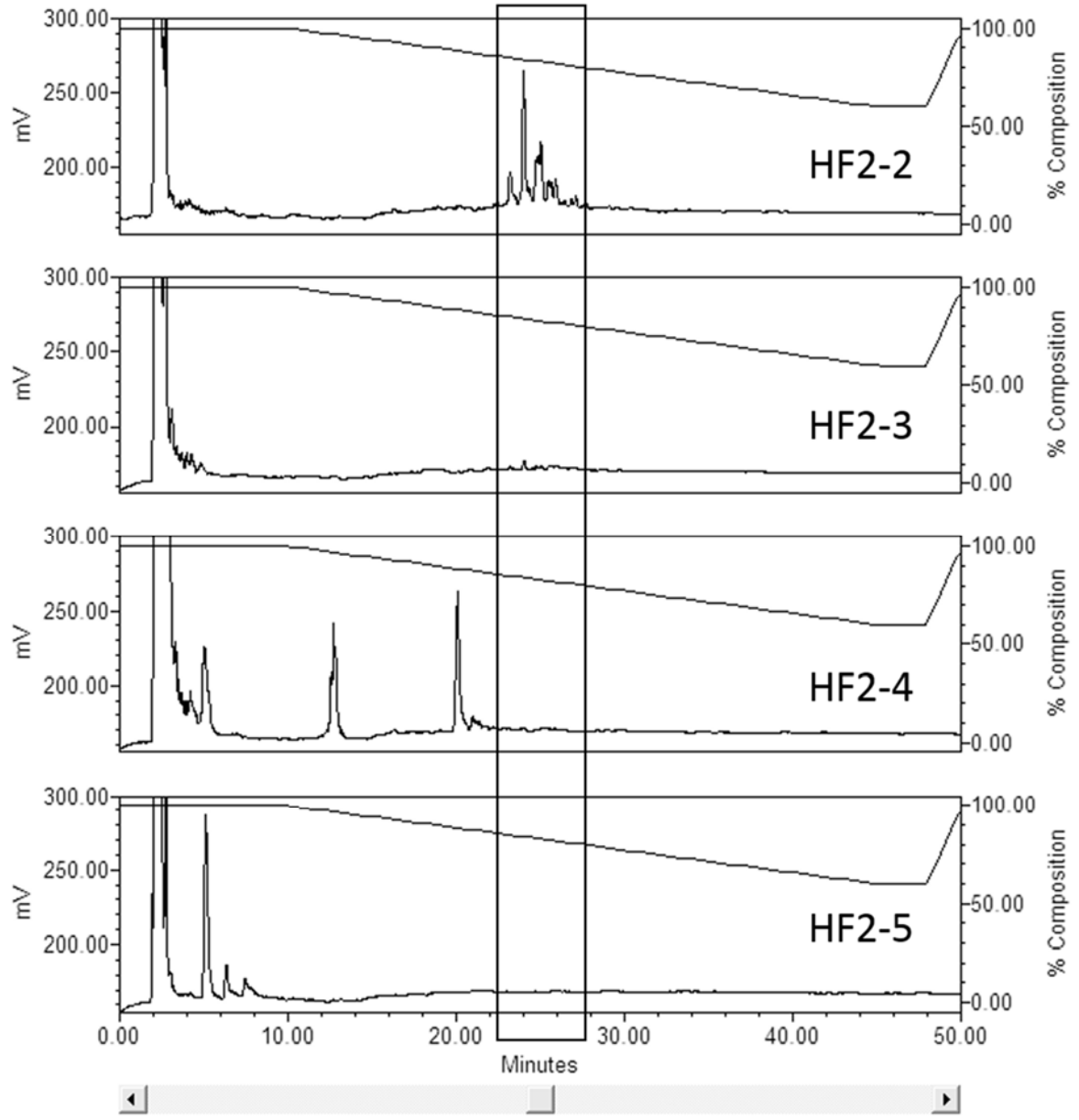

Visible	Vial	SampleName	Date Acquired	SampleWeight	Dilution	Injection Volume (uL)	Acq Method Set	
☑	5	HF2-2 AtldC18-A R2	7/5/2009 6:51:24 AM CDT	2.40000	240.00000	20.00	AtldC18 A	7/
☑	6	HF2-3 AtldC18-A R2	7/5/2009 7:57:37 AM CDT	2.40000	240.00000	20.00	AtldC18 A	7/
☑	9	HF2-4 AtldC18-A R2	7/5/2009 11:16:22 AM CDT	2.00000	200.00000	50.00	AtldC18 A	7/
☑	10	HF2-5 AtldC18-A R2	7/5/2009 12:22:27 PM CDT	4.00000	200.00000	10.00	AtldC18 A	7/

Figure S26. Analytical HPLC-UV (Max Plot) chromatograms for HF2-2, HF2-3, HF2-4 and HF2-5 (Atlantis dC_{18}).

This chromatogram set shows that the components of interest (22–28 min) present in Sephadex LH-20 fraction HF2-2 were not detectable by UV and the HF2-2 fraction could not be readily distinguished from the other fractions using only UV detection.

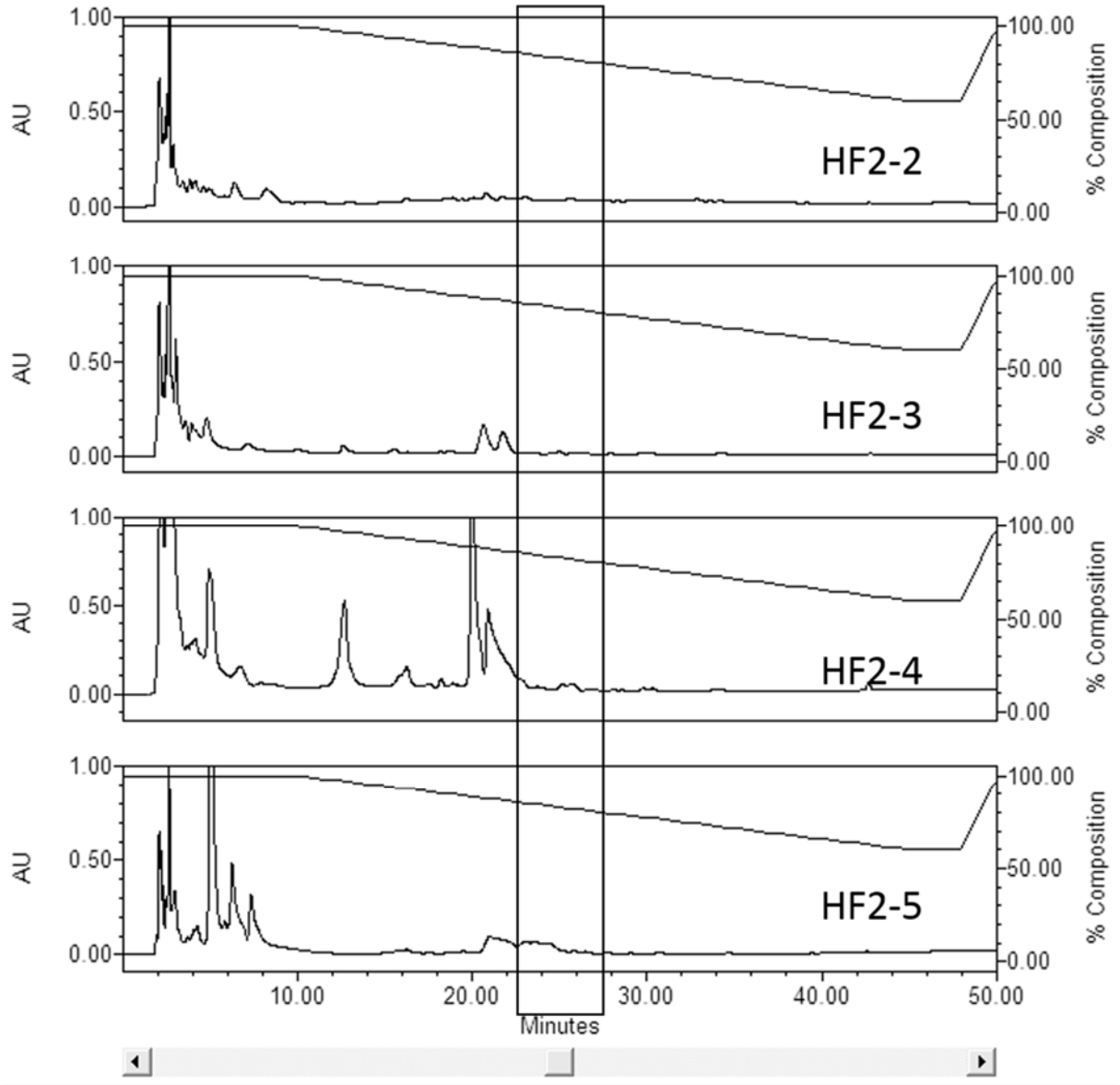

Visible	Vial	SampleName	Date Acquired	Acq Method Set	Injection Volume (uL)	Channel Name	Manua
☑	5	HF2-2 AtldC18-A R2	7/5/2009 6:51:24 AM CDT	AtldC18 A	20.00	MaxPlot 210.0 to 400.0	☐
☑	6	HF2-3 AtldC18-A R2	7/5/2009 7:57:37 AM CDT	AtldC18 A	20.00	MaxPlot 210.0 to 400.0	☐
☑	9	HF2-4 AtldC18-A R2	7/5/2009 11:16:22 AM CDT	AtldC18 A	50.00	MaxPlot 210.0 to 400.0	☐
☑	10	HF2-5 AtldC18-A R2	7/5/2009 12:22:27 PM CDT	AtldC18 A	10.00	MaxPlot 210.0 to 400.0	☐

Section S3. Separation of Putative Active Components

a. Preparative Atlantis dC_{18} HPLC-ELSD Methods and Results

Selected Sephadex LH-20 fractions (Tables S8-S10) were determined to contain the components of interest and were separated by preparative HPLC on the Atlantis dC_{18} sorbent. Selected Atlantis dC_{18} fractions (Table S11) were further separated using semi-preparative HPLC on the Polyamine II sorbent. Samples were separated on the dates shown, and chromatographic separations with the same date were often performed back-to-back within a single session to minimize instrument variability between separations and provide comparable retention times. Insufficient amounts of most fractions of interest were obtained from the Polyamine II separations (Table S12) although available data indicated that these fractions contained various oligosaccharide-type compounds.

The majority of the HF1-1, HF1-2, and HF1-3 samples were used for method development. Attempts were made to resolve the components of these fractions using direct injection onto both Waters X-Terra MS-C_{18} (XTMSC18) and Polyamine II semi-preparative columns with both PDA and/or ELS detection, but were unsuccessful at yielding pure compounds. The fractions collected from these separations were not combined with later materials due to the differences in the chromatographic methods used.

Direct separation of HF1-1 via several different semi-preparative methods during the method development process yielded two fractions of interest, HF1-1P1t34 and HF1-1P1t36 (Figure S27). These were obtained from a series of semi-preparative injections on the Atlantis dC_{18} column using a variation of the final solvent method chosen. Both were complex mixtures, but later comparisons of the ^{1}H NMR spectra for these fractions to that of HF2-2P1t22 indicated that both fractions also contained oligosaccharides (Figure S28). Analysis of the parent material HF1-1 by ^{1}H and COSY NMR in D_2O (Figure S29), and retrospective comparisons to data collected for both HF2-2P1t20 and the cranberry oligosaccharides in both NMR solvents, further indicated that major components of HF1-1 and both fractions were also oligosaccharides. Other components of this mixture appeared similar in HPLC elution profile to those of HF2-1+IF1-1 (see below) but could not be isolated.

Similar variations of optimized methods were used for all subsequent preparative separations and the results are discussed in the Main Text with additional details included here (Tables S8-S13; Figures S30 and S31). H and I fractions were initially kept separate with the goal of identifying and comparing the components from both source animals. As isolation efforts

proceeded, however, analytical chromatographic profiles indicated that the components of both samples were similar, and selected fractions from both materials were combined (Figure 6, Main Text). Aliquots of fractions that were available in lower quantities were co-injected with samples from more abundant fractions to aid in the alignment of peaks, to account for instrument variations between separations, and to account for possible sample matrix effects. Retention times were similar across reversed-phase preparative separations and chromatographic resolution was not significantly affected by slight variations in injection volumes or sample injection amounts.

Attempts at method optimization during preparative separations led to several minor method variations. The method for HF2-2 Run 1 (R1) (not shown) used 5 min at 100% water, a 30 min gradient to 30% MeOH, and a 20 min gradient to 100% MeOH. The ELSD conditions were adjusted for HF2-2 R1; initial conditions were an evaporator temperature of 100 ºC, a nebulizer temperature of 50 ºC, and a gas flow rate of 1.0 SML. At 40 min into the separation, corresponding to 50% MeOH, the evaporator temperature was changed to 90 ºC to account for the increase in the percentage of organic solvent. This modification did not improve detector resolution, and changes to the evaporator temperature were not made in subsequent separations. The method for HF2-2 R2–R6, IF1-2 R1, and IF1-3 R1–R3 (Figures S30 and S31) used 5 min at 100% water, a 30 min gradient to 20% MeOH, and a 10 min gradient to 100% MeOH. The ELSD conditions for these separations were maintained at an evaporator temperature of 100 ºC, a nebulizer temperature of 50 ºC, and a gas flow rate of 1.0 SML.

The Sephadex LH-20 fractions of interest ultimately yielded the series of oligosaccharides discussed in the Main Text. Selected fractions of the Atlantis dC_{18} preparative separations were combined across different parent materials and further separated on the Polyamine II sorbent (Tables S9-S11 and Figure 6, Main Text). Fractions from the IF1-2 separation were combined with those of HF2-2 to give HF2-2P1 subfractions, and fractions from the IF1-3 and HF1-2 separations were combined to give IF1-3P1 subfractions. Subfractions HF2-2P1t20 and IF1-3P1t20 were combined into fraction HF2-2P1t20 (28.8 mg), and IF1-3P1t22, IF1-3P1t23 and IF1-3P1t23.5 were combined into fraction IF1-3P1t22 (9.3 mg), while HF2-2P1t22 (17.1 mg) was not combined with another fraction. Both 1D and 2D NMR data were acquired for HF2-2P1t20 and HF2-2P1t22 samples (Figures S32 and S33, Figure 14, Main Text). The HF2-2P1t20 sample was later determined to contain a single dominant component (compound **1**) while HF2-2P1t22 was determined to contain a mixture of components. The

anomeric, oxymethylene, and glycosyl ring regions are indicated for the HF2-2P1t22 spectrum (Figure 14, Main Text). Consideration of the anomeric regions of the ^{13}C and ^{1}H NMR spectrum for HF2-2P1t20 (Figures S32 and S33) and consideration of the 2D NMR data for both HF2-2P1t20 and HF2-2P1t22, led to the refined working hypothesis that the carbohydrates of interest were oligosaccharides with 7-9 monomeric units. It was later determined that a reducing glucosyl unit was responsible for two of the anomeric resonances and that two high intensity anomeric resonances were duplicate resonance sets corresponding to two Xyl and two Ara residues. See Main Text for additional discussion.

Separations of HF2-1+IF1-1 via similar methods as those given for the HF2-2 series did not result in sufficient quantities of pure components, and there were insufficient amounts of the resulting fractions mixtures for further investigations. Separation of HF2-1+IF1-1 (Table S13) yielded a major fraction (HF2-1P1t40) which was a complex mixture that appeared to have UV absorbance for some components at 215 nm (Figure S34) but not 254 nm (data not shown). ^{1}H NMR spectroscopy of 8 mg this mixture in DMSO-d_6 (Figure S35) yielded a spectrum that resembled those of FA1 and HF1-1 (Figure 3, Main Text), with a few weak resonances in the aromatic/amide regions (6.5-7.2 ppm), resonances in the aliphatic region (0.5-2.5 ppm), and resonances characteristic of glycans (3-5 ppm). The possible identities of these components could not be determined with the data available. As the HPLC fractions produced using UV detection from earlier active materials, FA1, FA2, and previous studies (e.g., D and E urine samples),[2] had shown negative or inconclusive results when tested in the bioassay (see Section 2), further investigation was not pursued as a priority.

The HI series of samples shown in Figure 6 (Main Text) was prepared in 2010, after the structure of compound **1** and been determined by combining the remaining reference material that had been set aside for each of the parent Sephadex LH-20 fractions. These materials were recombined based on their HPLC-ELSD and ^{1}H NMR profiles with the objective of obtaining a sufficient quantity for bioassay testing (Table 2, Main Text). All three samples (HI1+HI2+HI3) were later additionally combined and separated by the Atlantis dC_{18} preparative HPLC methods previously used to obtain compound **1** (Figure S36). The eluting fractions were divided into retention time blocks (t00-11, t11-12, t12-16, t16-19, t19-22, t22-30, and t30-50 min) based on the ELSD chromatogram. For each block fraction, 20-50 mg was submitted in duplicate to the bioassay in randomized, coded vials. Most fractions appeared to show some level of detectable anti-adhesion activity, but the results across replicates were inconsistent (e.g., a given sample

would result in a 2-4x higher dilution end-point than its duplicate). Fraction t00-11 was the only fraction that had a duplicated negative (inactive) result. This lack of bioassay reproducibility and sensitivity made it impossible to determine which chromatographic region contained the compounds with the highest anti-adhesion properties. The majority of the remaining fraction material was used in this final effort to assign bioactivity to the various components of the urinary fractions of interest and no further studies could be done.

Table S8. Details of Preparative-Scale Sample Preparations for Selected Atlantis dC_{18} Separations of Oligosaccharide-Containing Sephadex LH-20 Fractions.

parent fraction	amount (mg)	sample dissolved in water (µL)	filter wash (µL)	sample volume (µL)	injected per run (R) (mg/µL)	separation dates
IF1-1	12	200	200	400	R1: 6 mg/200 µL	2009/06/24
HF2-1 + IF1-1[c]	67.5 + 59.7	300	200	500	R1: 60/250 R2: 60/250	2009/07/14
HF2-2	122	675	500[a]	775	R1: 50/250 R2: 50/275 25/150[a] + IF1-2R1	2009/07/09
HF2-2	208	800	200	1000	R3: 50/250 R4: 50/250 R5: 50/250 R6: 50/250	2009/07/10
IF1-2	53.3	250 (HF2-2 wash)[b]	100	250	R1: 53.3+/250 (contained small amount of HF2-2)	2009/07/10
IF1-3	182	600 (+ IF1-2 wash)[b]	150 (IF1-2 wash)[b]	750	R1: 60/250 R2: 60/250 R3: 60/250	2009/07/10

[a] This material was combined with the sample shown, [b] The filter wash collected from the fraction shown was used as the dilution solvent for this material, [c] These fractions were determined to be sufficiently similar by analytical HPLC-ELSD to justify combining them.

Table S9. Combined Preparative HPLC Fractions Resulting from HF2-2 and IF1-2 Separations, Designated HF2-2P1.

retention time (min)[a]	fraction number	mg	notes
1.7–3.7	03	92.9	
3.7–4.57	04	14.4	
4.57–5.52	05	10.4	
5.52–9	06-09	13.1	
18.3–19.4	19	10.6	
19.4–20.0	20 *	11.9	Major fraction of interest
20.0–20.8	21	8.0	
20.8–22.0	22 *	17.1	Major fraction of interest
22.0–24.0	24	14.7	
24.0–25.0	25	-	
25.0–26.0	26	5.1	
Baseline[b]	B	-	

[a] Time points for fraction numbers were based on HF2-2 R4 and R5.
[b] Baseline contains all peaks not accounted for by other time points.

Table S10. Combined Preparative HPLC Fractions Resulting from IF1-3 Separations, Designated IF1-3P1.

retention time (min)	fraction number	mg	notes
1.7–3.7	03	77.6	
3.7–5.0	04	10.1	
5.0–8.3	05-08	14.2	
8.3–11	08-11	8.0	
18.5–19.4	19	4.3	
19.4–20.0	19.5	2.4	
20.0–20.5	20 *	4.3	Major fraction of interest
20.5–21.4	21	16.4	
21.4–22.0	22 *	3.5	Major fraction of interest
22.0–22.8	22.5	2.7	
22.8–23.5	23	2.1	
23.5–24.1	24	2.3	
24.1–25.0	25	1.7	
25.0–60	B	25.4	

Table S11. Details of Semi-Preparative-Scale Sample Preparations Used for Polyamine Separations of HF and IF Atlantis dC_{18} Column Fractions.

parent fraction	amount (mg)	sample dissolved in (μL)	filter wash (μL)[a]	sample volume (μL)	injected per run (mg/μL)	separation date
HF2-2P1t19	10.6	75	0	80	R1: 4.0/30 6.6/50 added to MixR1–R2	2009/10/11
IF1-3P1t19 + IF1-3P1t19.5[c]	4.3 + 2.4	60	20	80	R1: 3.3/40 3.4/40 added to MixR1–R2	2009/10/11
HF2-2P1t19 IF1-3P1t19[c]	(6.6)[d] (3.4)[d]	50 + 45	25	120	MixR1: 4.2/50 MixR2: 5.8/70	2009/10/12
HF2-2P1t20	11.9	50	90	140	R1: 4/50 R2: 2/25 R3, R4: 2.4/30 1.1/10 added to HF2-2P1t22 R3	2009/10/14
IF1-3P1t20	4.3	30	0	30	R1: 4.3/30	2009/10/12
HF2-2P1t21 + IF1-3P1t21[c]	8.0 16.4	200	0	200	R1: 4.3/35 R2: 5.5/45 R3: 4.9/40	2009/10/04
HF2-2P1t21 + IF1-3P1t21[c]	(9.76)[d]	80 (prev. sample)	40	120	R4: 5/60 R5: 5/60	2009/10/11
HF2-2P1t22	17.1	100	50	130	R1: 5.3/40 R2: 4/30 R3[e]: 5.3/40 R3: 5.0/40[b]	2009/10/14
IF1-3P1t22	3.5	25	45	70	R1: 2.5/50 1.0/20 added to IF1-3P1t23 R2	2009/10/12
IF1-3P1t23 + IF1-3P1t22.5[c]	2.1 + 2.7 + (1.0)[d]	50	40	90	R1: 3.2/60 R2: 2.6/50[a]	2009/10/12
HF2-2P1t24	14.7	150	0	150	R1: 2/20 R2: 4/40 R3: 4.5/45 R4, R5: 3.5/35[b]	2009/10/04
IF1-2P1t24 + HF2-2P1t24[c]	6.8	45[b]	25	70	Added to HF2-2P1t24 R4 & R5	2009/10/04

[a] Samples for which the filter wash amount is 0 μL were not filtered. [b] Contained material from an additional parent fraction. [c] These fractions were determined to be sufficiently similar by analytical HPLC-ELSD to justify combining them during separations. [d] Material from a previously prepared sample. [e] Sample and data were lost due to instrument/operator malfunction.

Table S12. Descriptions of Polyamine II Fractions Obtained from HF and IF Combined Materials.

Fraction Name	Amount (mg)	Results of Analytical HPLC-ELSD on Atlantis dC_{18}	NMR Data	Interpretation of Data/ Structural Info Proposed/ Outcome
HF2-2P1t21A15	1.1	mixture: three components	none[a]	End of analysis.
IF1-3P1t23A15	0.6	mixture: six components	none	End of analysis.
IF1-3P1t23A16	0.5	mixture: three components	none	End of analysis.
HF2-2P1t24A16	0.8	mixture: two major, one minor components	none	Possibly the same as t23A16 based on elution profile. End of analysis.
HF2-2P1t19A17	1.9	mixture: one major, three minor components	none	Uncertain relation to t20A17. End of analysis.
HF2-2P1t20A17	8.8	single component	Full Set	Sufficient purity and quantity for full structural elucidation to yield compound **1**.
HF2-2P1t21A17	1.2	mixture: one major, three minor components	none	Possibly the same main component as t20A17 based on elution profile. End of analysis.
HF2-2P1t22A17	1.9	mixture: one major, multiple minor components	^{1}H NMR	Possibly the same main component as t20A17 but NMR data poorly resolved. End of analysis.
HF2-2P1t19A18	0.5	single component	none	End of analysis.
HF2-2P1t22A18	1.8	single component	^{1}H NMR	Possibly the same as t19A18 based on elution profile. NMR data poorly resolved. End of analysis.
IF1-3P1t23A18	1.0	single component	none	Possibly the same as t19A18 based on elution profile. End of analysis.
HF2-2P1t24A18	1.6	mixture: six components	none	End of analysis.
HF2-2P1t22A19	1.9	mixture: two components	^{1}H NMR	NMR data poorly resolved. End of analysis.
HF2-2P1t24A20	1.7	mixture: two components	none	End of analysis.
HF2-2P1t21A21	1.2	mixture: two components	none	End of analysis.
HF2-2P1t24A22	0.8	mixture: two components	none	End of analysis.

[a] Insufficient amount of pure or enriched fraction available for meaningful ^{1}H NMR data acquisition.

Figure S27. Representative Atlantis dC_{18} semi-preparative separation of HF1-1 yielding fractions t34 and t36 with detection by ELS and UV (215 and 254 nm).

The solvent system used for this separation was: 20 min at 100% water, 30 min gradient from water to 25% MeOH, 3 min at 25% MeOH, 7 min gradient from 25% MeOH to 100% MeOH.

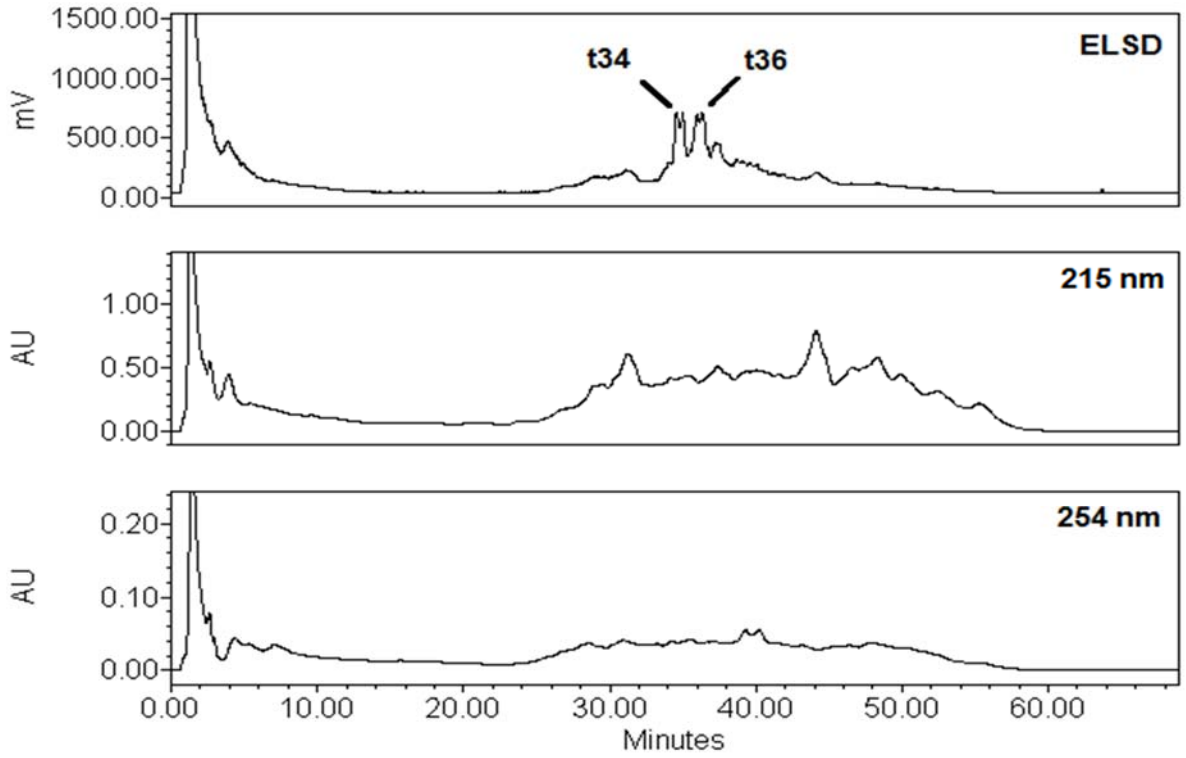

Figure S28. ^{1}H NMR spectra for fractions HF1-1P1t34 and HF1-1P1t36 compared to HF2-2P1t22 (DMSO-d_6, 400 MHz).

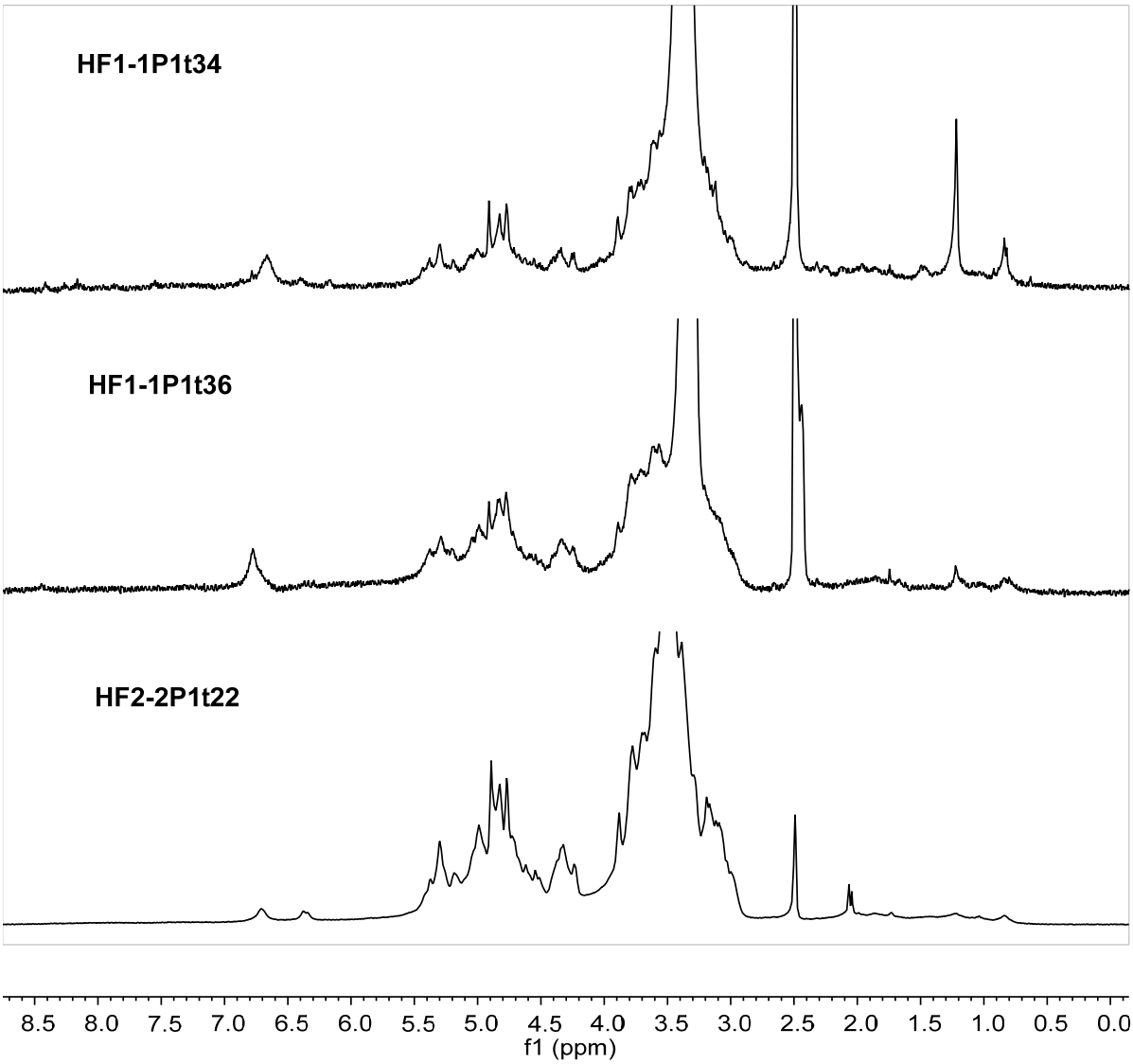

Figure S29. COSY spectrum of fraction HF1-1 (D_2O, 400 MHz).

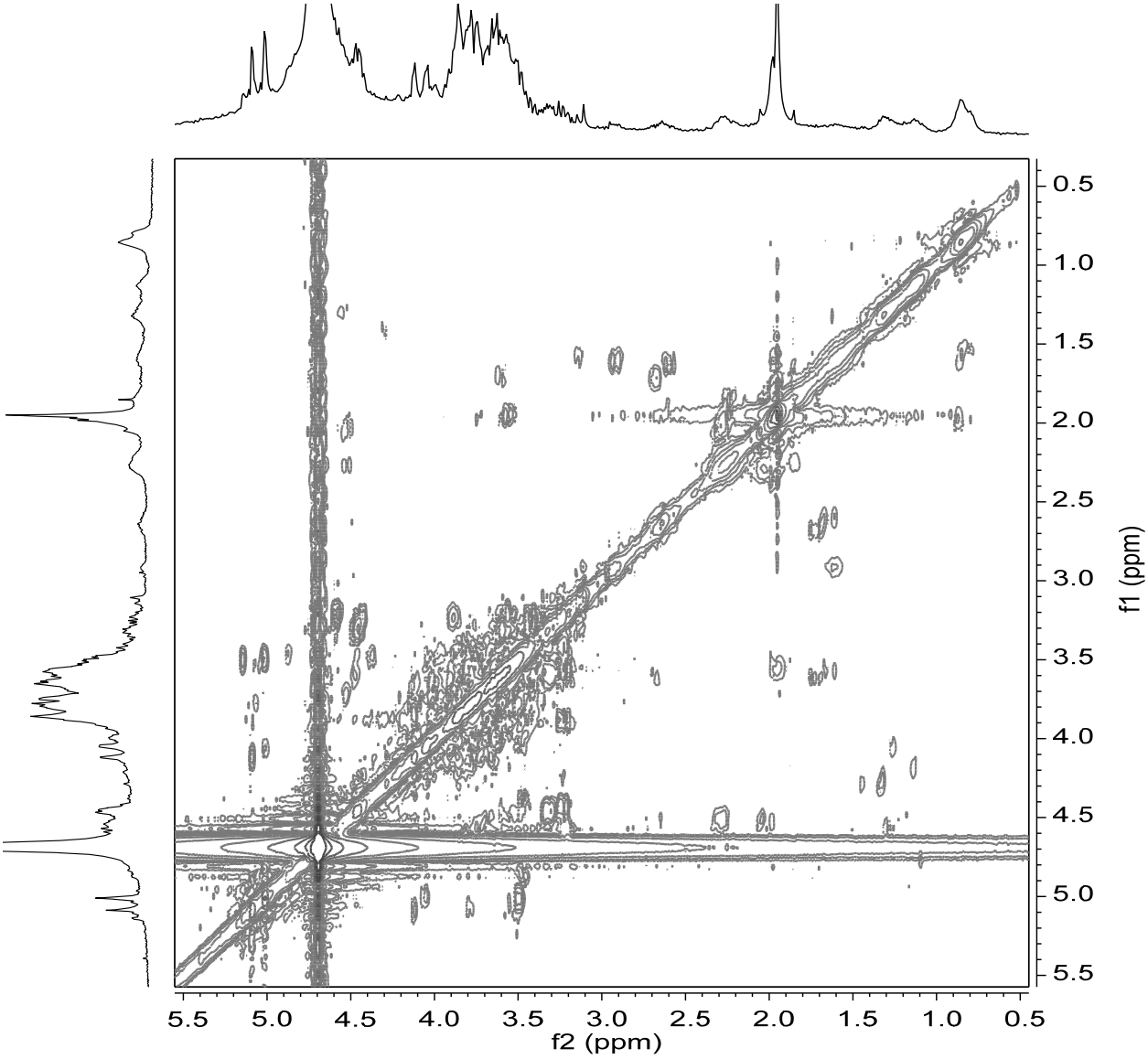

Figure S30. Preparative HPLC-ELSD of HF2-2, R2 (top chromatogram) through R6 (bottom chromatogram) (Atlantis dC_{18}).

This set of chromatograms shows the repeatability of the preparative separation. R1 of this series (not shown) has a similar profile but slightly different retention times as a result of differences in the solvent method used.

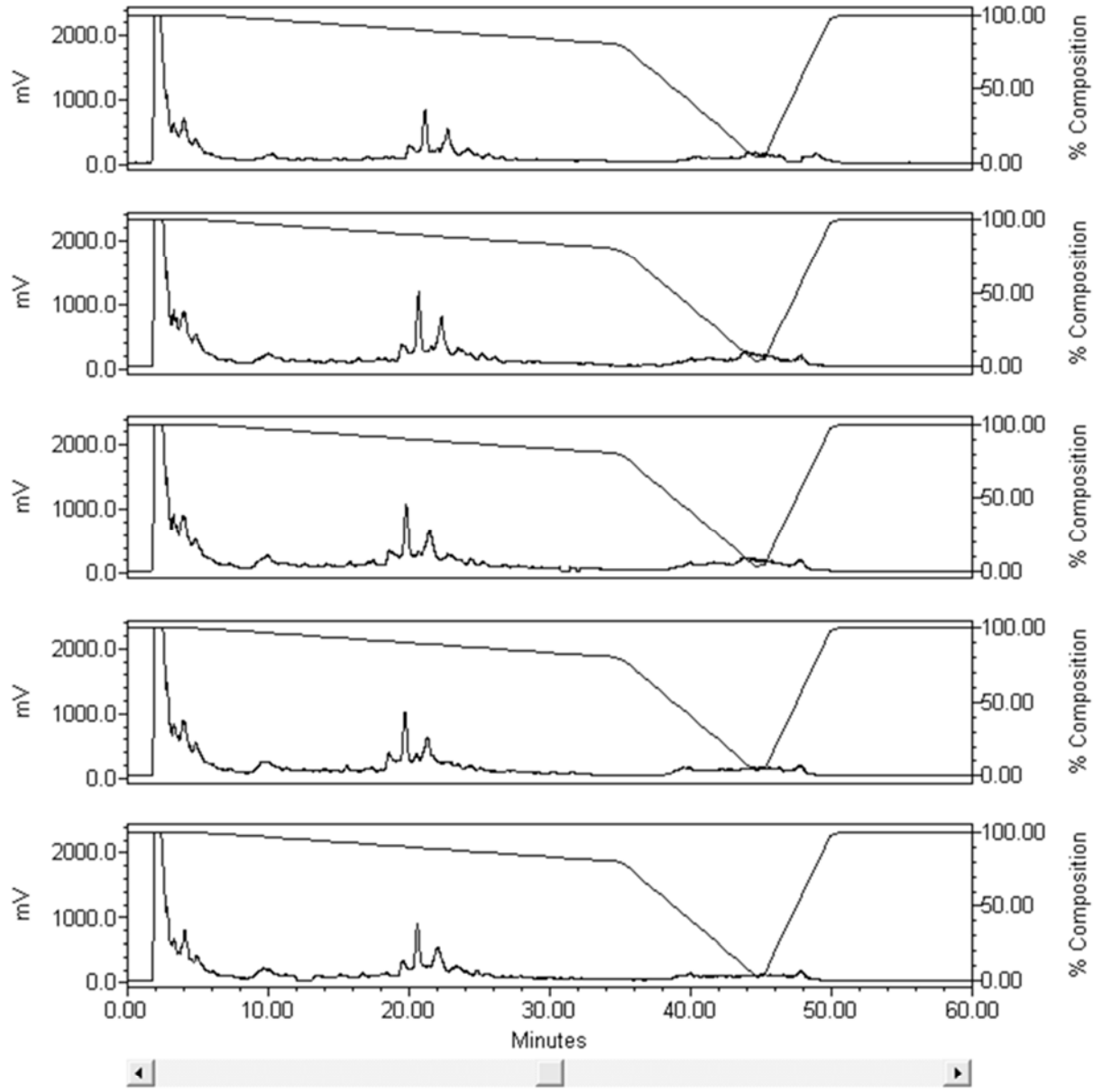

Visible	SampleName	Date Acquired	Acq Method Set	Injection Volume (uL)	Run Time (Minutes)	Barcode / BCD	Auto Ac
☑	HF2-2 AtldC18-P R2	7/9/2009 6:38:51 PM CDT	Atlantis dC18 P vB	275.00	100.00		
☑	HF2-2 AtldC18-P R3	7/9/2009 9:21:13 PM CDT	Atlantis dC18 P vB	250.00	100.00		
☑	HF2-2 AtldC18-P R4	7/9/2009 10:38:49 PM CDT	Atlantis dC18 P vB	250.00	100.00		
☑	HF2-2 AtldC18-P R5	7/9/2009 11:56:34 PM CDT	Atlantis dC18 P vB	250.00	100.00		
☑	HF2-2 AtldC18-P R6	7/10/2009 1:11:35 AM CDT	Atlantis dC18 P vB	250.00	100.00		

Figure S31. Preparative HPLC-ELSD of IF1-2 and IF1-3, R1 through R3 (Atlantis dC_{18}).

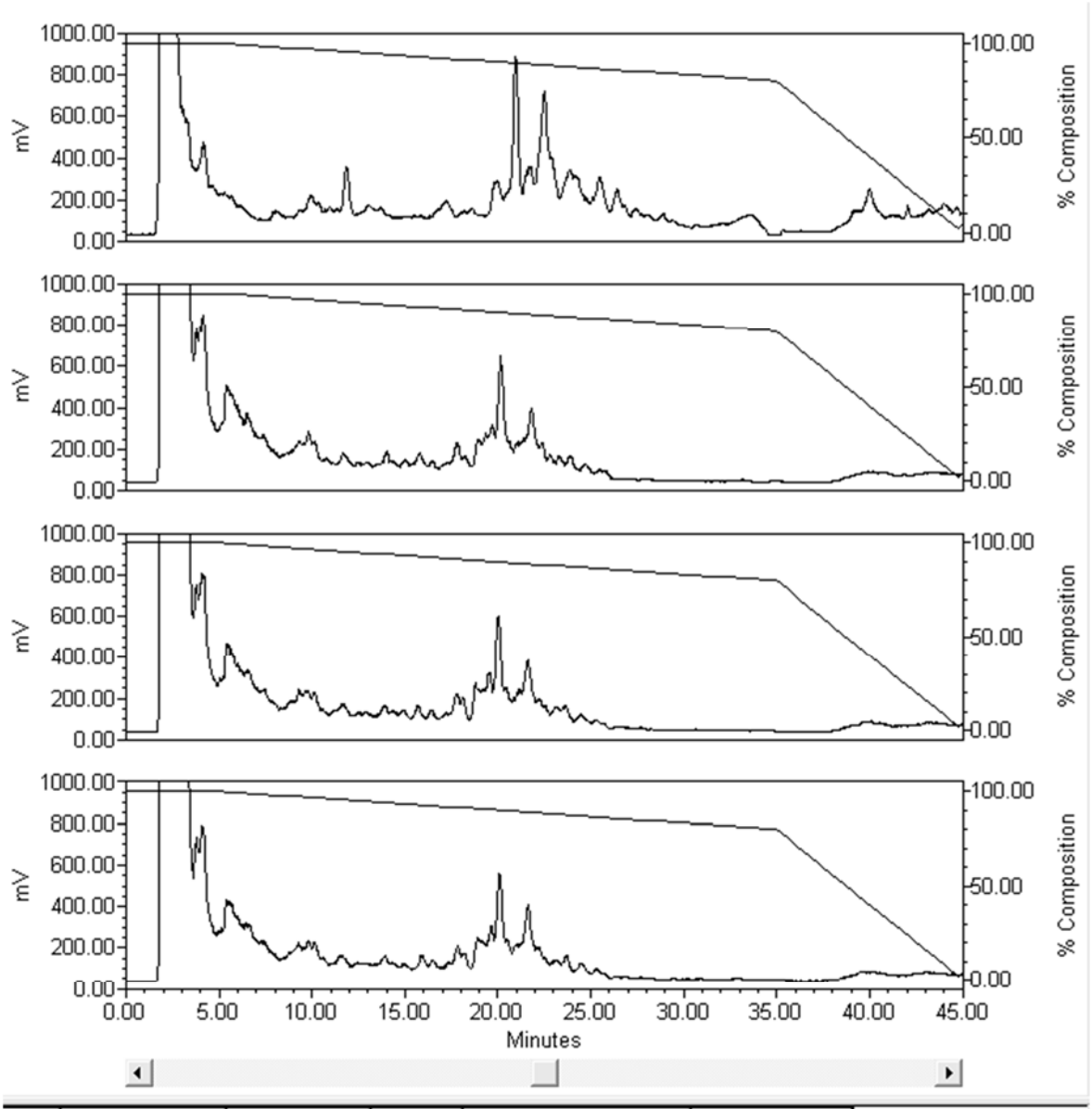

Visible	SampleName	Injection Volume (uL)	Det. Units	Date Acquired	Acq Method Set
☑	IF1-2 AtldC18-P R1	275.00	mV	7/9/2009 8:01:07 PM CDT	Atlantis dC18 P vB
☑	IF1-3 AtldC18-P R1	250.00	mV	7/10/2009 4:22:03 AM CDT	Atlantis dC18 P vB
☑	IF1-3 AtldC18-P R2	250.00	mV	7/10/2009 5:44:05 AM CDT	Atlantis dC18 P vB
☑	IF1-3 AtldC18-P R3	250.00	mV	7/10/2009 7:04:42 AM CDT	Atlantis dC18 P vB

Figure S32. Comparison of the ^{1}H NMR spectra for HF2-2P1t20 and HF2-2P1t22 showing highly similar composition, DMSO-d_6, 400 MHz.

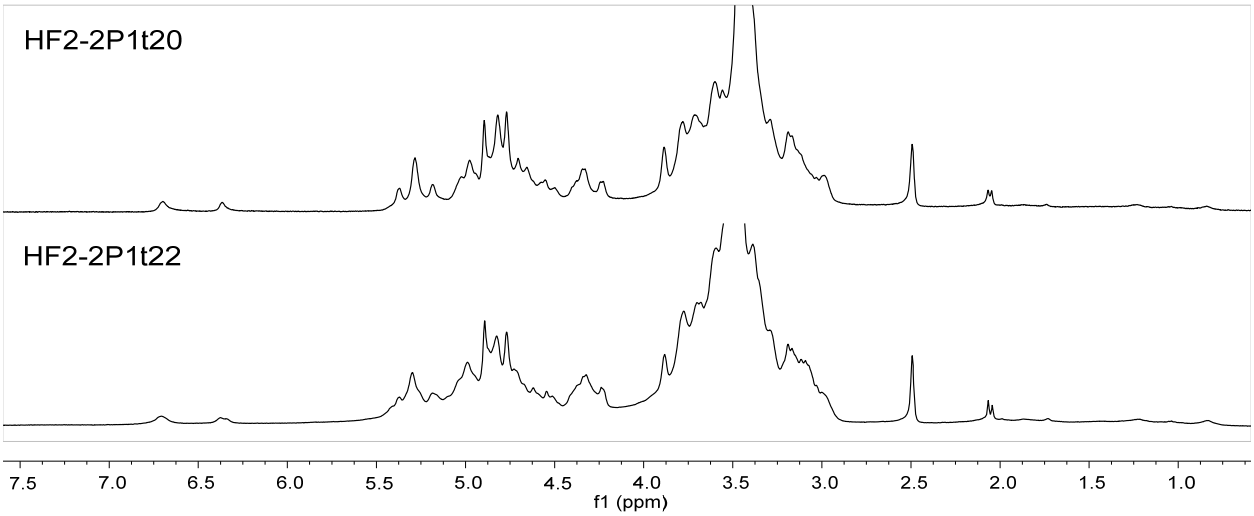

Figure S33. Comparison of the ^{13}C NMR spectra for HF2-2P1t20 and HF2-2P1t22 showing highly similar composition, DMSO-d_6, 400 MHz.

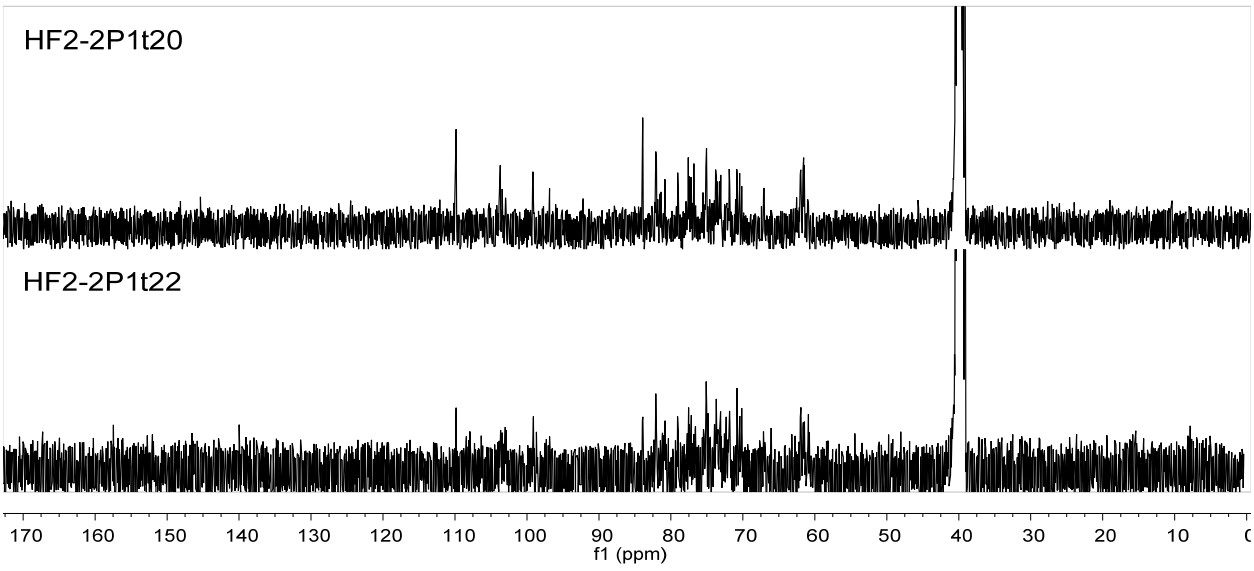

Figure S34. Atlantis dC_{18} preparative separations of HF2-1+IF1-1 R1 (a and b) and R2 (c and d) with detection by ELS (a and c) and UV (215 nm) (b and d).

The initial separation method attempted for HF2-1+IF1-1 (a.k.a. HI1) R1 was the same as that for the HF2-2, IF1-2, and IF1-3 samples. As this method did not appear to resolve the detectable components in the fraction, an alternate method was employed for R2 with modified gradient times of 5 min at 100% water, a 10 min gradient from water to 20% MeOH, and a 30 min gradient from 20 to 100% MeOH. The ELSD conditions for both separations were maintained at an evaporator temperature of 100 ºC, a nebulizer temperature of 50 ºC, and a gas flow rate of 1.0 SML. The change in elution method did not help with resolution of the detectable components of this mixture.

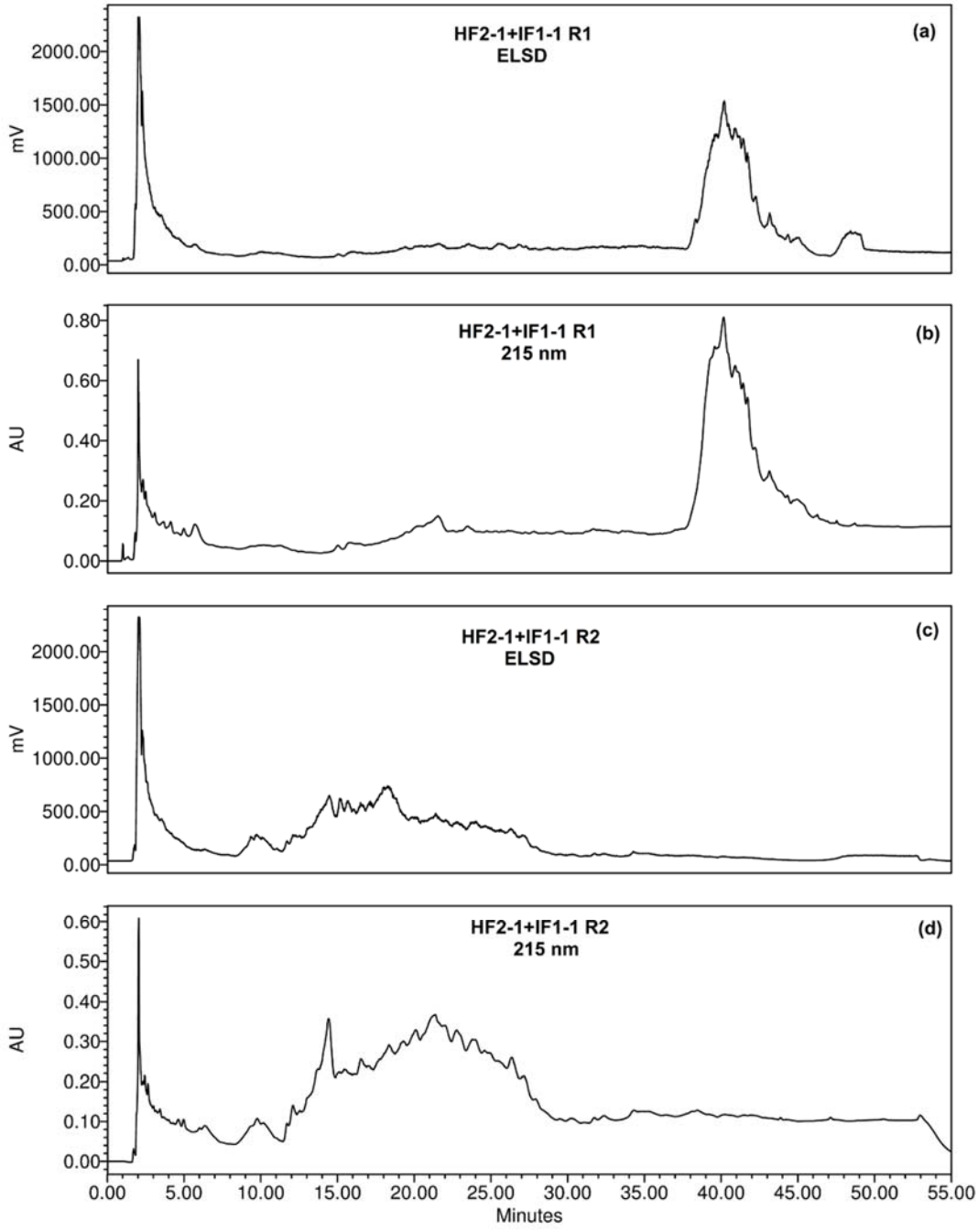

Table S13. Combined Preparative HPLC Fractions Resulting from HF2-1+IF1-1 Separations R1 and R2, Designated HF2-1P1.

Multiple further separations using different sorbents and methods were attempted with the material designated HF2-1P1t40, but none yielded sufficient amounts of pure compounds suitable for structural elucidation.

retention time (min)		fraction number	mg	notes
R1	R2	R1 + R2		
1.5–7.0	1.5–8.5	02	24.2	
7.0–14	8.5–11.5	B	-	Part of baseline
14–22.6	11.5–15.0	20	12.6	Fraction of interest due to R_t in R1
22.6–37.7	15.0–17.5	25	17.0	
37.7–48.0	17.5–30.0	40	32.9	Mixture of interest
48.0–70.0	30.0–60.0	B	-	Part of baseline

Figure S35. ^{1}H NMR spectrum for fraction HF2-1P1t40 (8 mg), DMSO-d_6, 400 MHz.

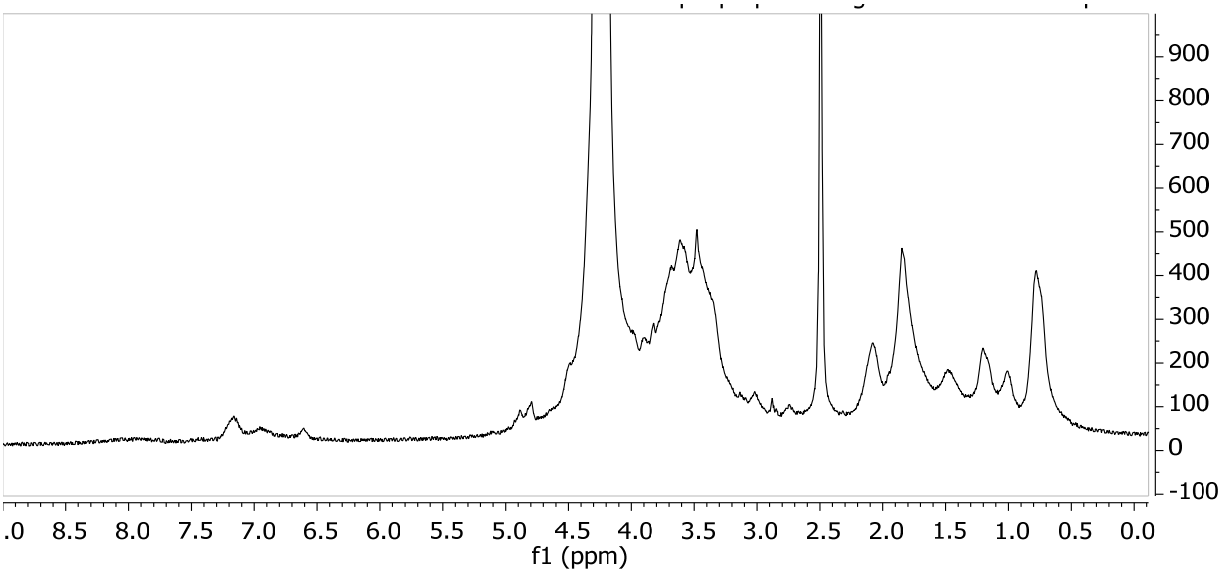

Figure S36. Preparative HPLC separation of HI1+HI2+HI3 on Atlantis dC_{18} with detection by ELS and UV (215 and 254 nm).

The method used for this separation was 5 min water, a 30 min gradient from water to 20% MeOH, a 10 min gradient from 20 to 100% MeOH, 3 min at 100% MeOH, and a return to starting conditions. This solvent gradient is shown by the sloped line in the ELSD panel; vertical lines in the ELSD panel represent fraction break time points. The material eluting initially from the column at t00-04 min overloaded the detector with a reading of >1100 mV.

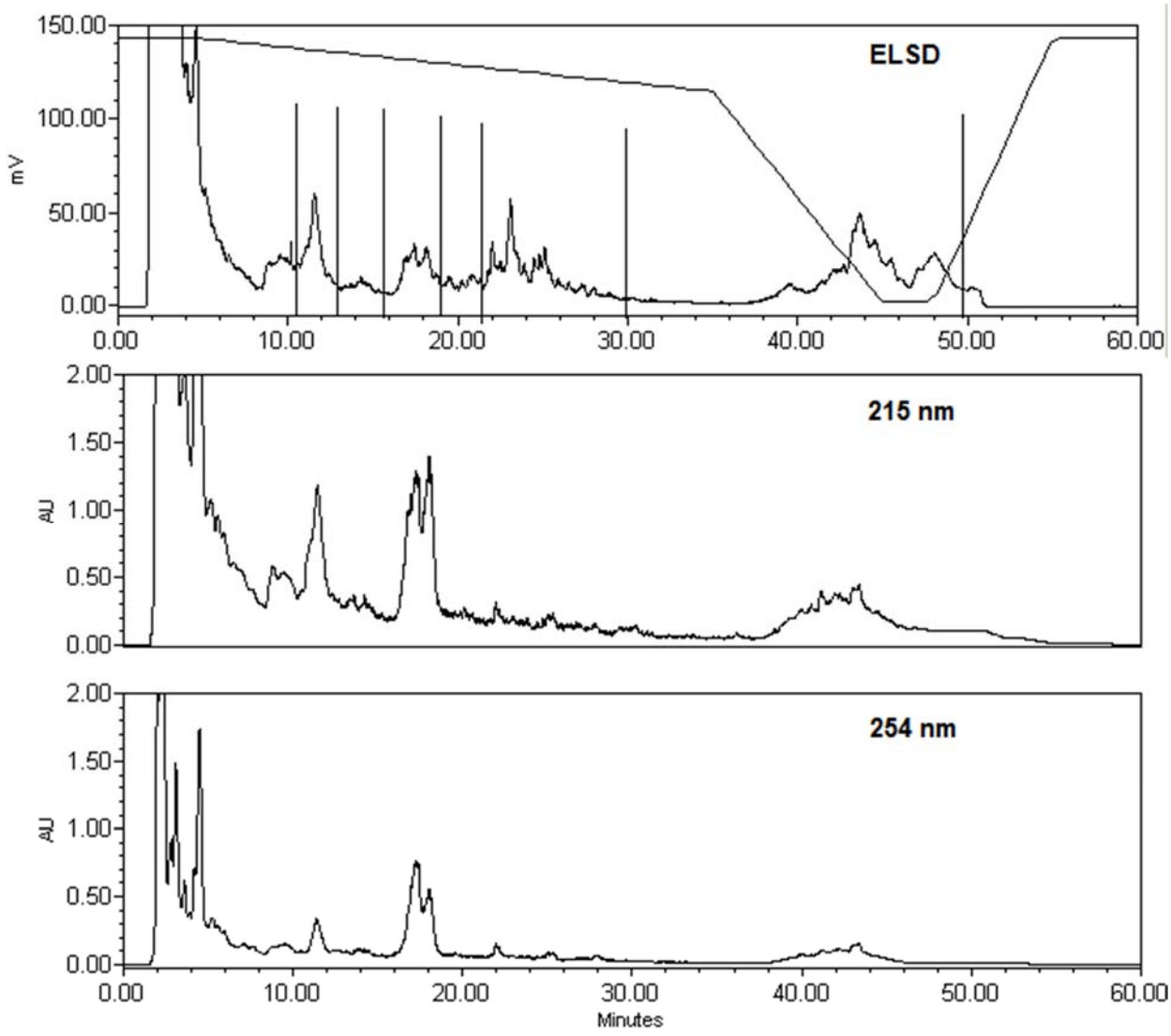

b. Semi-Preparative Polyamine HPLC-ELSD Methods and Results

Methods for semi-preparative separations were developed using the working hypothesis that the compounds of interest were oligosaccharides. Analytical scale HPLC-ELSD data and considerations of the results of sample co-injections (Table S11) were both used to aid in comparisons and sample fraction combinations (Tables S14-S19). The fractions of interest resulting from these separations are summarized in Table S12 and in Figure 6 (Main Text).

Fraction HF2-2P1t24 was used to evaluate the effects of changes in starting solvent percentages and gradient length on the resolution of semi-preparative separations. A consistent flow rate of 4 mL/min was used for all separations. The method for HF2-2P1t24 R1 used MeCN:water, with 10 min at 70% MeCN, a 30 min gradient to 40% MeCN, and a 3 min gradient to 70% MeCN. The method for HF2-2P1t24 R2 used MeCN:water, with 5 min at 65% MeCN, a 30 min gradient to 40% MeCN, and a 3 min gradient to 65% MeCN. The method for HF2-2P1t24 R3–R5 (Figure S37) used MeCN:water, with 5 min 65% MeCN, a 25 min gradient to 45% MeCN, and a 3 min gradient to 65% MeCN. This last method was also used for HF2-2P1t21 R1–R5 and later separations.

Initial ELSD conditions used for HF2-2P1t24 were an evaporator temperature of 90 ^{o}C, a nebulizer temperature of 45 ^{o}C, and a gas flow rate of 1.0 SLM. The instrument configuration and ELSD conditions were modified for HF2-2P1t21 and later separations with changes in the ELSD inlet tubing to give 3.9 mL/min to collection and 0.1 mL/min to ELS detection. These changes dictated that the ELSD gas flow rate be decreased to 0.8 SLM to maintain sensitivity; other temperature conditions remained the same.

Fractions from Polyamine separations (Figures S37-S40) were minimally combined (Tables S12 and S14-S19) due to minor shifts in retention times between samples and the difficulties of obtaining NMR data on small quantities of material. Most Polyamine fractions of interest were reinjected on the analytical Atlantis dC_{18} column to check for purity. An example of this (Figure S41) is included for HF2-2P1t20A17 compared to the HF2-2P1t22 series (A17, A18, A19). While HPLC-ELSD indicates the presence of impurities in HF2-2P1t22A17, retention times indicate that it may contain the same primary component as that of HF2-2P1t20A17 (**1**). While ^{1}H NMR (in D_2O) could be obtained for this sample (Figure S42), the amount available (1.9 mg) was insufficient for obtaining ^{13}C NMR or any usable 2D NMR spectra at 400 MHz.

The low relative recovery (~ 30.5%) of compound **1** (8.8 mg from a total of 28.8 mg of parent fractions containing t20 from Atlantis dC$_{18}$ separations) can be partly attributed to the requirement for destructive, ELSD-based detection and collection. The preparative HPLC configuration involved the placement of a flow splitter after the UV detector but before the ELSD. This splitter directed the majority of the flow to collection vessels, with a smaller portion directed to the detector. Typically, 2–4% of the eluting solvent entered the detector for the flow rates of 20–25 mL/min used with the preparative Atlantis dC$_{18}$ column, but this percentage may have been as high as 10% for the slower flow rates (5–10 mL/min) used with the semi-preparative Polyamine column. This arrangement meant that as much as 10% of an injected sample would be lost to the detector with every separation. All attempts were made with available resources to decrease this percentage of sample loss but such efforts were limited by the sensitivity and configuration of the detector and by the flow dynamics of the system.

Table S14. Combined Semi-Preparative HPLC Fractions Resulting from HF2-2P1t21 and IF1-3P1t21 Separations, Designated HF2-2P1t21A.

retention time (min)[a]	fraction	mg	notes
0–2.5	02	-	large peak, inconsistent profile, large % of sample
2.5–14	04	2.9	multiple peaks between start and 8 min – inconsistent retention times
14–15	14	1.2	
15–16	15 *	1.1	Major component of interest
16–17	16	0.9	
17–18	17 *	1.2	Major component of interest
18–18.5	18	0.5	
18.5–19.2	19	0.9	first of 19–20 double peak
19.2–20	20	1.0	second of 19–20 double peak
20–21	21 *	1.2	Major component of interest
21–21.5	21.5	0.4	shoulder of 21
21.5–23	22	0.6	

Table S15. Combined Semi-Preparative HPLC Fractions Resulting from HF2-2P1t24 Separations, Designated HF2-2P1t24A.

retention time (min)[a]	fraction	mg	notes
1.2–15	02	1.2	few compounds between 0–6, low % of sample
15.0–16.0	15	0.5	
16–16.8	16 *	0.8	Major component of interest
16.8–17.6	17	0.6	
17.6–18.7	18 *	1.6	Major component of interest
18.7–19.8	19	0.9	
19.8–20.8	20 *	1.7	Major component of interest
20.8–21.5	21	0.3	
21.5–22.5	22 *	0.8	Major component of interest
22.5–24.0	23	0.4	

[a] Time points for fraction numbers were based on R2, as R1 had an extended gradient time.

Table S16. Combined Semi-Preparative HPLC Fractions Resulting from HF2-2P1t19, IF1-3P1t19 and IF1-3P1t19.5 Separations, Designated HF2-2P1t19A.

retention time (min)[a]	fraction	mg	notes
0–3	2	4.6	
3–4	4	0.5	
4–13	B	3.0	flat line before eluting peak set
13–14.5	14	0.2	first minor peak
14.5–16.5	15	0.6	baseline peaks between 14 and 17
16.5–17.5	17 *	1.9	major peak for t19 fractions, possibly same as HF2-2P1t20A17
17.5–18.5	18	0.5	side peak of 17 (minor component)
18.5–20	19	0.4	last minor peak of set
20–22	21	0.3	baseline peaks tailing off end of separation

[a] Time points for fraction numbers were based on HF2-2t19R1 & IF1-3t19R1.

Table S17. Combined Semi-Preparative HPLC Fractions Resulting from IF1-3P1t22, IF1-3P1t23, and IF1-3P1t23.5 Separations, Designated IF1-3P1t23A.

retention time (min)[a]	fraction	mg	notes
1.3–4.0	2	-	
4.0–13.5	B	-	baseline between early eluting impurity and major peak set
14.5–16	15 *	0.6	Major component of interest
16–17	16 *	0.5	Major component of interest
17–18	17	0.5	
18–19	18 *	1.0	Major component of interest
19–20	19	0.9	
20–21.5	21	0.9	mix of baseline minor components
21.5–22.5	22	0.8	mix of baseline minor components

[a] Times points for fraction numbers were based on IF1-3P1t23 R1.

Table S18. Combined Semi-Preparative HPLC Fractions Resulting from HF2-2P1t22 Separations, Designated HF2-2P1t22A.

retention time (min)[a]	fraction	mg	notes
1.3–4.0	2	-	
4.0–13.5	B	-	baseline between early eluting impurity and major peak set
13.5–14.5	14	0.9	
14.5–15.5	15	0.4	minor – almost baseline relative percent
15.5–16.5	16	0.5	
16.5–17.5	17 *	1.9	same compound as major component of HF2-2t20
17.5–18.5	18 *	1.8	first major peak of set found in HF2-2t22 sample
18.5–20.0	19 *	1.9	second major peak of set found in HF2-2t22 sample
20.0–22	21	0.4	minor baseline peak set

[a] Times points for fraction numbers were based on HF2-2P1t22 R2 as this sample contained a portion of the HF2-2Pt120 sample.

Table S19. Combined Semi-Preparative HPLC Fractions Resulting from HF2-2P1t20 and IF1-3P1t20 Separations, Designated HF2-2P1t20A.

retention time (min)[a]	fraction	mg	notes
1.3–4.0	02	3.2	
4.0–12.5	B	1.1	baseline between early eluting impurity and major peak set
12.5–13.5	13	1.0	
13.5–14.5	14	1.6	
14.5–15.8	B	-	baseline peaks just before major component – perhaps one primary component
15.8–17.8	17 *	8.8	major peak/major component of sample mass
17.8–19	18	0.8	baseline minor peak (mixture)
19–21	20	0.9	baseline minor peak set (mixture)

[a] Time points for fraction numbers were based on HF2-2P1t20 R2 & R3.

Figure S37. Semi-preparative HPLC-ELSD chromatograms for HF2-2P1t24, R2 through R5 (Polyamine).

This chromatogram set shows the repeatability of the separations. See Table S15 for recovered amounts of each fraction.

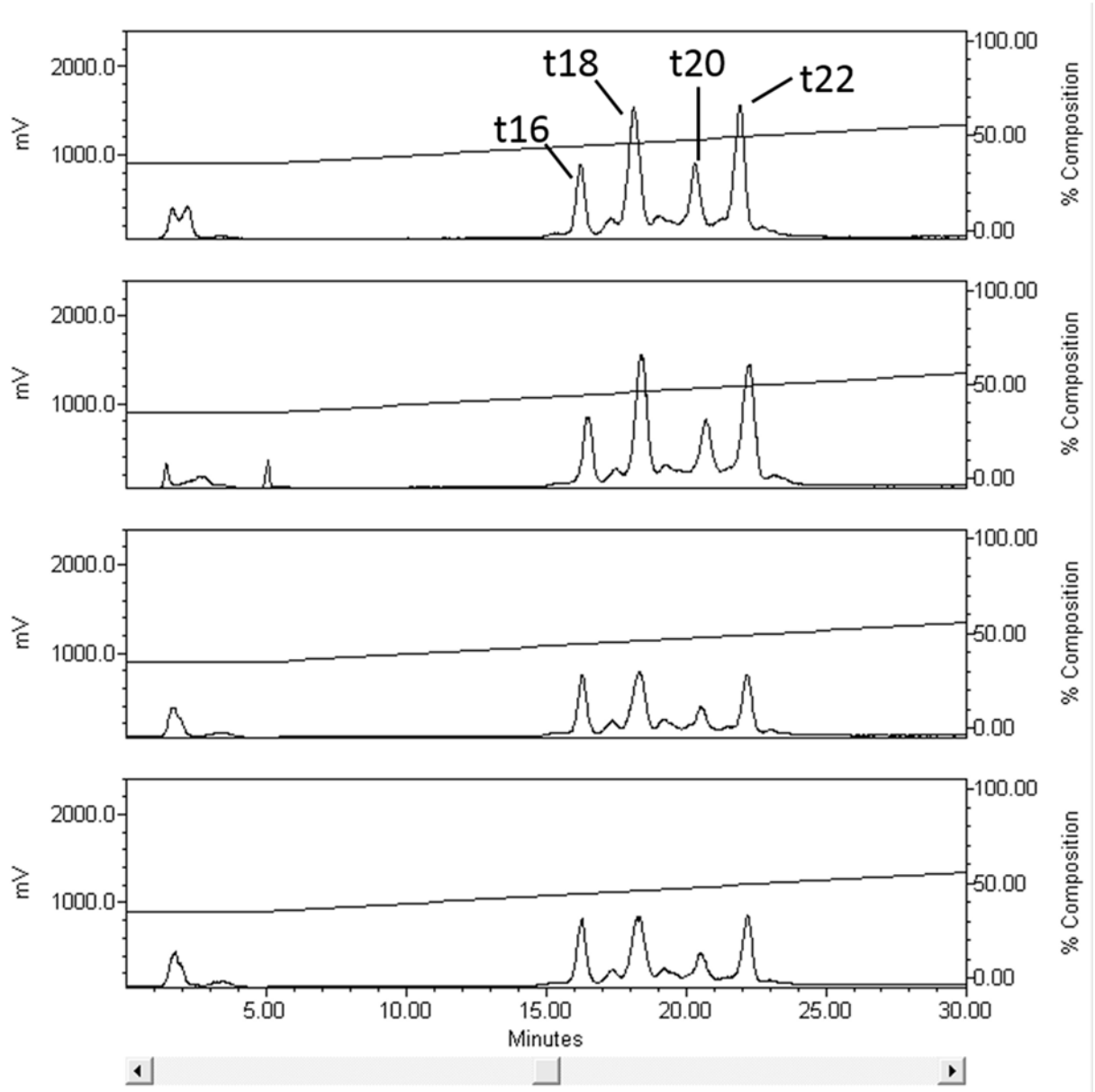

Visible	SampleName	Injection Volume (uL)	Det. Units	Date Acquired	Acq Method Set
☑	HF2-2P1t24 YMC-PolyA-SP R2	40.00	mV	10/4/2009 6:27:46 PM CDT	YMC PolyAmine SP vB
☑	HF2-2P1t24 YMC-PolyA-SP R3	45.00	mV	10/4/2009 7:36:07 PM CDT	YMC PolyAmine SP vB
☑	HF2-2P1t24 YMC-PolyA-SP R4	35.00	mV	10/4/2009 8:35:26 PM CDT	YMC PolyAmine SP vB
☑	HF2-2P1t24 YMC-PolyA-SP R5	35.00	mV	10/4/2009 11:15:08 PM CDT	YMC PolyAmine SP vB

Figure S38. Semi-preparative HPLC-ELSD of HF2-2P1t21, R1 through R5 (Polyamine).

(% MeCN shown)

Slight retention time shifts were observed for these separations. See Table S14 for recovered quantities.

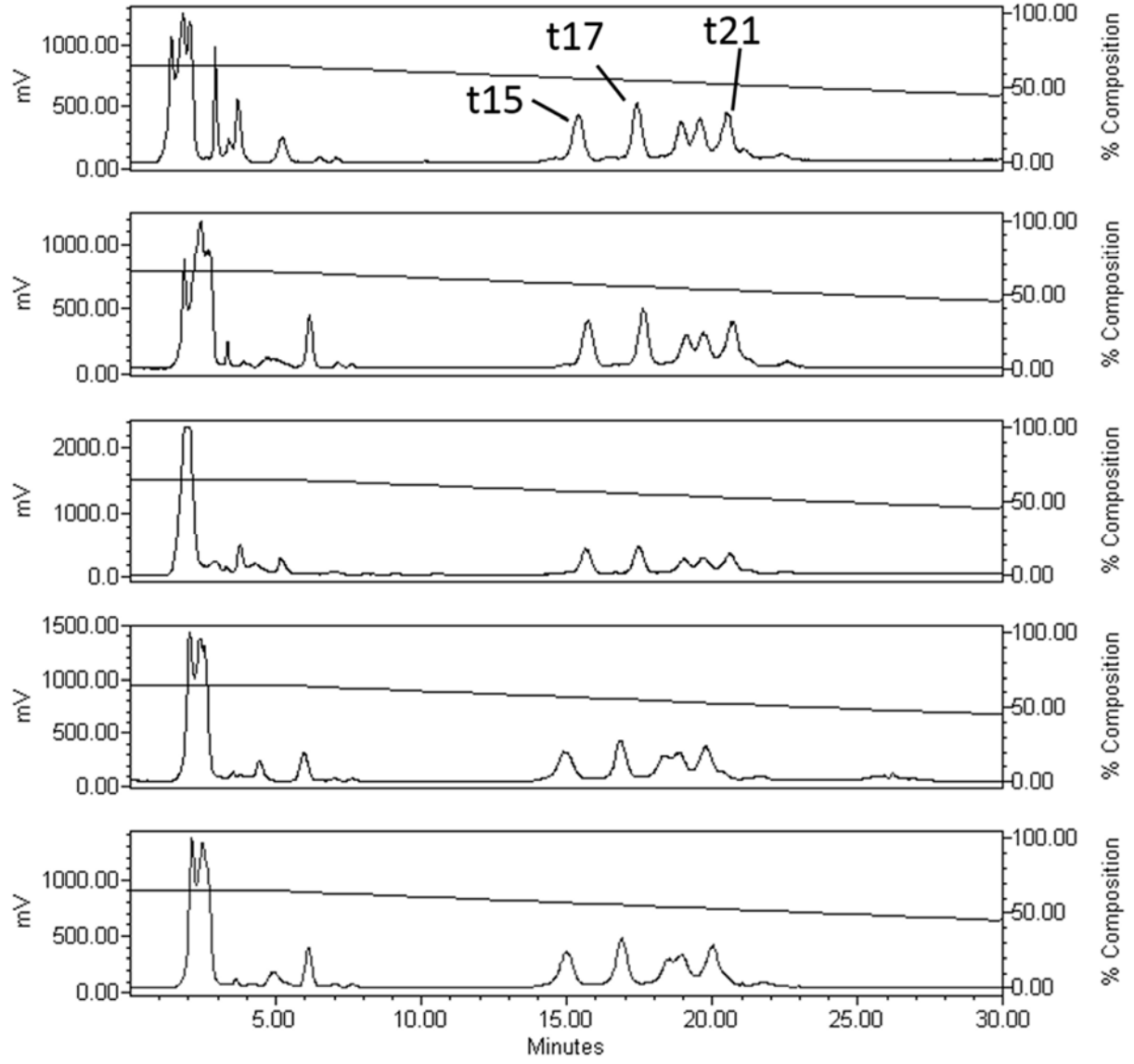

Visible	SampleName	Date Acquired	Injection Volume (uL)	Run Time (Minutes)	Instrument Method Name	Acq Me
☑	HF2-2P1t21 YMC-PolyA-SP R1	10/5/2009 12:08:54 AM CDT	35.00	100.00	YMC PolyAmine SP vB	YMC PolyA
☑	HF2-2 P1t21 YMC-PolyA-SP R2	10/5/2009 2:23:08 PM CDT	45.00	100.00	YMC PolyAmine SP vB	YMC PolyA
☑	HF2-2 P1t21 YMC-PolyA-SP R3	10/5/2009 4:36:34 PM CDT	45.00	80.00	YMC PolyAmine SP vB	YMC PolyA
☑	HF2-2 P1t21 YMC-PolyA-SP R4	10/11/2009 1:40:29 PM CDT	60.00	90.00	YMC PolyAmine SP vB	YMC PolyA
☑	HF2-2 P1t21 YMC-PolyA-SP R5	10/11/2009 2:51:11 PM CDT	60.00	90.00	YMC PolyAmine SP vB	YMC PolyA

Figure S39. Semi-preparative HPLC-ELSD of HF2-2P1t22, R1 through R3 (Polyamine).

The ratios of t17, t18 and t19 varied with each injection due to the co-injection of HF2-2P1t22 with related fractions to aid in subfraction recombinations. For Run 3 (bottom panel) material from HF2-2P1t20 was co-injected, indicating that the t17 peak may contain the same component as the major component of HF2-2P1t20A17 (Compound **1**). Retention time shifts were observed for these injections. See Table S18 for fraction quantities.

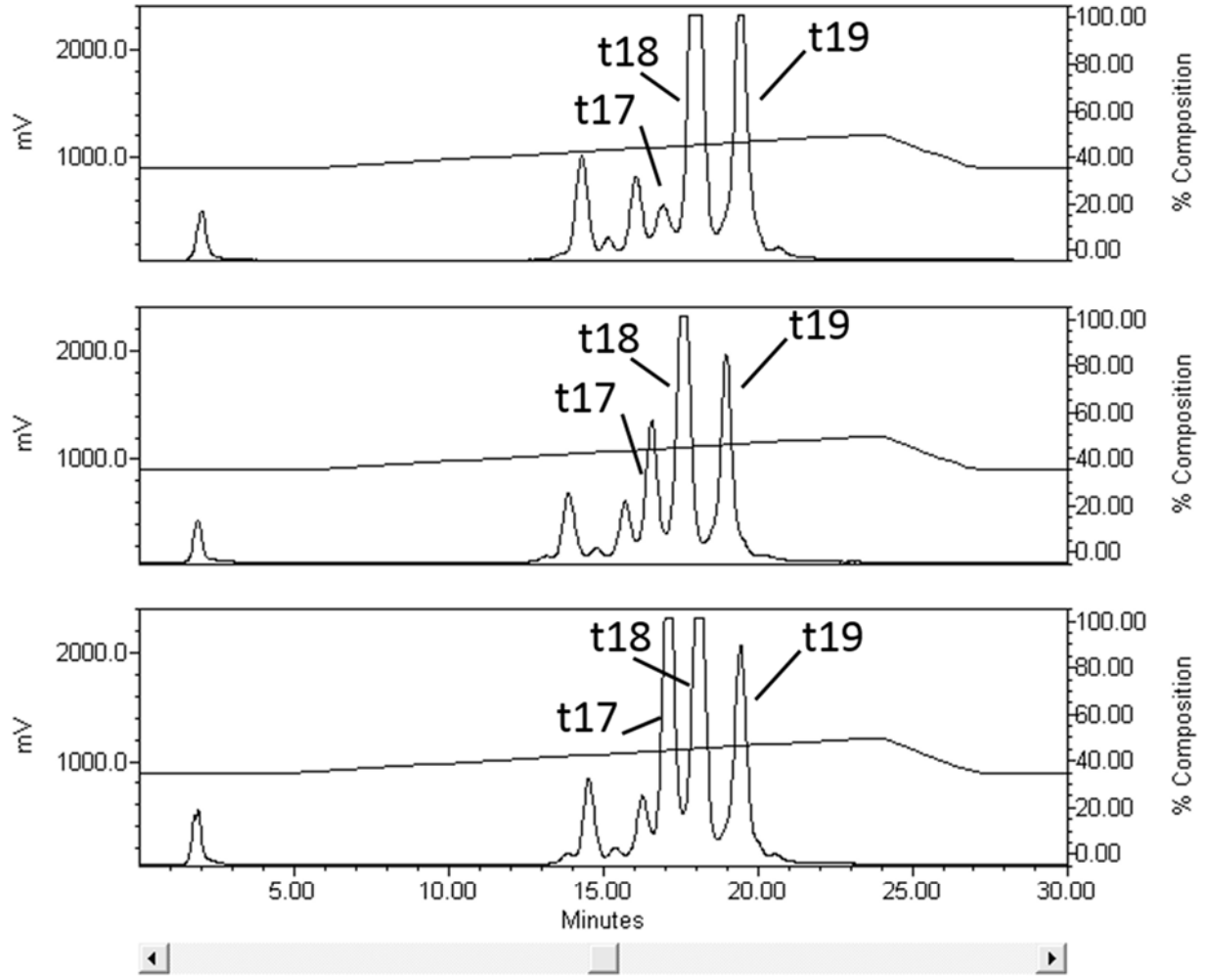

Visible	SampleName	Injection Volume (uL)	Det. Units	Date Acquired	Acq Method Set
☑	HF2-2 P1t22 YMC-PolyA-SP R1	40.00	mV	10/13/2009 10:07:35 PM CDT	YMC PolyAmine SP vB
☑	HF2-2 P1t22 YMC-PolyA-SP R2	30.00	mV	10/14/2009 2:02:20 AM CDT	YMC PolyAmine SP vB
☑	HF2-2 P1t22 YMC-PolyA-SP R3	40.00	mV	10/14/2009 2:51:17 AM CDT	YMC PolyAmine SP vB

Figure S40. Semi-preparative HPLC-ELSD of HF2-2P1t20, R1 through R4 (Polyamine). (% MeCN shown)

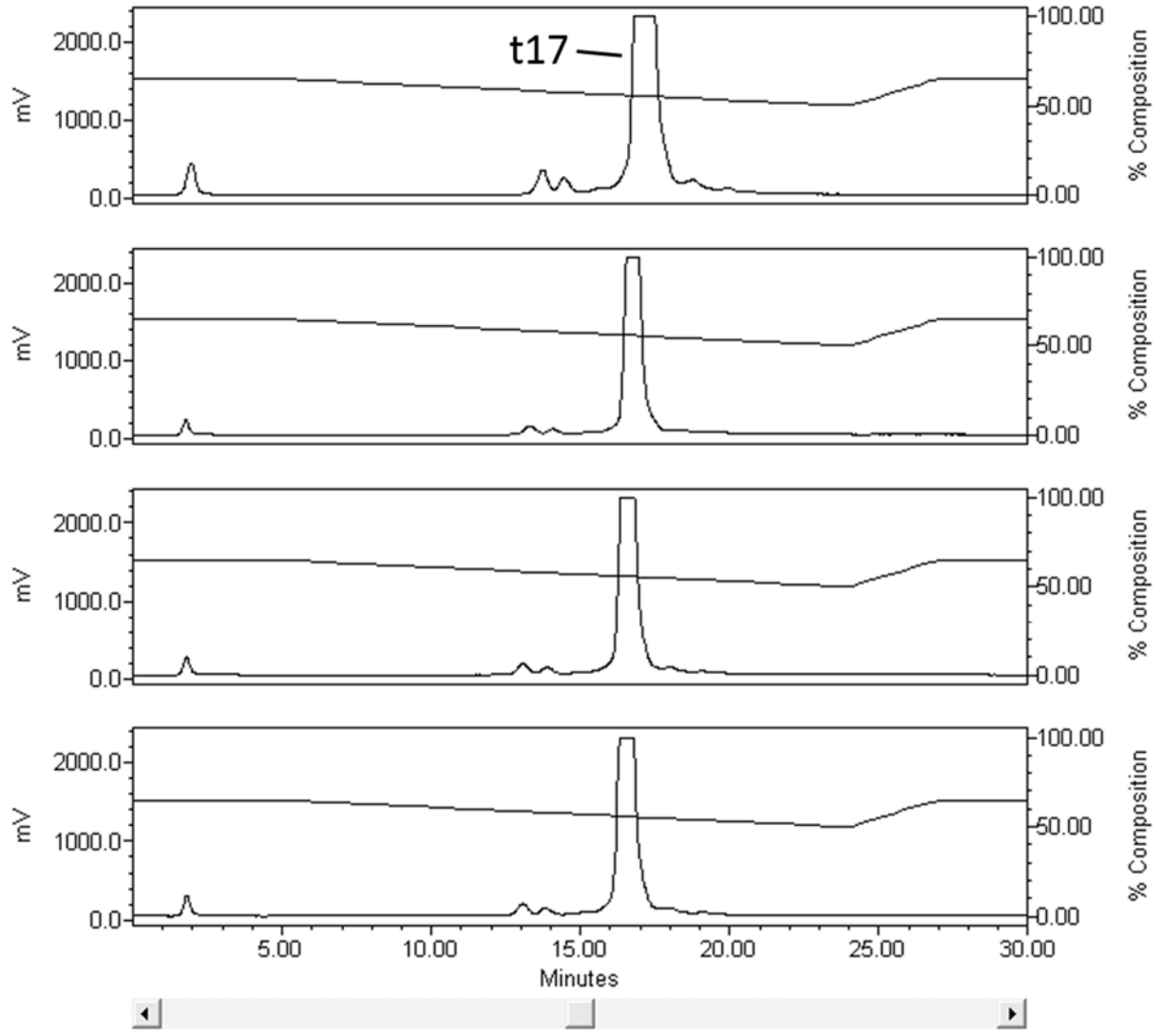

Visible	SampleName	Date Acquired	Injection	Injection Volume (uL)	Run Time (Minutes)	Instrument Method Name
☑	HF2-2 P1t20 YMC-PolyA-SP R1	10/13/2009 10:54:15 PM CDT	2	50.00	80.00	YMC PolyAmine SP vB
☑	HF2-2 P1t20 YMC-PolyA-SP R2	10/13/2009 11:38:42 PM CDT	3	25.00	60.00	YMC PolyAmine SP vB
☑	HF2-2 P1t20 YMC-PolyA-SP R3	10/14/2009 12:25:13 AM CDT	4	30.00	60.00	YMC PolyAmine SP vB
☑	HF2-2 P1t20 YMC-PolyA-SP R4	10/14/2009 1:14:02 AM CDT	5	30.00	60.00	YMC PolyAmine SP vB

Figure S41. Analytical HPLC-ELSD showing the relative purity for the Polyamine II fractions HF2-2P1t20A17, HF2-2P1t22A17, HF2-2P1t22A18, HF2-2P1t22A19 on the Atlantis dC_{18} sorbent.

All fractions were separated by the same analytical method on the same system as part of the same sample set. Different amounts were injected for each sample.

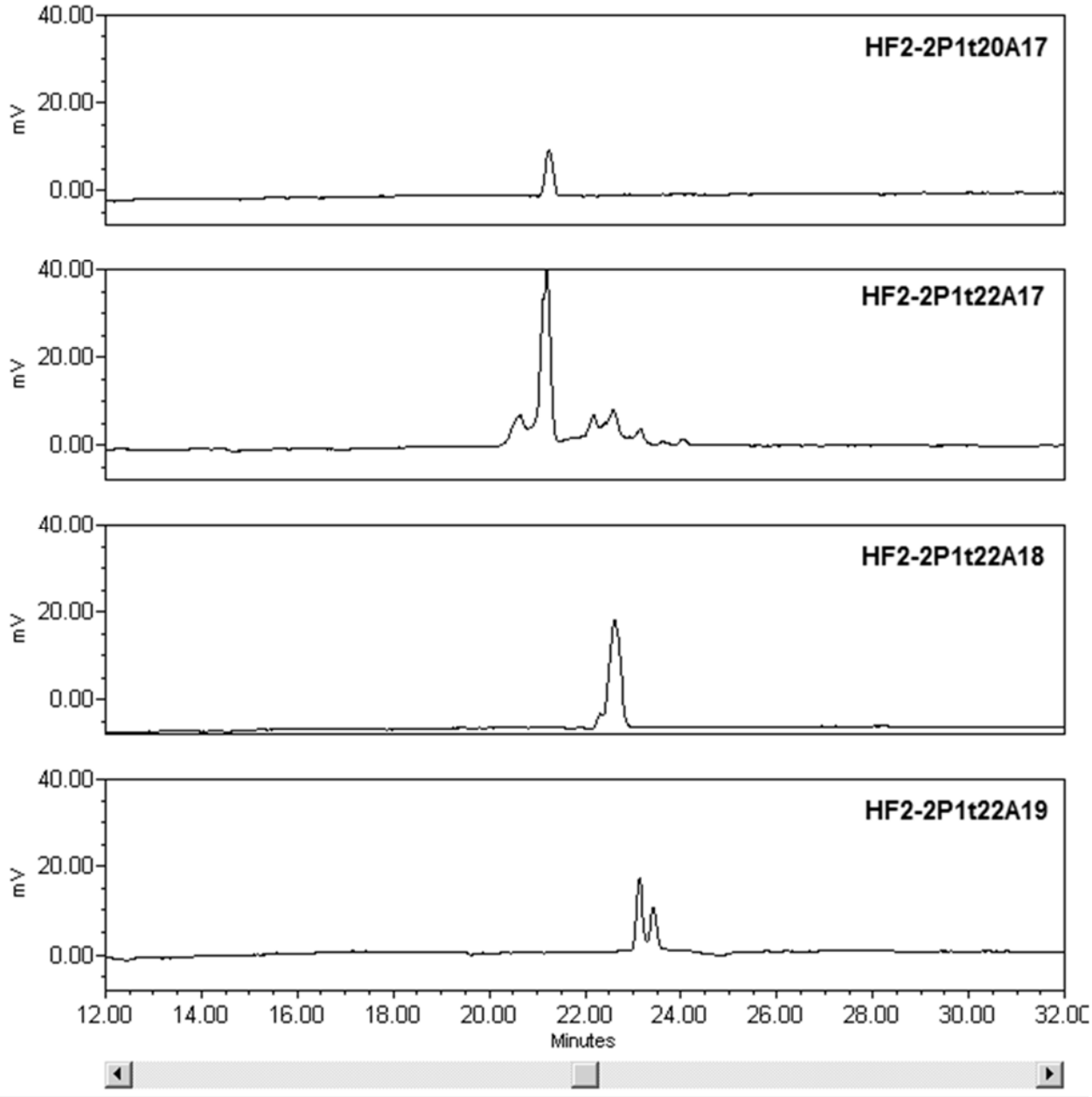

Visible	SampleName	Date Acquired	SampleWeight	Dilution	Injection Volume (uL)	Channel
☑	HF2-2P1t20A17 AtldC18-A R1	2/6/2010 8:06:08 PM CST	0.02000	200.00000	40.00	SATIN
☑	HF2-2P1t22A17v2 AtldC18-A R1	2/6/2010 6:13:53 PM CST	0.02000	200.00000	60.00	SATIN
☑	HF2-2P1t22A18 AtldC18-A R1	2/7/2010 10:58:51 AM CST	0.02000	200.00000	80.00	SATIN
☑	HF2-2P1t22A19 AtldC18-A R1	2/10/2010 7:45:00 AM CST	0.04000	200.00000	50.00	SATIN

Figure S42. ^{1}H NMR spectrum for HF2-2P1t22A17 in D2O with peak picking (400 MHz).

This fraction was determined to contain one major component with the same retention time as HF2-2P1t20A17 (the octasaccharide, compound **1**) on both the Polyamine and Atlantis dC$_{18}$ sorbents, indicating the presence of similar structural features and possibly the same primary component. An insufficient amount of material was available, however, for obtaining 2D NMR data to confirm whether or not this sample contained the same compound as HF2-2P1t20A17. Minor components could be detected in this material by HPLC-ELSD (Figure S41). This spectrum was acquired using all sample material available (1.9 mg) in a minimum amount of solvent.

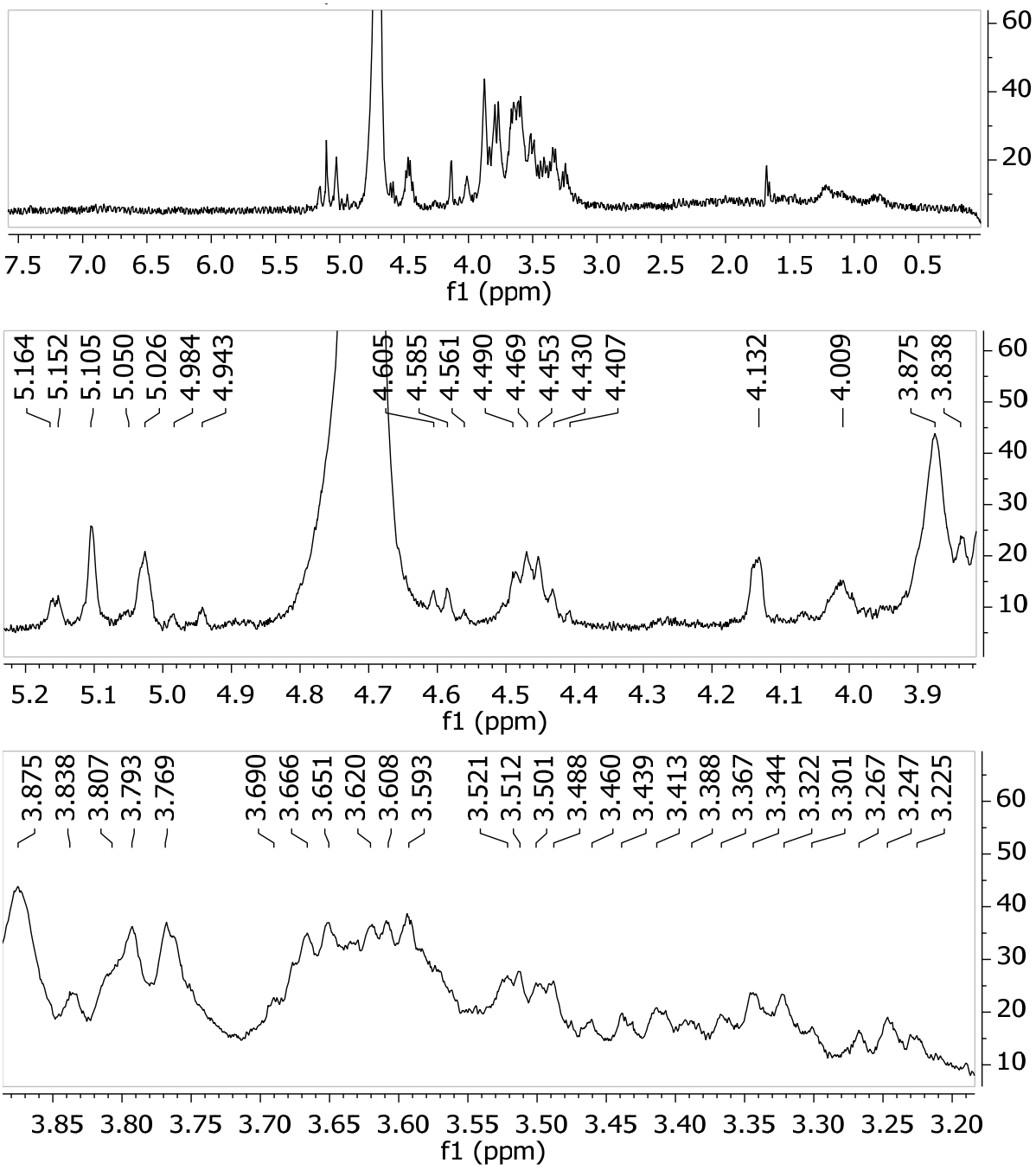

c. The Complexity of the Oligosaccharide Profile

Fractions collected from a single Atlantis dC$_{18}$ separation (e.g., IF1-3; Figure S31) were sequentially analyzed using the polyamine sorbent with an optimized analytical instrument and controlled, repeated conditions. Comparisons of the resulting analytical HPLC-ELSD spectra showed that fractions eluting with different Atlantis dC$_{18}$ retention times, and therefore different major components, contained compounds that had similar retention times on the polyamine sorbent (Figures S43–S45). For example, during semi-preparative separation, the IF1-3P1t20 subfraction collected from the Atlantis dC$_{18}$ column contains a major compound that appears at 16–17 min on the Polyamine column (Figure S46). This component overlaps in retention time with compounds in the t22 and t23 subfractions of IF1-3P1 even though they are derived from different parent Atlantis dC$_{18}$ fractions and are unlikely to contain the same components. Peaks that appear to contain single or major components in the Atlantis dC$_{18}$ chromatogram (e.g., the peak at 22 min; Figure S31) were also found to contain multiple components when examined on the Polyamine stationary phase (Figure S44). In non-enriched parent fractions, all such compounds would have overlapped and led to the observed poor resolution. These phenomena made the recombination of fractions from multiple separations especially challenging, as there was little certainty, based solely on retention time data, that any two peaks from related fractions represented the same compounds.

The amounts of material obtained for Atlantis dC$_{18}$-Polyamine purified fractions (0.5–5 mg or less; Tables S12 and S14-S19) were typically insufficient to obtain high quality ^{1}H NMR data suitable for guiding fraction recombinations. This was likely due partly to the high molecular weights of the compounds in question and partly to the high resonance overlap inherent to oligosaccharides. The general oligosaccharide nature of many purified compounds could be established by ^{1}H NMR, but the data obtained could not reliably distinguish two components with different retention times and different parent fractions. For most samples, sufficient purity could not be assured for the pursuit of chemically based structure elucidation approaches, and the limited quantities available made additional ELSD-based separations impractical due to the losses inherent to the split detection-collection design of the preparative system. The difficulty of obtaining baseline resolution between the components of the series indicated that compounds present possessed similar chromatographic properties, likely due to similar structures. Similarities in the NMR data that could be obtained indicated that many of the distinct compounds present have structures closely related to that subsequently established for **1**.

Figure S43. Analytical Polyamine HPLC-ELSD comparisons of IF1-3 Atlantis dC_{18} fractions t03, t05-t08, t08-11, t19, and B, showing the changes in elution profile associated with the change in sorbent.

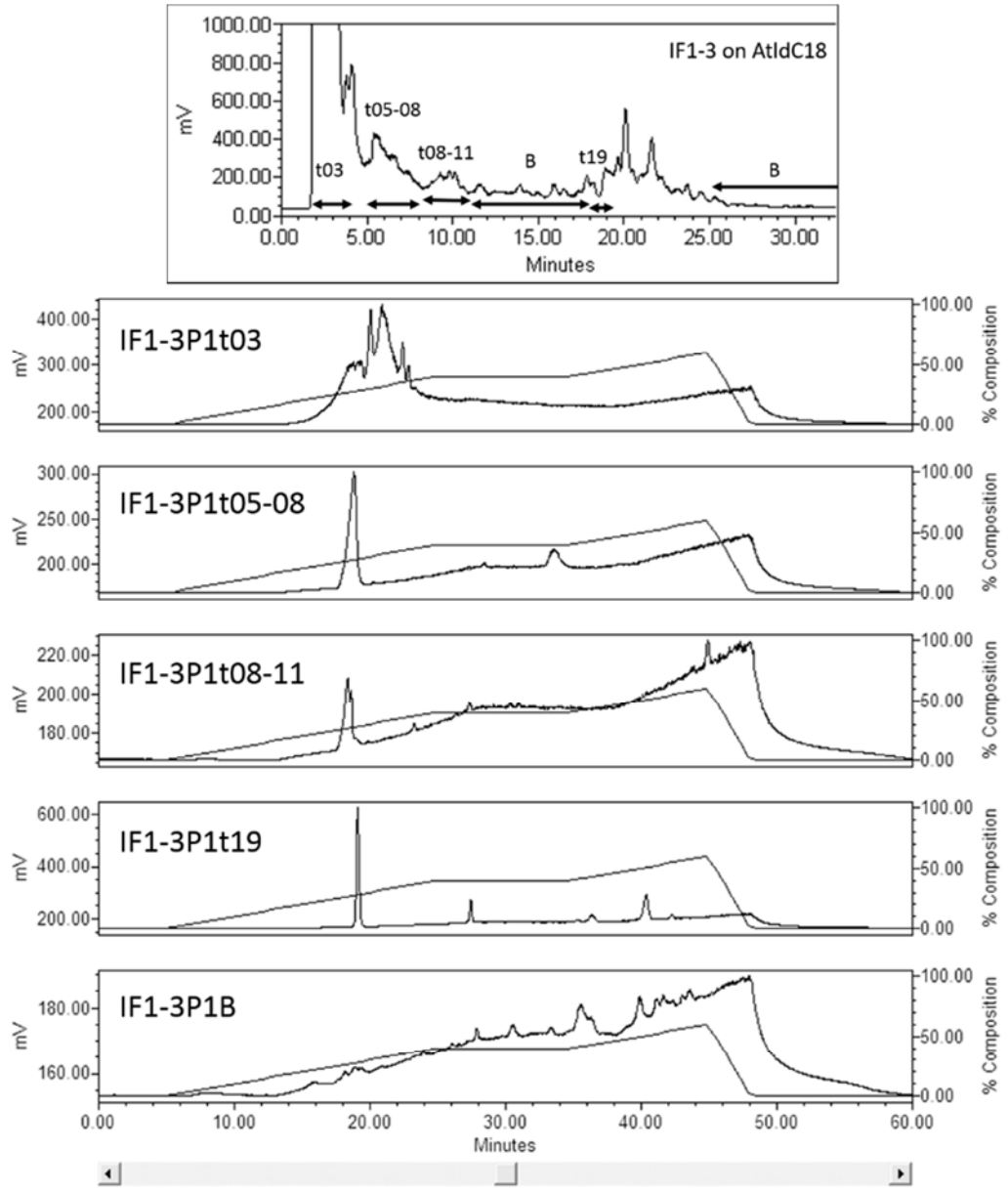

Visible	SampleName	SampleWeight	Dilution	Injection Volume (uL)	Channel Name	Date Acquired	Acq Method Set
☑	IF1-3 P1t03 YMC-PolyA-SP R2	1.80000	200.00000	25.00	SATIN	9/3/2009 10:26:29 PM CDT	YMC PolyA SP
☑	IF1-3 P1t05-08 YMC-PolyA-SP R1	0.40000	100.00000	45.00	SATIN	9/4/2009 12:39:30 AM CDT	YMC PolyA SP
☑	IF1-3 P1t08-11 YMC-PolyA-SP R1	0.30000	75.00000	30.00	SATIN	9/4/2009 1:45:49 AM CDT	YMC PolyA SP
☑	IF1-3 P1t19 YMC-PolyA-SP R1	0.40000	100.00000	40.00	SATIN	9/4/2009 3:58:30 AM CDT	YMC PolyA SP
☑	IF1-3 P1-B YMC-PolyA-SP R2	1.00000	250.00000	80.00	SATIN	9/4/2009 11:27:11 PM CDT	YMC PolyA SP

Figure S44. Analytical Polyamine HPLC-ELSD comparisons of IF1-3 Atlantis dC_{18} fractions t19.5, t20, t21, t22, and t22.5, showing the changes in elution profile associated with the change in sorbent.

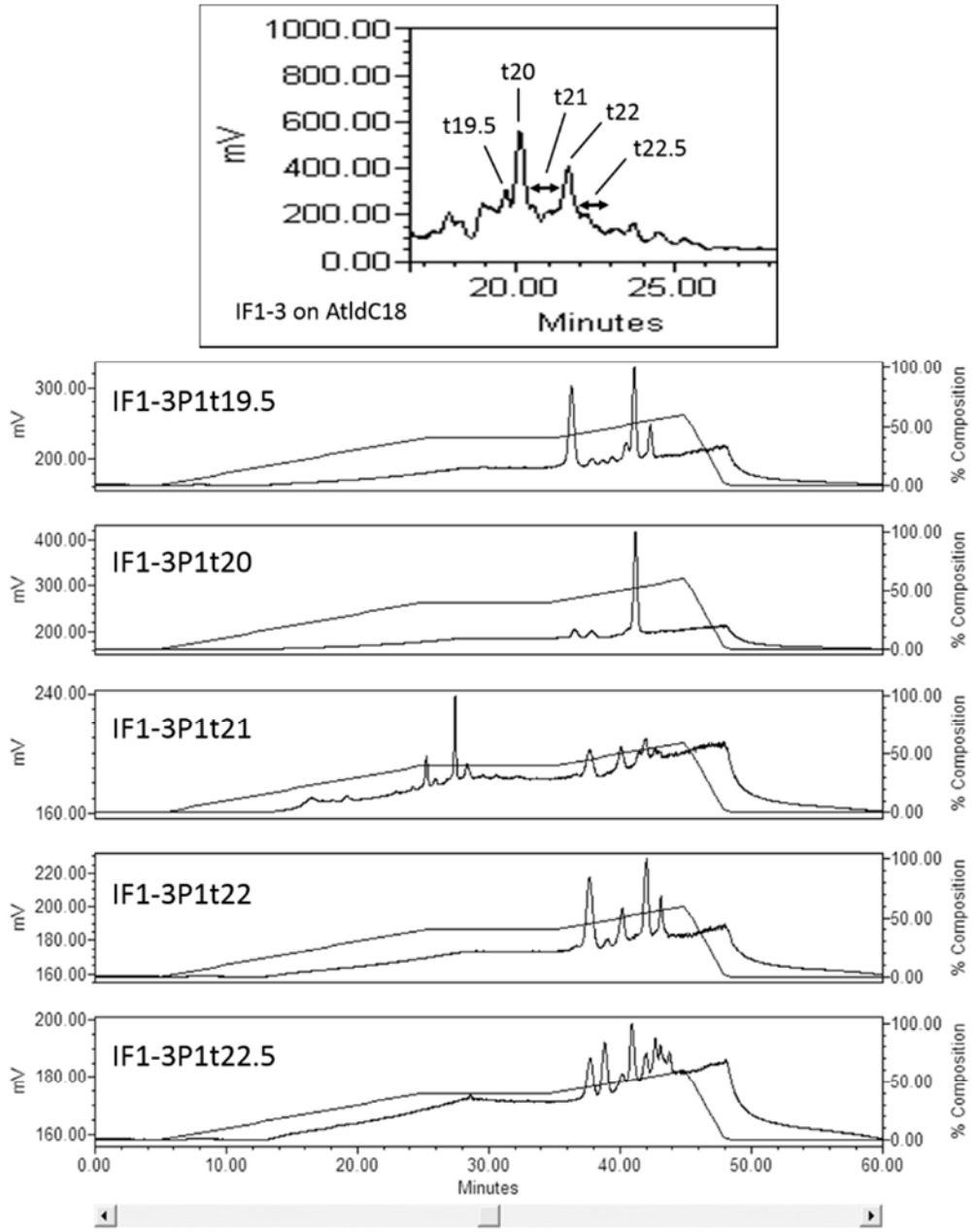

Visible	SampleName	SampleWeight	Dilution	Injection Volume (uL)	Channel Name	Date Acquired	Acq Method Set
☑	IF1-3 P1t19.5 YMC-PolyA-SP R1	0.20000	50.00000	25.00	SATIN	9/4/2009 5:04:50 AM CDT	YMC PolyA SP
☑	IF1-3 P1t20 YMC-PolyA-SP R2	0.50000	100.00000	30.00	SATIN	9/4/2009 6:11:24 AM CDT	YMC PolyA SP
☑	IF1-3 P1t21 YMC-PolyA-SP R1	0.50000	125.00000	40.00	SATIN	9/4/2009 7:18:00 AM CDT	YMC PolyA SP
☑	IF1-3 P1t22 YMC-PolyA-SP R1	0.30000	75.00000	30.00	SATIN	9/4/2009 9:30:38 AM CDT	YMC PolyA SP
☑	IF1-3 P1t22.5 YMC-PolyA-SP R1	0.40000	100.00000	40.00	SATIN	9/4/2009 10:36:59 AM CDT	YMC PolyA SP

Figure S45. Analytical Polyamine HPLC-ELSD comparisons of IF1-3 Atlantis dC_{18} fractions t22.5, t23, t24, and t25, showing the changes in elution profile associated with the change in sorbent.

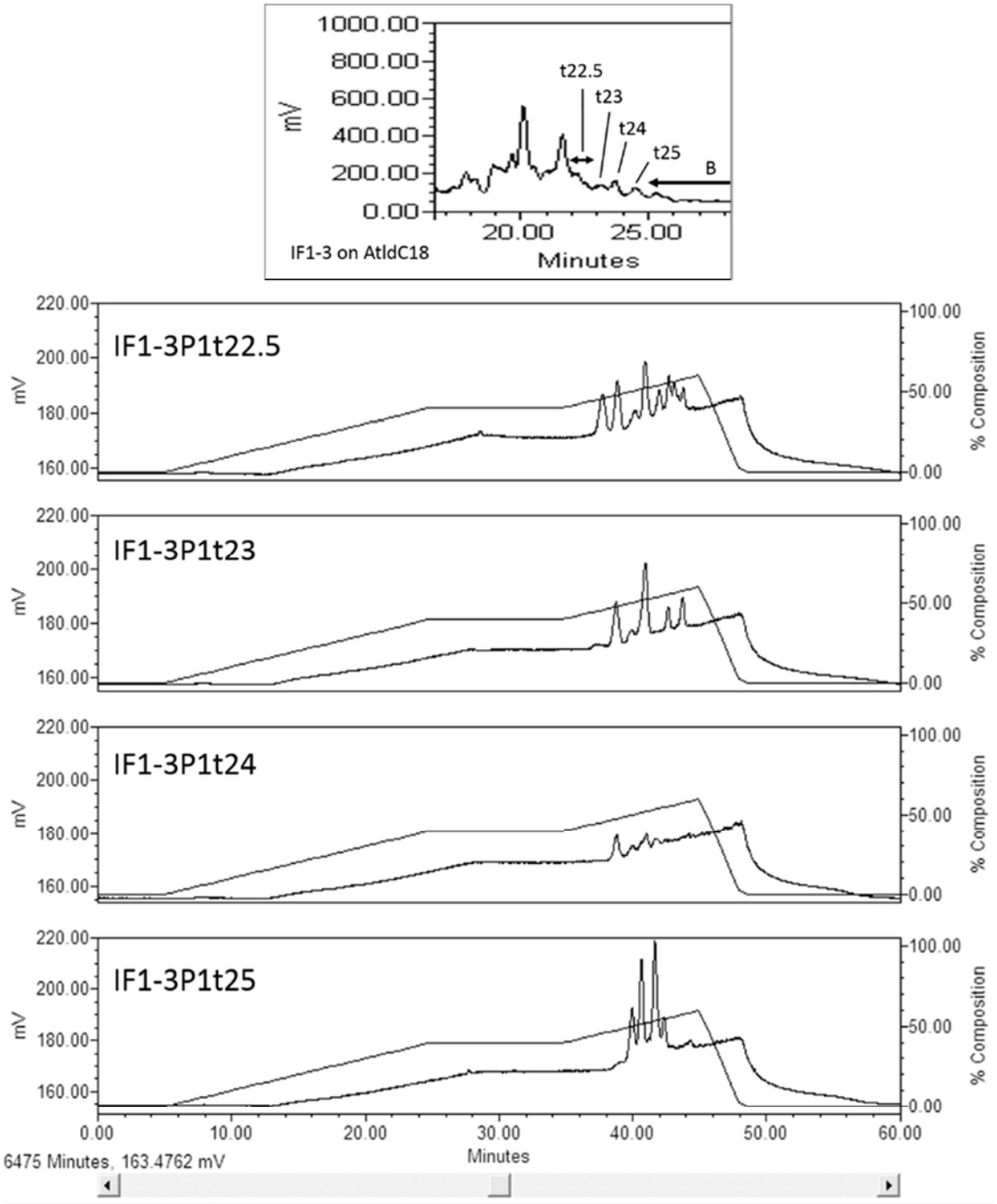

Visible	SampleName	SampleWeight	Dilution	Injection Volume (uL)	Channel Name	Date Acquired	Acq Method Set
☑	IF1-3 P1t22.5 YMC-PolyA-SP R1	0.40000	100.00000	40.00	SATIN	9/4/2009 10:36:59 AM CDT	YMC PolyA SP
☑	IF1-3 P1t23 YMC-PolyA-SP R1	0.30000	75.00000	30.00	SATIN	9/4/2009 11:43:16 AM CDT	YMC PolyA SP
☑	IF1-3 P1t24 YMC-PolyA-SP R1	0.20000	50.00000	25.00	SATIN	9/4/2009 3:06:56 PM CDT	YMC PolyA SP
☑	IF1-3 P1t25 YMC-PolyA-SP R1	0.20000	50.00000	25.00	SATIN	9/4/2009 4:12:56 PM CDT	YMC PolyA SP

Figure S46. Semi-preparative HPLC-ELSD separations for IF1-3P1 subfractions (Polyamine). The arrow indicating the peak at t17 min corresponds to compound **1**.

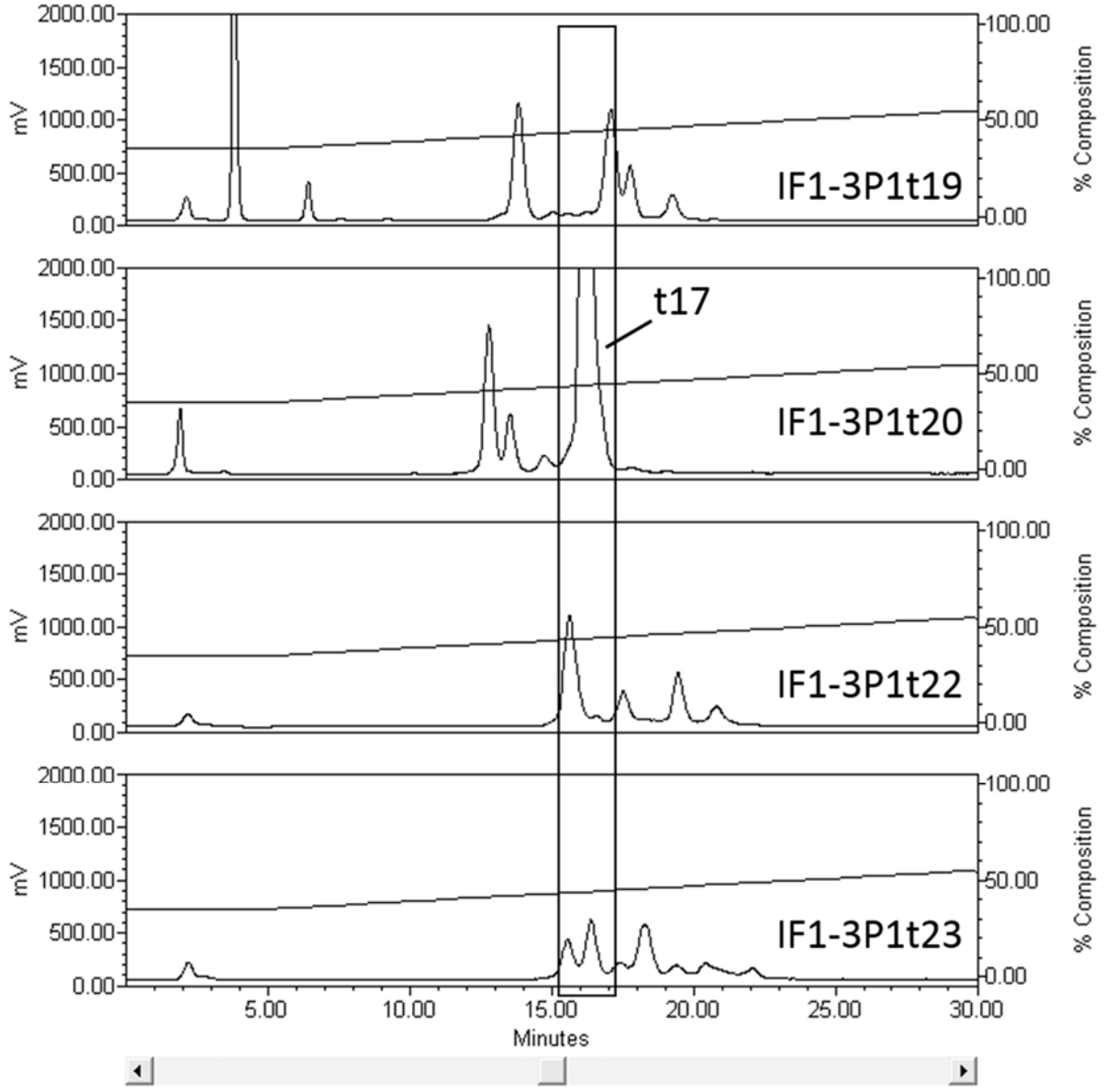

Visible	SampleName	Injection Volume (uL)	Det. Units	Date Acquired	Acq Method Set
☑	IF1-3 P1t19 YMC-PolyA-SP R1	40.00	mV	10/11/2009 4:43:24 PM CDT	YMC PolyAmine SP vB
☑	IF1-3 P1t20 YMC-PolyA-SP R1	30.00	mV	10/12/2009 11:03:51 PM CDT	YMC PolyAmine SP vB
☑	IF1-3 P1t22 YMC-PolyA-SP R1	50.00	mV	10/13/2009 12:38:13 PM CDT	YMC PolyAmine SP vB
☑	IF1-3 P1t23 YMC-PolyA-SP R1	60.00	mV	10/13/2009 1:34:33 PM CDT	YMC PolyAmine SP vB

Section S4. Carbohydrate Derivatization Analyses for Structure Elucidation

a. Glycosyl Composition

Glycosyl composition was determined using gas chromatography/mass spectrometry (GC-MS) of per-*O*-trimethylsilyl (TMS) derivatives of the sample. Monosaccharide methyl glycosides were produced by acidic methanolysis (1 M HCl in MeOH at 80 °C, 18–22 h), followed by re-*N*-acetylation with pyridine and acetic anhydride in MeOH for detection of amino sugars. The sample was then per-*O*-trimethylsilylated by treatment with Tri-Sil (Pierce) at 80 °C (30 min) as described previously.[4,5] Inositol was added to the sample before derivatization as an internal standard (20 μg per sample). GC-MS analysis of the TMS methyl glycosides was performed on an HP 6890 GC interfaced to a 5975b mass selective detector, using an All Tech EC-1 fused silica capillary column (30 m × 0.25 mm ID). Monosaccharides were identified by comparisons of retention times to those of standards, and mass spectra were used to authenticate the carbohydrate nature of the derivatives.

b. Glycosyl Linkage (NaOH method)

For glycosyl linkage analysis, the sample was permethylated, depolymerized, reduced, and acetylated. The resulting partially methylated alditol acetates (PMAAs) were analyzed by GC-MS.[5] Initially, an aliquot of the sample after dialysis was suspended in about 200 μL of DMSO. The sample was then permethylated using treatment with NaOH and CH_3I in dry DMSO.[6] The sample was subjected to NaOH base for 10 min and CH_3I was added and left for 20 min. This process was repeated to ensure complete methylation. Following sample workup, the permethylated material was reduced by superdeuteride to the methyl ester of uronic acid, hydrolyzed using 2 M TFA (2 h in a sealed tube at 121 °C), reduced with $NaBD_4$, and acetylated using Ac_2O/TFA. The resulting PMAAs were analyzed on a Hewlett Packard 5890 GC interfaced to a 5970 mass selective detector (electron impact ionization mode). Separation was performed on a Supelco 2330 bonded phase fused silica capillary column (30 m).

c. MALDI-MS

The sample was dissolved in deionized water (1 mg/mL) and 1 µL of the solution was deposited on a spot of 2,5-dihydroxybenzoic acid matrix dried from MeCN:water (1:1). This material was subjected to MALDI-MS on a Bruker MicroFlex Mass Spectrometer (positive ion mode). All masses were calibrated to malto-oligosaccharide controls analyzed immediately before the sample.

d. Monomer Configuration

The absolute configuration of monomeric glycosyl units was determined by comparisons between derivatized compound substituents and derivatized standards. The sample was hydrolyzed in 2 M TFA (500 µL) at 120 ºC for 1.5 h, the hydrolysate was dissolved in 200 µL (*S*)-(+)-2-BuOH (Fluka 19025), 15 µL acetyl chloride (Aldrich 236691) was added, and N_2 was bubbled through the solution for 30 s. The mixture was capped tightly and incubated at 80 ºC for 16 h. The mixture was dried under N_2 and absolute MeOH was added to ensure sample dryness. To the dry sample, 250 µL TMS was added and derivatization was carried out at 121 ºC for 20 min. The same procedure was applied to authentic standards D-Glc, L-Ara, and D-Xyl; two sets of standards were derivatized to which either (*S*)-(+)-2-BuOH or (*R*)-(-)-2-BuOH was added separately. The sample and standard derivatives were analyzed on an Agilent 5975C GC interfaced with a 7890A MS detector.

e. Oligosaccharide Sequence

Glycosyl sequence was determined using per-*O*-methylated glycans analyzed by Nanospray Ionization-Linear Ion Trap Mass Spectrometry (NSI-MS^n).[7] The sample was dissolved in DMSO, permethylated as previously described,[7] extracted with DCM, and dried under N_2. The resulting per-*O*-methylated glycan was dissolved in 1 mM NaOH in 50% MeOH and directly infused with a syringe flow rate of 0.5 µL/min into an LTQ Orbitrap Discoverer mass spectrometer (Thermo Scientific) equipped with a nanospray ion source. The capillary temperature was set to 210 °C, and MS analysis was performed in positive ion mode with fragmentation by CID (25% collision energy) in MS/MS and MS^n modes. Indicative partial-fragmentation patterns from NSI-MS^n analysis of the per-*O*-methylated derivative of **1** were used to confirm side chain linkage positions and establish monomer connectivity.

Section S5. Interpretation of the MS^n Fragmentation Pattern Results.

A pure sample of **1** was derivatized via per-*O*-methylation and then subjected to NSI-MS with fragmentation by CID in MS/MS and MS^n modes using direct infusion of the sample. As the only material in the sample was the compound of interest, resulting fragment ions were presumed to have been generated from this material. The derivative produced from **1** was detected as singly and doubly (2+) charged species (Figure S47) and selected ions were subjected to additional fragmentation.

Two possible structures for **1** were consistent with the data from previous analyses (Figure S48). These could be distinguished using the results of the fragmentation pattern analysis, even though mass fragments were only generated at unit resolution due to the nature of the method used. Methylation patterns and knowledge of typical fragmentation sites (glycosidic bonds) and fragmentation sequences for oligosaccharides made it possible to distinguish between different mass fragments and associate the resulting mass losses with the two putative structures for **1**.[8-11] Terminal, internal, and reducing glucopyranosyl residues could be distinguished based on unit mass differences of 218 (terminal), 190 (internal), and 236 (reducing) amu. Arabinofuranosyl and xylopyranosyl residues could also be distinguished based on mass losses of 174 and 160 amu, respectively, or 334 amu for an Ara-Xyl side chain.

Figure S47. Results of the NSI-MS-based glycosyl linkage analysis showing mass fragments for the per-*O*-methylated derivative of **1**.

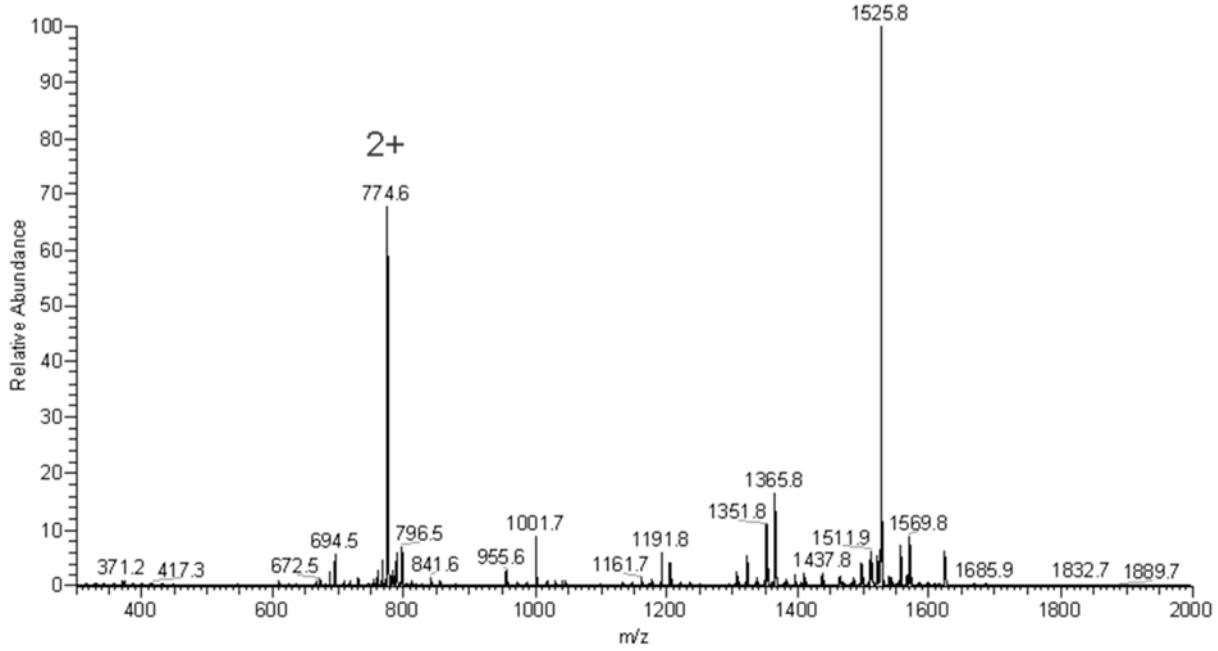

Figure S48. Possible structures for **1** showing placement of a Xyl-Ara side chain on either Glc*p*-B (a) or Glc*p*-A (b).

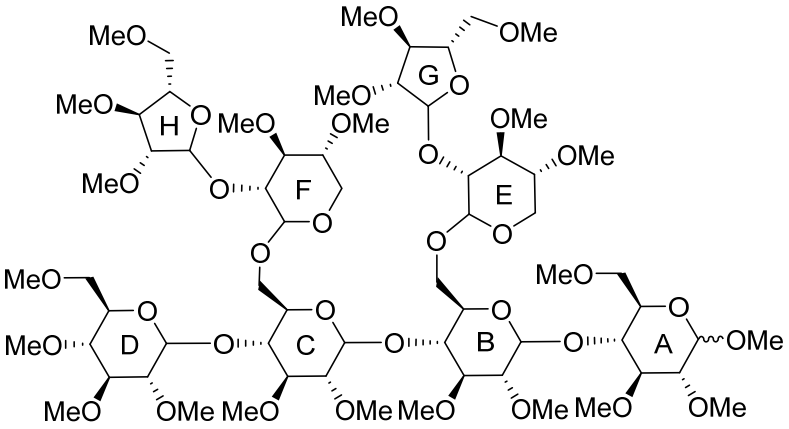

(a)

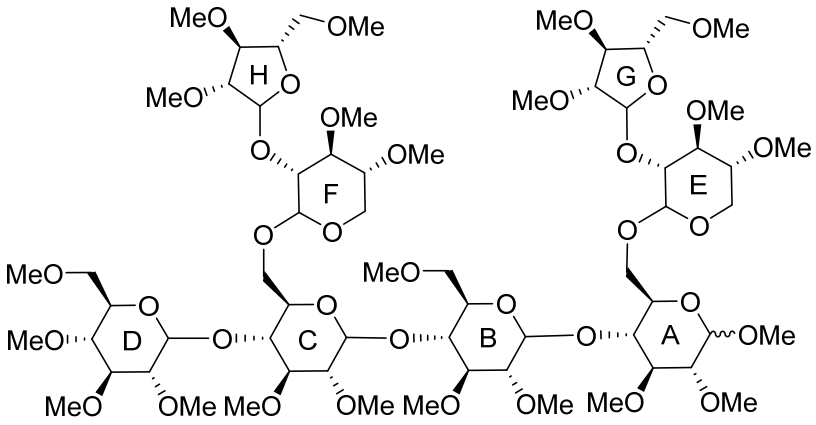

(b)

The NSI-MS^2 fragmentation at *m/z* 1526 for the per-*O*-methylated derivative of **1** (Figure S49) gave indicative mass fragments of *m/z* 1352, 1308, 1290, 1192, and 784. The mass fragment of *m/z* 1352 is consistent with the loss of a terminal arabinose (Δ*m/z* = 174), *m/z* 1308 is consistent with the loss of terminal glucose (Δ*m/z* = 218), *m/z* 1290 is consistent with the loss of reducing end glucose (Δ*m/z* = 236), *m/z* 1192 is consistent with the loss of a terminal arabinose and an internal xylose (Δ*m/z* = 334), and *m/z* 784 is consistent with the loss of a terminal arabinose, an internal xylose, an internal glucose and a terminal glucose (Δ*m/z* = 742). These mass fragments were consistent with structure (a) (Figure S50), as structure (b) (Figure S51) did not result in the production of an *m/z* 1290 fragment corresponding to the loss of a reducing end glucose (Δ*m/z* = 236). Ions at *m/z* 1308 and 1352 were selected for further fragmentation.

Figure S49. The NSI-MS^2 fragmentation at *m/z* 1526 for the per-*O*-methylated derivative of **1**.

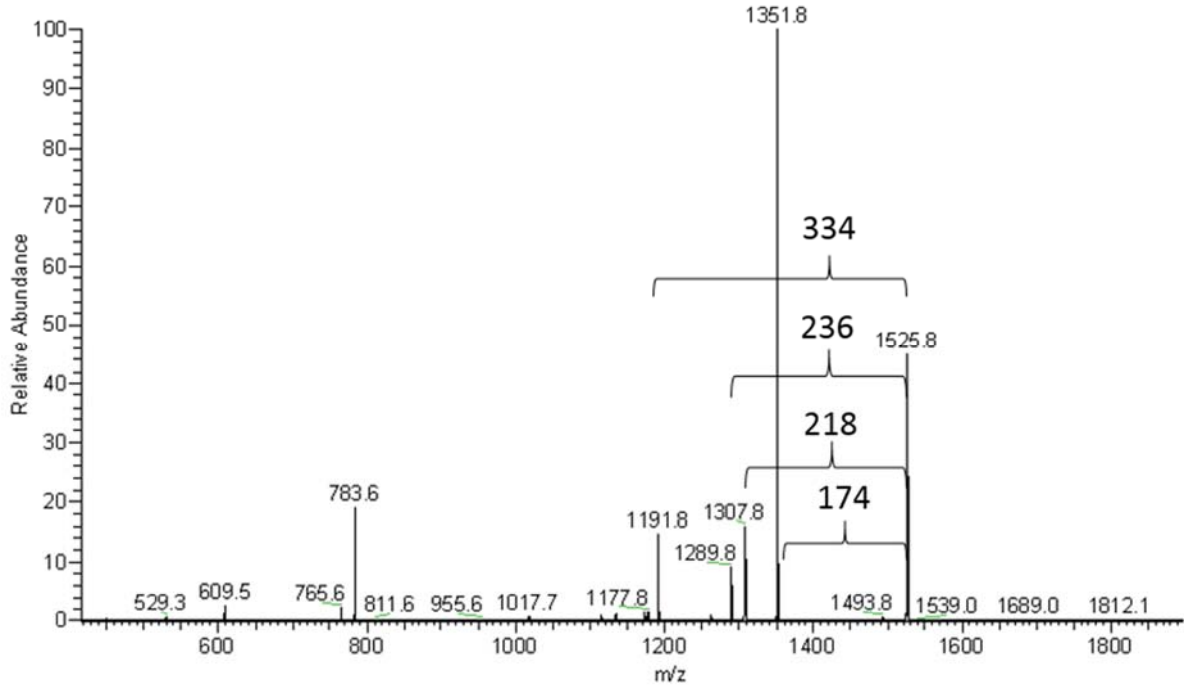

Figure S50. Structure (a) putative mass fragments produced from the *m/z* 1526 parent ion of per-*O*-methylated **1**.

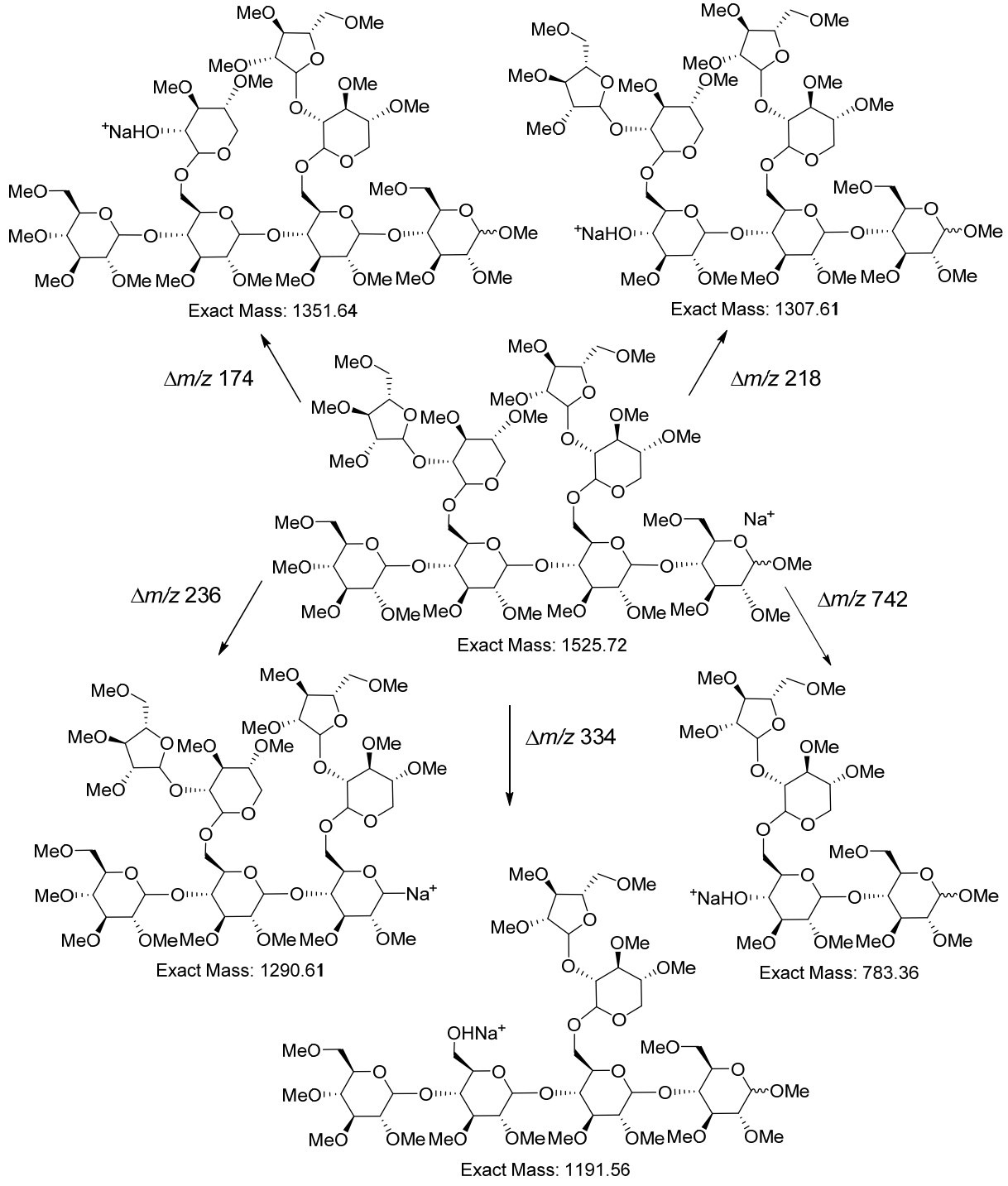

Figure S51. Structure (b) putative mass fragments produced from the *m/z* 1526 parent ion of per-*O*-methylated **1**.

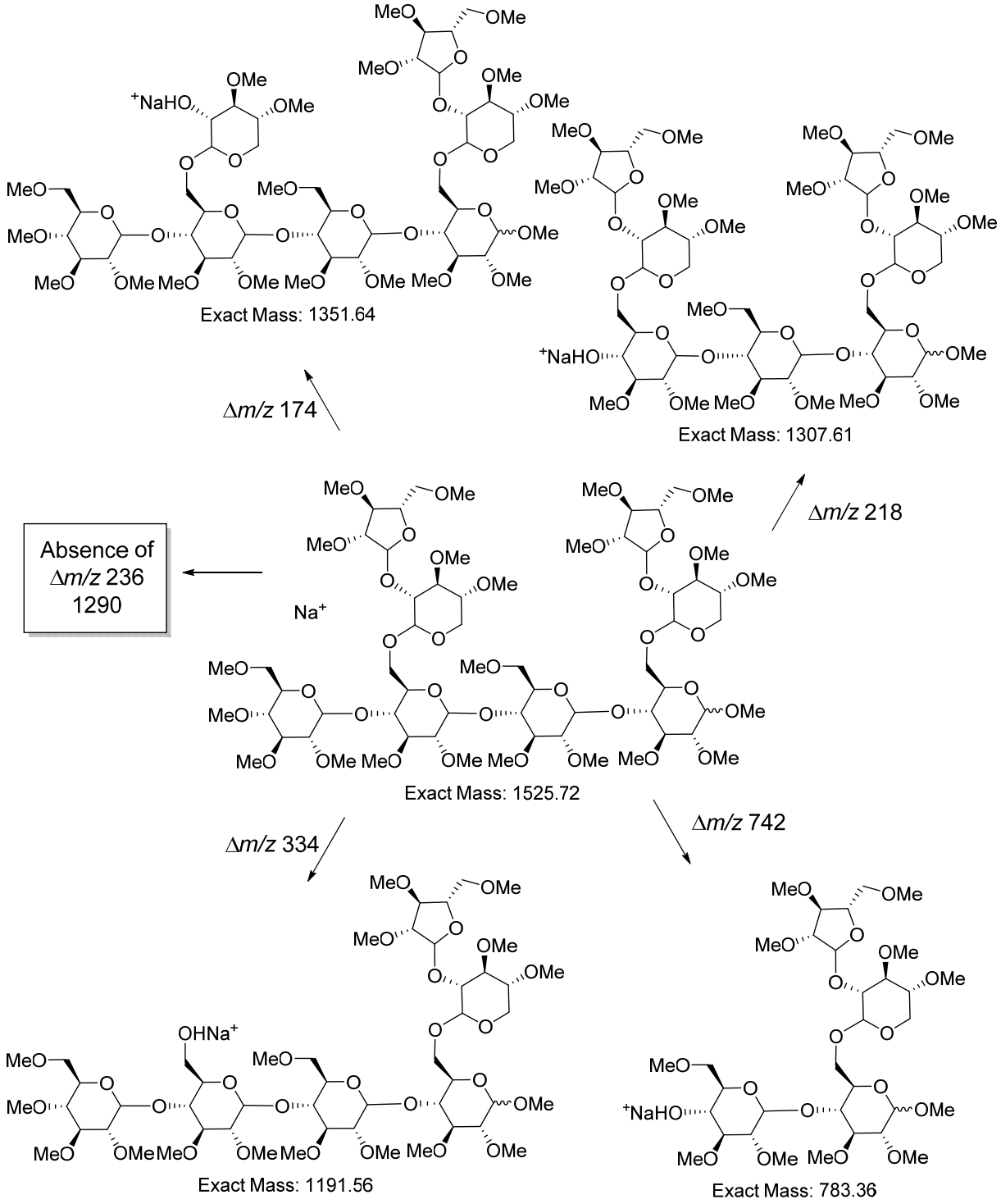

The NSI-MS^3 fragmentation at *m/z* 1526 → 1308 for the per-*O*-methylated derivative of **1** (Figure S52) gave indicative mass fragments of *m/z* 1134, 1072, 974, and 784. This spectrum was generated using CID = 30%. The mass fragment of *m/z* 1134 is consistent with the loss of a terminal arabinose (Δ*m/z* = 174), *m/z* 1072 is consistent with the loss of a reducing end glucose (Δ*m/z* = 236), *m/z* 974 is consistent with the loss of a terminal arabinose and an internal xylose (Δ*m/z* = 334), and *m/z* 784 is consistent with the loss of a terminal arabinose, an internal xylose, and an internal glucose (Δ*m/z* = 524). These mass fragments were consistent with structure (a) (Figure S53), as the putative *m/z* 1308 fragment of structure (b) (Figure S54) did not produce a fragment at *m/z* 1072 corresponding to the loss of a reducing end glucose (Δ*m/z* = 236).

Figure S52. The NSI-MS^3 fragmentation at *m/z* 1526 → 1308 for the per-*O*-methylated derivative of **1**.

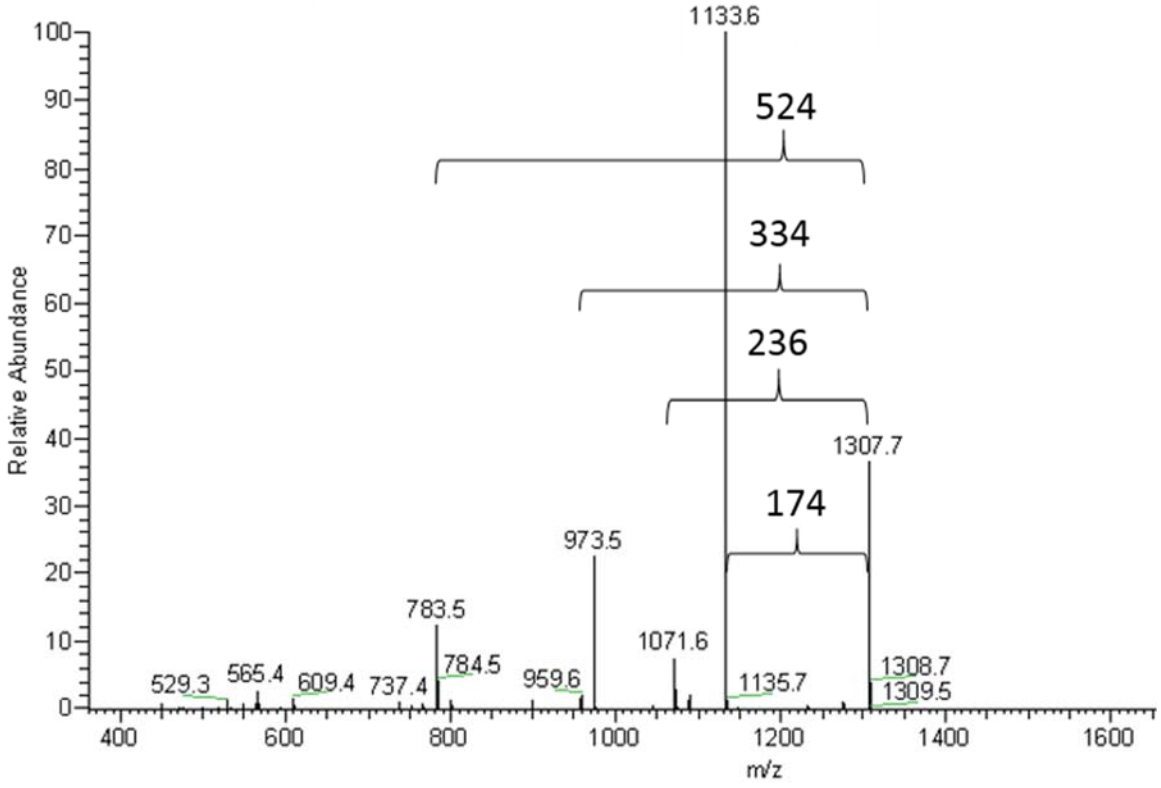

Figure S53. Structure (a) putative mass fragments produced from the *m/z* 1308 fragment of per-*O*-methylated **1**.

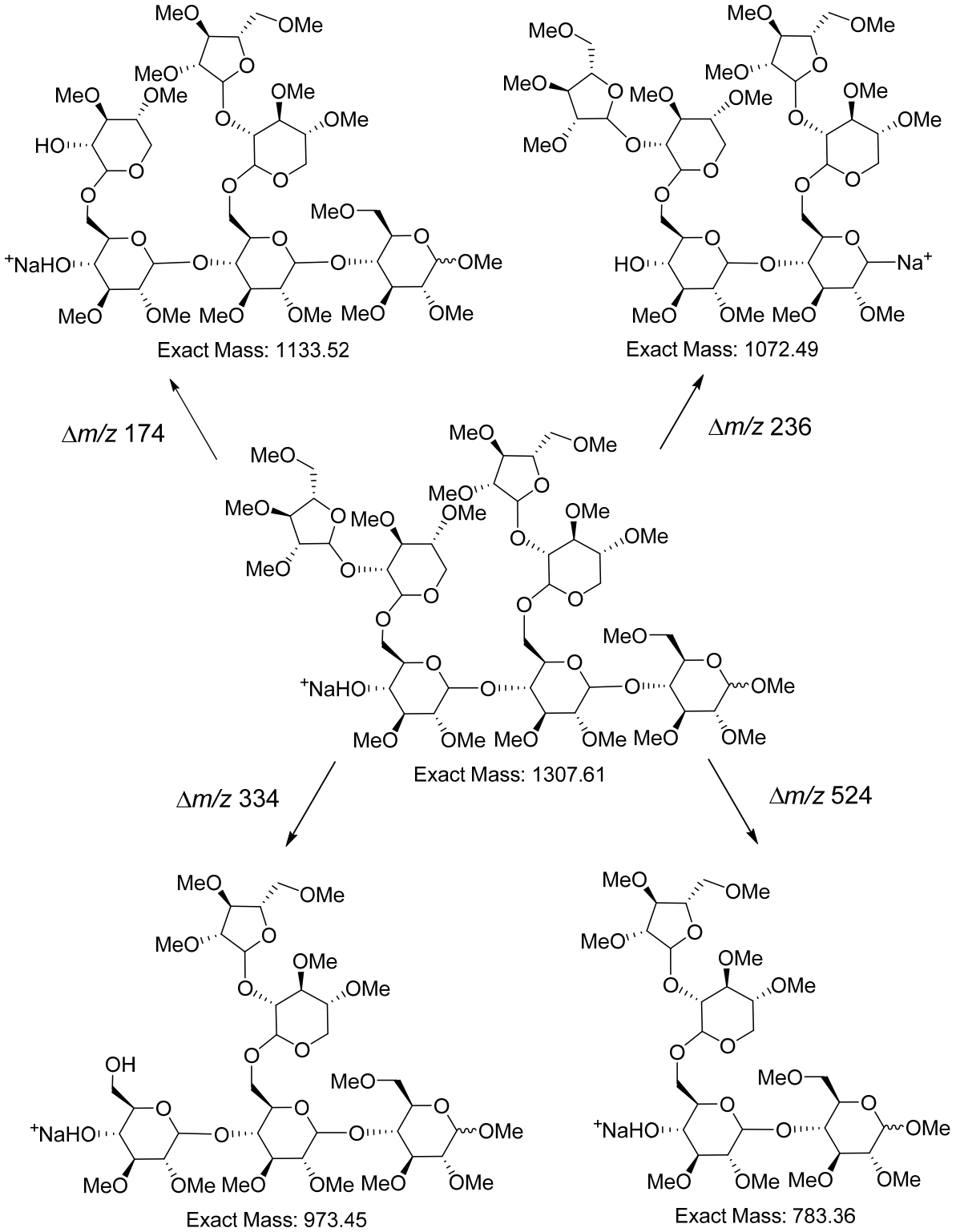

Figure S54. Structure (b) putative mass fragments produced from the *m/z* 1308 fragment of per-*O*-methylated **1**.

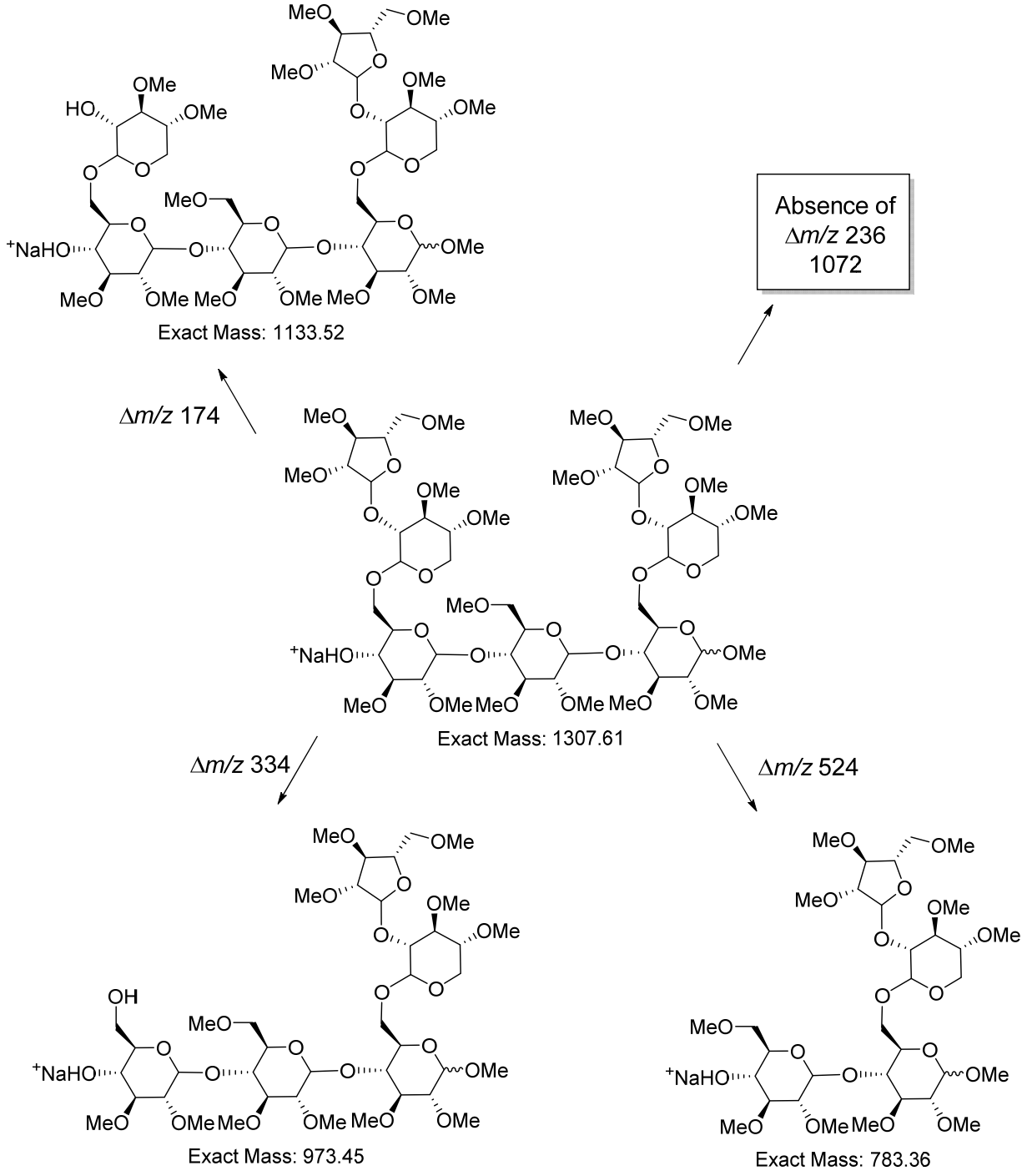

The NSI-MS^3 fragmentation at *m/z* 1526 → 1352 for the per-*O*-methylated derivative of **1** (not shown; see Figures S50 and S51 for putative structures of the *m/z* 1352 ion) yielded a high intensity, indicative fragment at *m/z* 1192, with additional low intensity mass fragments of *m/z* 1178, 1017, 955, 857, and 784. The *m/z* 1178 fragment was consistent with the loss of a terminal arabinose (Δ*m/z* = 174), and the *m/z* 1192 fragment was consistent with the loss of an internal xylose (Δ*m/z* = 160). The fragmentation pattern for the *m/z* 1352 ion was of minimal utility in distinguishing between the two putative structures for **1**, and the highest intensity ion at *m/z* 1192 was therefore selected for further fragmentation.

The NSI-MS^4 fragmentation at *m/z* 1526 → 1352 → 1192 for the per-*O*-methylated derivative of **1** (Figure S55) gave indicative mass fragments of *m/z* 1017, 974, 955, 857, and 784. The mass fragment of *m/z* 1017 is consistent with the loss of a terminal arabinose (Δ*m/z* = 174), *m/z* 974 is consistent with the loss of a terminal glucose (Δ*m/z* = 218), *m/z* 955 is consistent with the loss of a reducing end glucose (Δ*m/z* = 236), *m/z* 857 is consistent with the loss of an internal xylose and a terminal arabinose (Δ*m/z* = 334), and *m/z* 784 is consistent with the loss of a terminal and an internal glucose (Δ*m/z* = 408). These mass fragments were consistent with structure (a) (Figure S56), as the putative *m/z* 1192 fragment of structure (b) (Figure S57) did not produce a fragment at *m/z* 955 corresponding to the loss of a reducing end glucose. The *m/z* 1192 fragment of structure (b) would also have been expected to result in a fragment at *m/z* 579 corresponding to the loss of a terminal glucose and two internal glucose units (Δ*m/z* = 612). This fragment was not present in the NSI-MS^4 data at *m/z* 1192. The ion at *m/z* 784 was selected for further fragmentation.

Figure S55. The NSI-MS^4 fragmentation at *m/z* 1526 → 1352 → 1192 for the per-*O*-methylated derivative of **1**.

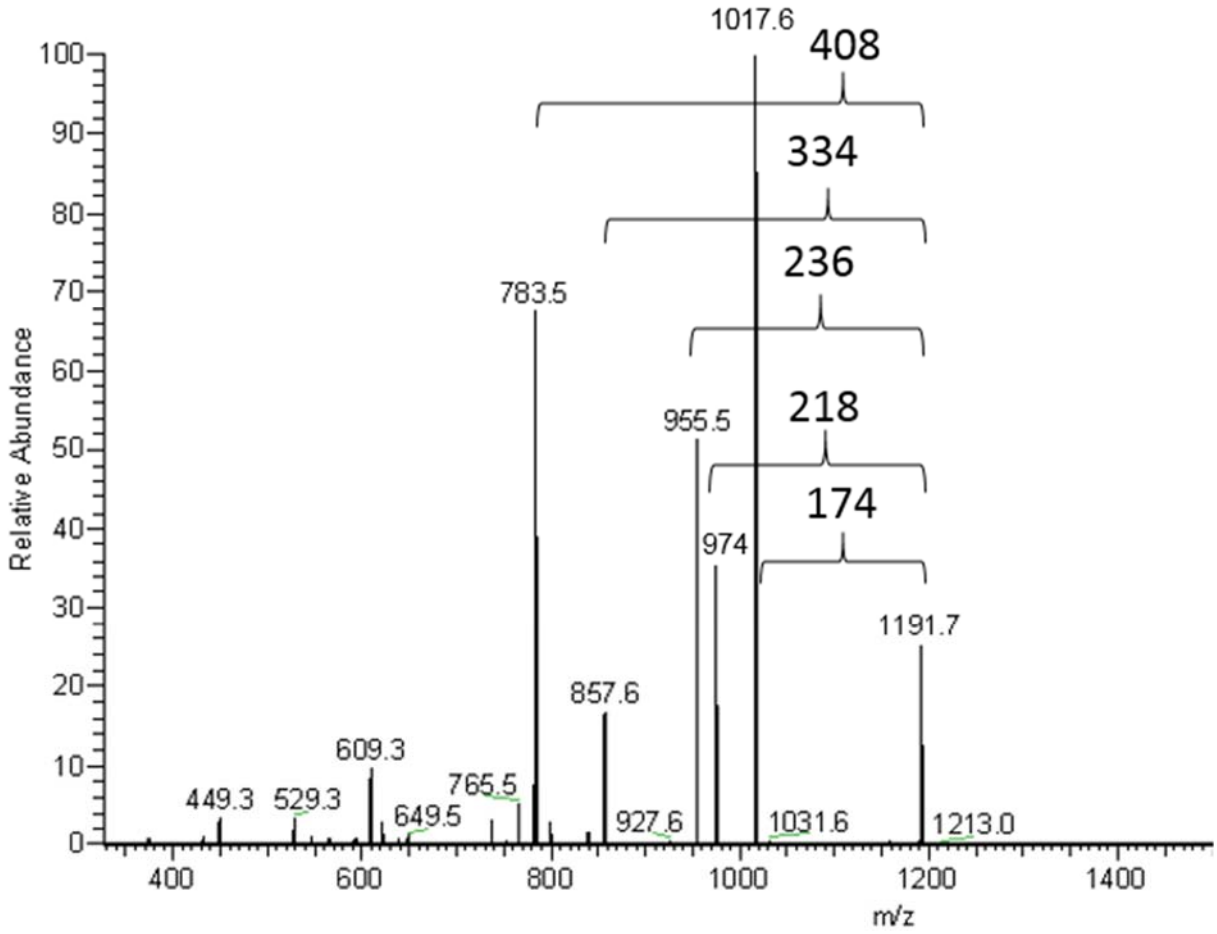

Figure S56. Structure (a) putative mass fragments produced from the *m/z* 1192 fragment of per-*O*-methylated **1**.

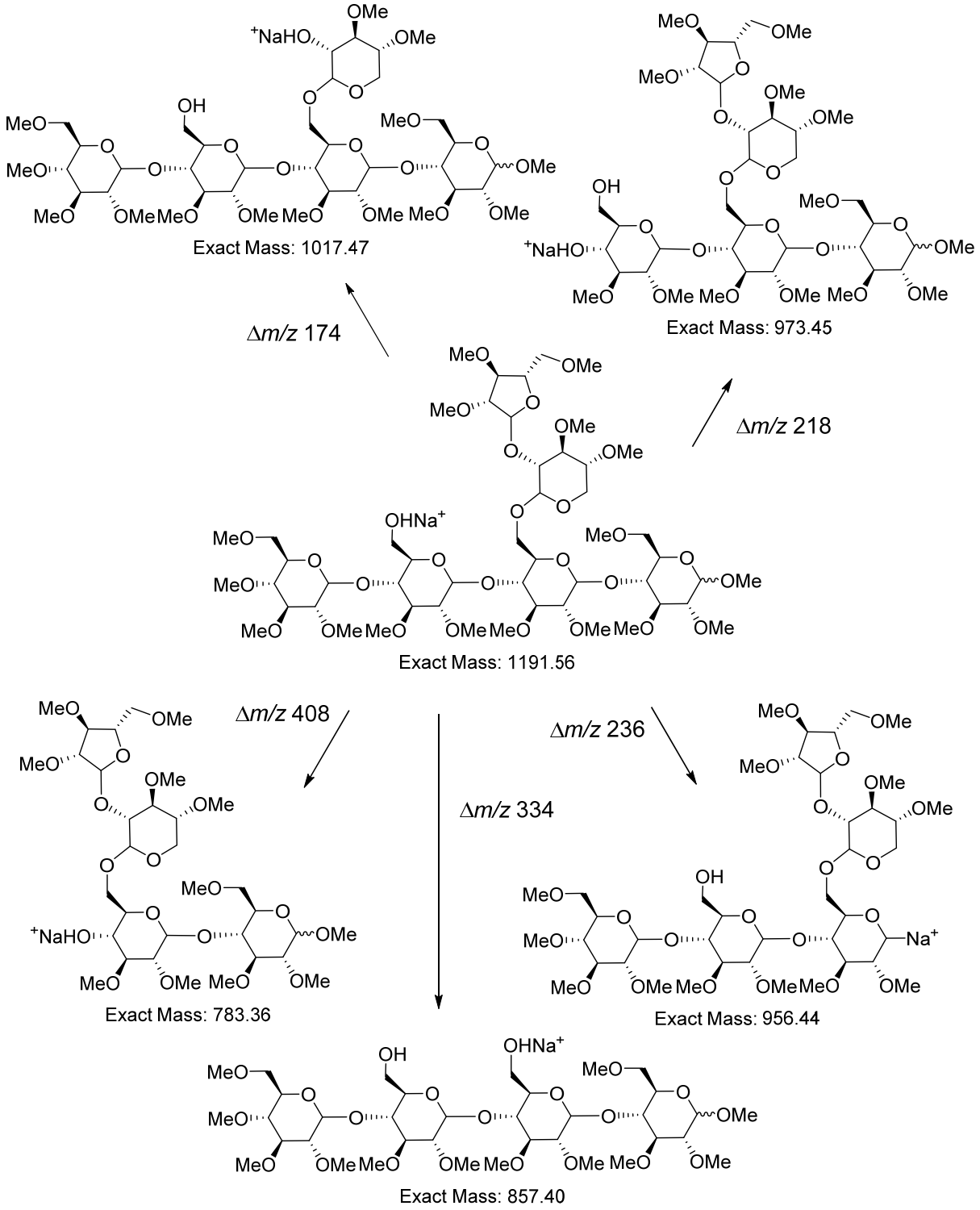

Figure S57. Structure (b) putative mass fragments produced from the *m/z* 1192 fragment of per-*O*-methylated **1**.

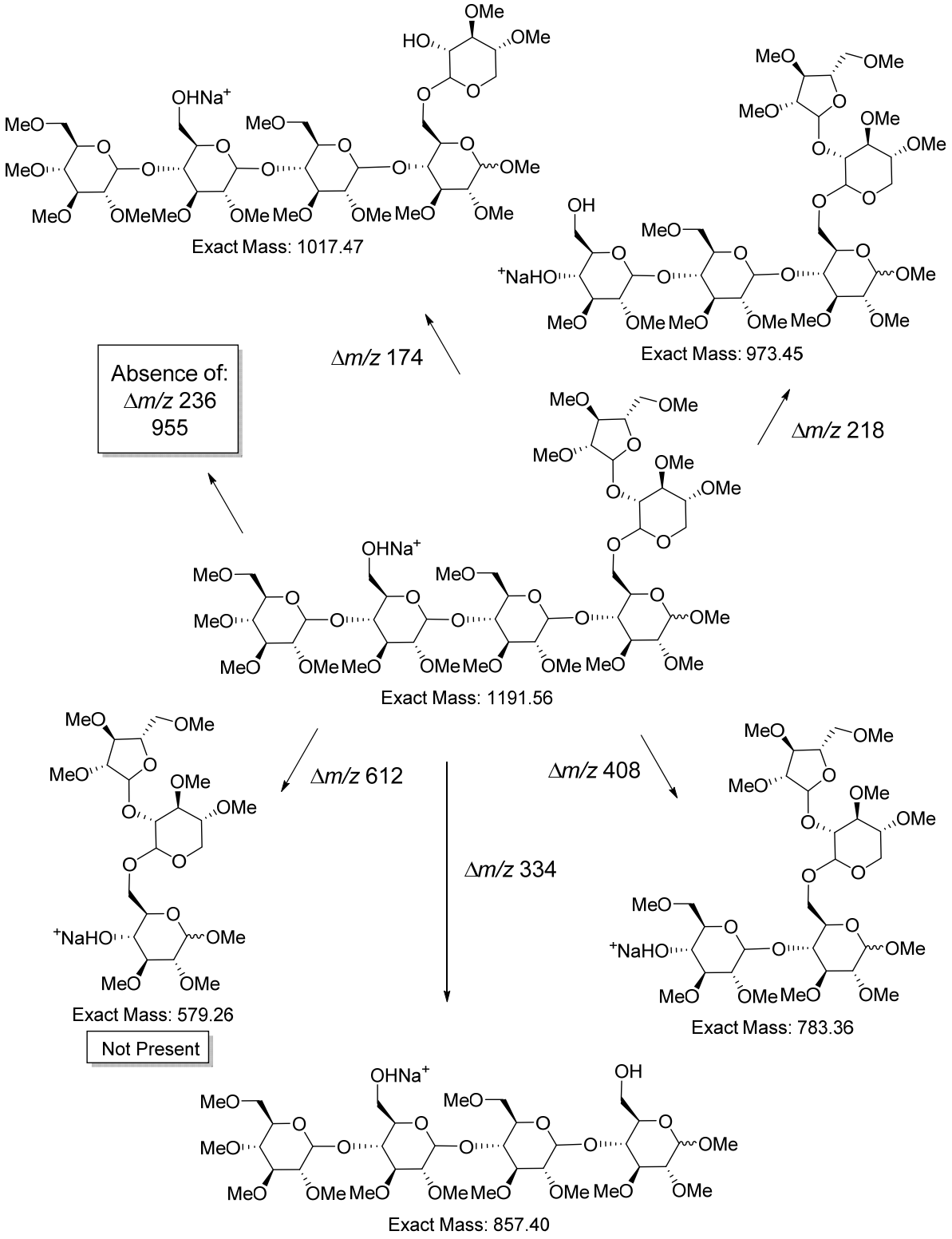

The NSI-MS^5 fragmentation at *m/z* = 1526 → 1352 → 1192 → 784 for the per-*O*-methylated derivative of **1** (Figure S58) gave indicative mass fragments of *m/z* 609, 565, 547, and 449. The mass fragment of *m/z* 609 is consistent with the loss of a terminal arabinose (Δ*m/z* = 174), *m/z* 565 is consistent with the loss of a reducing end glucose minus an oxygen (Δ*m/z* = 219), *m/z* 547 is consistent with the loss of a reducing end glucose (Δ*m/z* = 236), and *m/z* 449 is consistent with the loss of an internal xylose and a terminal arabinose (Δ*m/z* = 334). These mass fragments were consistent with structure (a) (Figure S59), as the putative *m/z* 784 fragment of structure (b) (Figure S60) did not produce fragments at *m/z* 547 or 565 corresponding to the loss of a reducing end glucose. The *m/z* 784 fragment of structure (b) would also have been expected to result in fragments at *m/z* 579, corresponding to the loss of an internal glucose (Δ*m/z* = 204), and at *m/z* 563, corresponding to the loss of an internal glucose minus an oxygen (Δ*m/z* = 221). These fragments were not present in the NSI-MS^5 data.

Figure S58. NSI-MS^5 fragmentation at *m/z* 1526 → 1352 → 1192 → 784 for the per-*O*-methylated derivative of **1**.

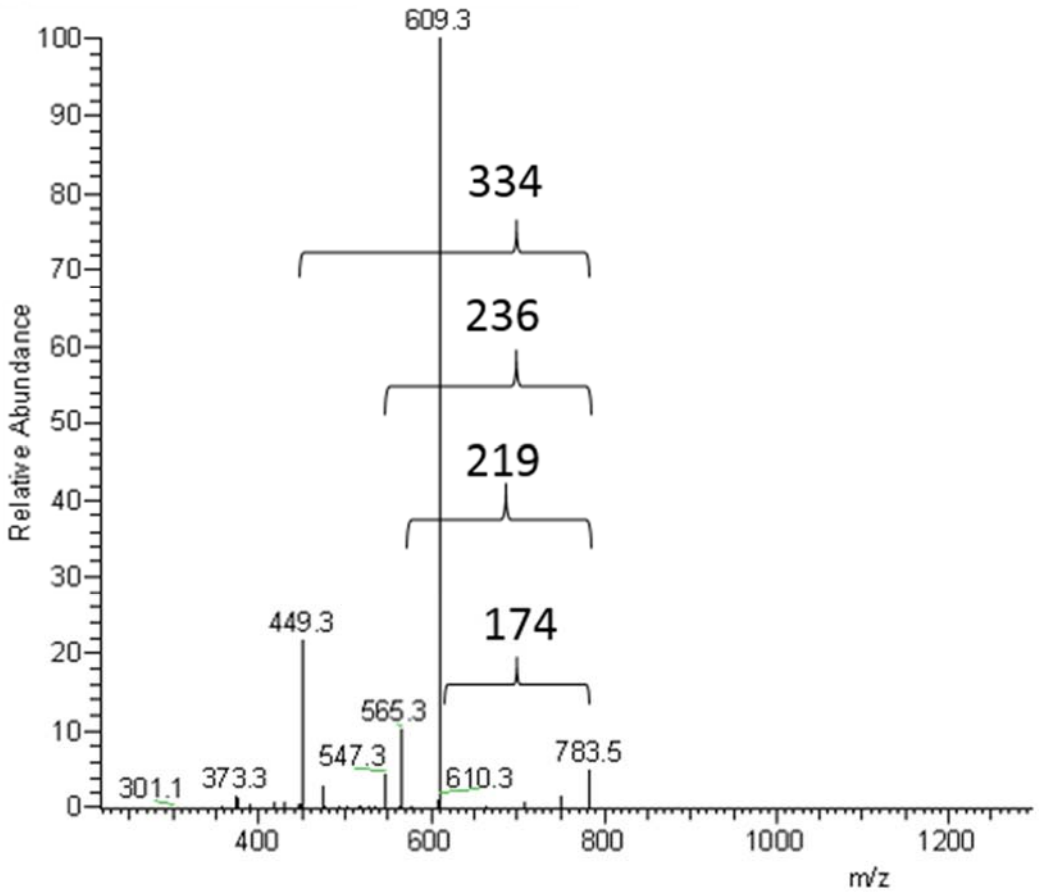

Figure S59. Structure (a) putative mass fragments produced from the *m/z* 784 fragment of per-*O*-methylated **1**.

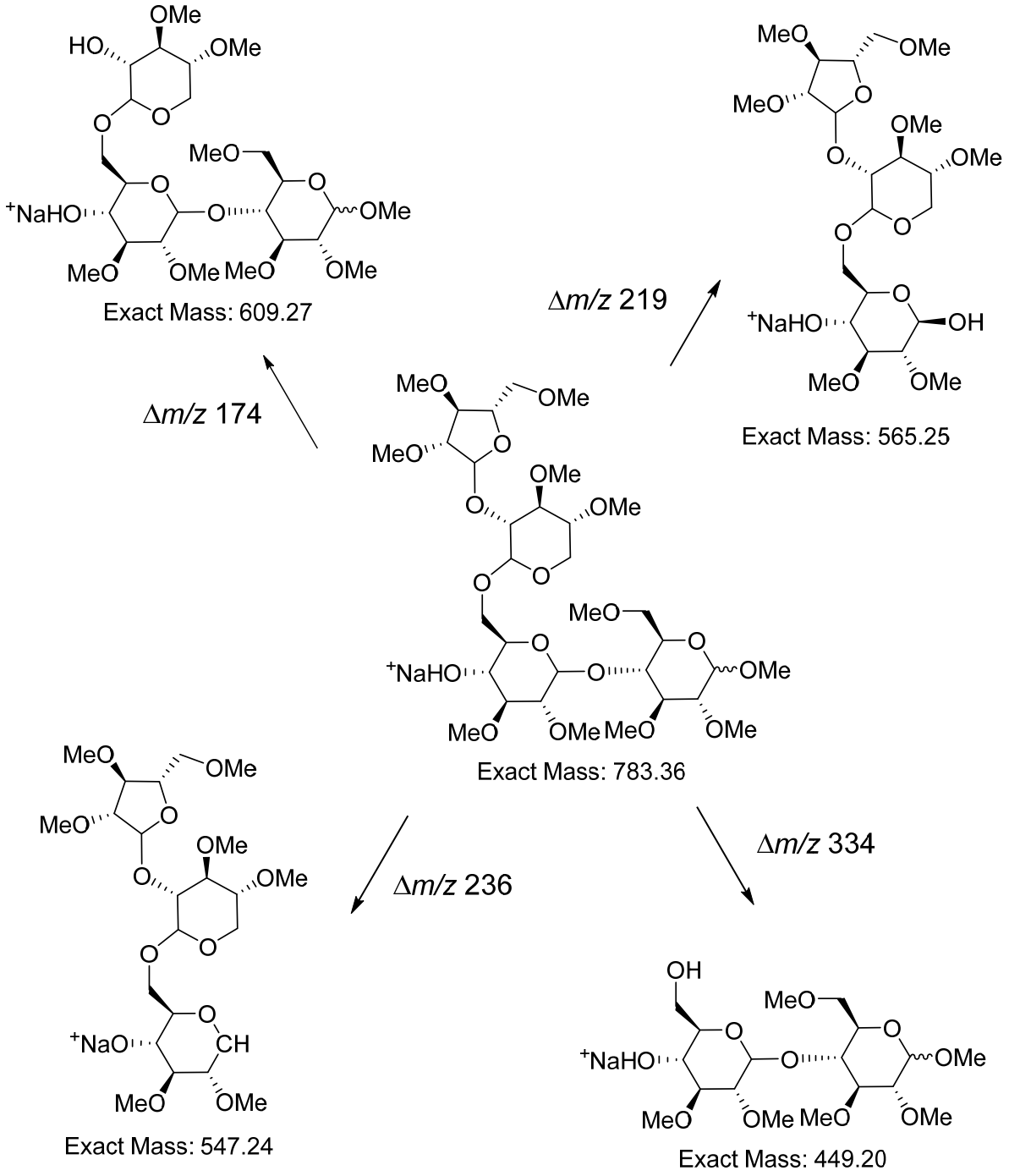

Figure S60. Structure (b) putative mass fragments produced from the *m/z* 784 fragment of per-*O*-methylated **1**.

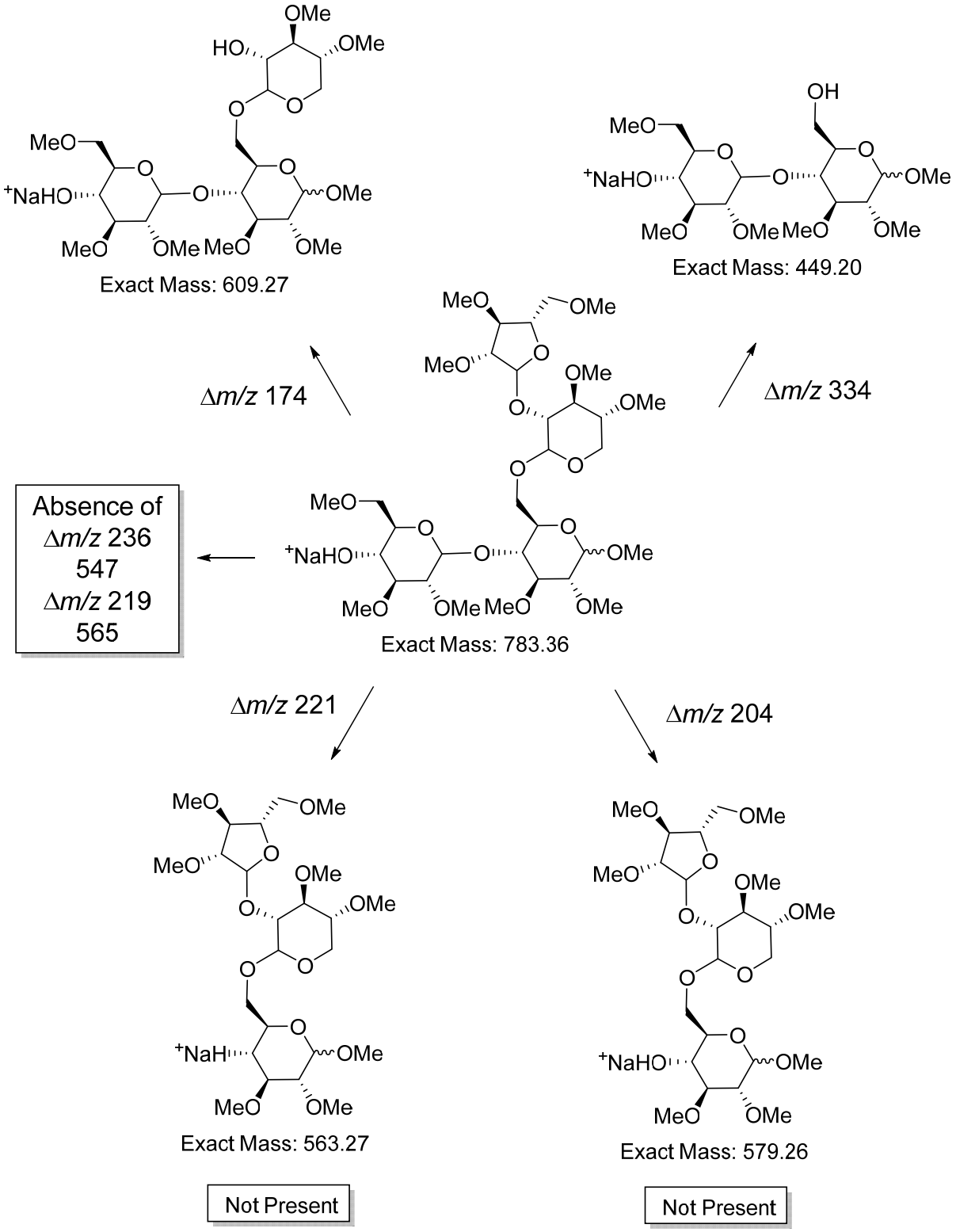

Structure (a) was therefore confirmed as the structure of **1** through the presence of key putative fragments produced from partial and sequential fragmentation of the *m/z* 1526 parent ion. These data supported the presence of a reducing, unsubstituted glucosyl moiety connected via a single glycosidic bond to the remainder of the compound, and allowed placement of the two Xyl-Ara side chains on the two internal glucosyl residues of the tetrameric backbone. Alternative placement of one of the side chains on the reducing glucosyl unit (structure b) would have resulted in a different pattern of MS^n fragments. A key indicator of the presence of the 4-linked glucosyl unit was a mass loss of $\Delta m/z = 236$ from the fragment ions analyzed (*m/z* 1526, 1308, 1192, and 784). If the reducing glucosyl unit had instead been substituted with a side chain on C-6, the mass loss of $\Delta m/z = 236$ would not have been detected and additional fragments indicative of C-6 substitution on the reducing glucosyl unit would instead have been detected. Placement of the Xyl-Ara side chains was further confirmed using NMR analyses.

All data obtained from the carbohydrate derivatization analyses were used to assign the structure of **1** as shown (Figure S61), with a D-glucopyranosyl-(1→4)-D-glucopyranosyl backbone and two L-arabinofuranosyl-(1→2)-D-xylopyranosyl side chains connected to the internal glucosyl residues via D-xylopyranosyl-(1→6)-D-glucopyranosyl linkages. Configurations at the C-1 positions were determined using NMR analyses.

Figure S61. The structure of **1** as determined by the carbohydrate derivatization analyses.

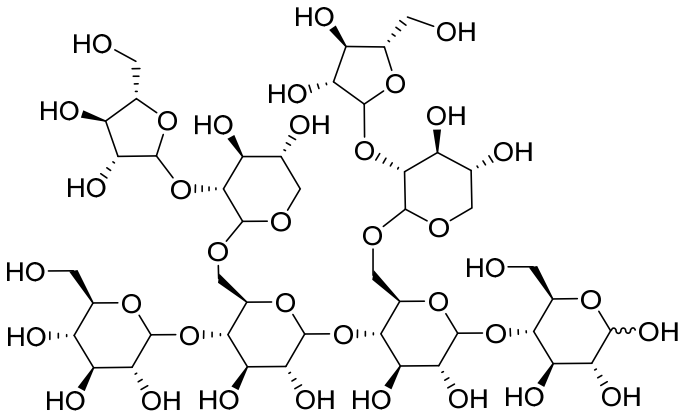

(**1**)

Supplementary References

(1) Foo, L. Y.; Lu, Y.; Howell, A. B.; Vorsa, N. A-type proanthocyanidin trimers from cranberry that inhibit adherence of uropathogenic P-fimbriated *Escherichia coli. J. Nat. Prod.* **2000**, *63*, 1225-1228. (a)

(2) Coleman, Christina M. Cranberry Metabolites with Urinary Anti-adhesion Activity. Doctoral Dissertation, University of Mississippi, University, MS, **2014**.

(3) Atlantis™ Columns Brochure - Applications Notebook. Literature Code 720000793EN. Waters Corporation, 2004. www.Waters.com.

(4) Merkle, R. K.; Poppe, I. Carbohydrate composition analysis of glycoconjugates by gas-liquid chromatography/mass spectrometry. *Methods Enzymol*. **1994**, *230*, 1-15.

(5) York, W. S.; Darvill, A. G.; McNeil, M.; Stevenson, T. T.; Albersheim, P. Isolation and characterization of plant cell walls and cell wall components. *Methods Enzymol.* **1986**, *118*, 3-40.

(6) Ciucanu, I.; Kerek, F. A simple and rapid method for the permethylation of carbohydrates. *Carbohydr. Res.* **1984**, *131* (2), 209-217.

(7) Anumula, K. R.; Taylor, P. B. A comprehensive procedure for preparation of partially methylated alditol acetates from glycoprotein carbohydrates. *Anal. Biochem*. **1992**, *203* (1), 101-108.

(8) Domon, B.; Mueller, D. R.; Richter, W. J. High performance tandem mass spectrometry for sequence, branching and interglycosidic linkage analysis of peracetylated oligosaccharides. *Biomed. Environ. Mass Spectrom.* **1990**, *19* (6), 390-2.

(9) Costello, C. E.; Vath, J.E. Tandem mass spectrometry of glycolypids. *Methods Enzymol.* **1990**, *193* (Mass Spectrom.), 738-768.

(10) Hisamatsu, M.; York, W. S.; Darvill, A. G.; Albersheim, P. Characterization of seven xyloglucan oligosaccharides containing from seventeen to twenty glycosyl residues. *Carbohydr. Res.* **1992**, *227*, 45-71.

(11) York, W. S.; Kolli, V. S. K.; Orlando, R.; Albersheim, P.; Darvill, A. G. The structures of arabinoxyloglucans produced by solanaceous plants. *Carbohydr. Res.* **1996**, *285*, 99-128.